Lipid droplet regulation by the differentially spliced proteins Osw5L and Osw5S

Lisa Johnsen

TESI DOCTORAL UPF / 2016

THESIS SUPERVISOR

Dr. Pedro Carvalho

CELL AND DEVELOPMENTAL BIOLOGY PROGRAM

CENTER FOR GENOMIC REGULATION (CRG)

Universitat Pompeu Fabra Barcelona

In the face of overwhelming odds,

I'm left with only one option: I'm gonna have to science the shit out of this.

-Marc Watney (The Martian)

Acknowledgements

To start with, I would like to thank Pedro to give me the opportunity to do my PhD thesis in his group. Furthermore, the CRG and all its people, scientist as well as administrative staff, to make my stay here a success. Finally, La Caixa, to do at least one good deed: fund me!

Big thanks go to the current, past and futur members of the Great TupperClub for the introduction to southern culinary science. Visca el pa amb tumacat! You guys made every lunch worthwile.

També vull agrair a "Els Xilens" Anna, Montse i Marc de acollir-me amb els braços oberts a la vostra bonica ciutat i el vostre entusiasme a integrar a aquesta alemanya quadrada al vostre increïble grup d'amics.

I would also like to thank the members of Hostal Sant Domènec to keep up with me from the very beginning to the bitter end. Montse, Marc, Mike, Micha and our ninja roomy Marta, you made every hangover and sleep deprivation worth it!

Vero, Vicky and Maria. You are the embodyment of female power and I wish you all the best. I had so much fun with you!

Many thanks also to Freddy, Vicky and Fatima for correction of the current body of work.

Vielen Dank auch an meine Familie für eure Unterstützung, egal welche Entscheidung ich auch getroffen habe.

Abstract

The cell stores neutral lipids in specialized organelles termed lipid droplets (LDs). Lipid droplets are born at the Endoplasmic Reticulum (ER) and consist of a neutral lipid core enclosed by a phospholipid monolayer and associated LD proteins. Lipid droplet size and number are tightly regulated. In the yeast *Saccharomyces cerevisiae*, lack of *FLD1*, the functional homolog of human Seipin leads to supersized droplets and global rearrangements of the lipid droplet proteome. Fld1 forms a complex with Ldb16 at the LD-ER contact sites and is thought to coordinate the release of neutral lipids into the droplet with the enclosing phospholipid monolayer.

We identified a third interaction partner of the Fld1-Ldb16 complex called Osw5L/Osw5S. This protein has two isoforms (Osw5L and Osw5S) which are generated by a splicing event. Osw5S deletion leads to a moderate increase of LD size. Unlike in Seipin complex mutants, only few LD proteins are mislocalised upon Osw5L deletion. However, overexpression of Osw5L leads to a massive fat accumulation in the cell. We suggest that Osw5L and Osw5S are regulatory factors of the Seipin complex and that protein targeting defect might arise from a deregulation of the ER-LD contact site.

Resumen

Las células almacenan lípidos en compartimentos especializados, llamados gotas lipídicas. Las gotas lipídicas se forman en el retículo endoplasmático y consisten en un cuerpo de grasa (neutra) envuelto por una membrana unilaminar de fosfolípidos y proteínas asociadas. En la célula el número y el tamaño de las gotas lipídicas se encuentra altamente regulado. En la levadura *Saccharomyces cerevisiae* la deleción del gen *FLD1*, el homólogo de Seipin en humanos, causa gotas lipídicas de gran tamaño y reordenamientos globales de su proteoma. En la levadura, la proteína Fld1 está en complejo con Ldb16 y se localizan en el punto de unión del retículo endoplasmático y la gota lipídica. Aquí, el complejo Fld1-Ldb16 coordina la liberación de las grasas neutras desde el retículo endoplasmático al cuerpo de la gota con la envoltura de fosfolípidos.

En este estudio identificamos una proteína adicional en complejo con Fld1-Ldb16 llamada Osw5L/Osw5S. Esta proteína tiene dos isoformas (Osw5L e Osw5S) que se generan por una reación de splicing. La ausencia de Osw5S causa un leve aumento del tamaño de las gotas lipídicas. Al contrario de los mutantes de Fld1-Ldb16, pocas proteínas localizadas normalmente en las gotas lipídicas pierden su localización si Osw5L está ausente. Notablemente, la sobre-expressión de Osw5L causa la acumulación de grasa en la célula. Proponemos que las proteínas Osw5L/Osw5S son componentes reguladores del complejo de Seipin y afinan su función en el punto de unión del retículo endoplasmático y la gota lipídica.

Preface

The work described in this thesis has been entirely conducted in the Cell and Developmental Biology program at Center for Genomic Regulation (CRG) under the supervision of Dr. Pedro Carvalho.

The current study reports on the novel role of two proteins, Osw5L and Osw5S, generated by a splicing event, in complex with the Seipin complex. Together with the Seipin complex, these proteins are involved in lipid droplet regulation in *Saccharomyces cerevisiae*.

List of Figures

List of Tables

Table of Content

1. Introduction

1.1. A declaration of love: Yeast as a model organism in lipid research

The thesis on hand characterizes the role of a previously undescribed protein in lipid storage and lipid droplet formation in the yeast *Saccharomyces cerevisiae*. Lipid biology has attracted much attention during the last decades and the yeast *Saccharomyces cerevisiae* has become a reliable organism to answer those basic questions. In 1988, Botstein and Fink predicted yeast to be a suitable model to elucidate gene and protein structure (Botstein and Fink 1988). Indeed, since the genome sequence of *S. cerevisiae* was published in 1996, the number of studied genes has risen from 35 % to 85 %, which is the highest number in any eukaryotic organism. 17 % of this gene products belong to orthologous protein families associated with human disease and for most complement the deletion of their mammalian homologs (Botstein and Fink 2011). The ease of culturing and genome manipulation have made it easy to study not only the gene products themselves but also the biological consequences of failure in a cellular context. Lipid metabolism and lipid storage are highly conserved processes from yeast to mammals (Walther and Farese 2012) and therefore *Saccharomyces cerevisiae* is our model of choice in this study.

1.2. Setting the stage: The Endoplasmic Reticulum

1.2.1. The discovery of a net-like organelle

In 1665, the English natural philosopher and architect Robert Hooke was the first to view a cell under the microscope (Turner 1890). Limited by the microscopy technology of the 17th century it should take nearly two centuries until the first intracellular structure, the nucleus was described by the microbiologist Antony van Leuwenhook in 1833 (Harris 2000). Descriptions of mitochondria (Ernster and Schatz 1981), chloroplast (Schimper 1883) and the Golgi apparatus (Farquhar and Palade 1998) followed before the conclusion of the 19th century. In 1894 the German zoologist Karl August Möbius noted analogies between defined subcellular compartments and organs of the human body and named them “Organellulas” which was readily accepted and eventually changed to organelles (Möbius 1884). In 1902 Emilio Veratti, an Italian scientist and student of

Camillo Golgi, used Golgi´s staining procedures and discovered a new net-like organelle (Veratti 1961). Besides his careful studies and drawings, the scientific community did not accept the existence of this organelle until the development of suitable electron microscopy (EM) methods in 1953 by Keith Porter, which allowed for the visualization of the Endoplasmic Reticulum (ER) (Porter 1953). When Porter teamed up with George Palade in 1954 to obtain high-quality EM pictures, the ER was finally accepted as a *bona fide* organelle and piqued the curiosity of many scientists (Palade and Porter 1954).

1.2.2. ER structure and function

Over the last 60 years of research, it turned out that the ER is one of the most versatile and diversified cellular organelles. The ER is a single continuous membrane system delimiting a single luminal space. It is composed of multiple morphological domains thought to be associated to different functions (Shibata, Voeltz et al. 2006). Its main domains are the nuclear ER or nuclear envelope, perinuclear sheets and the peripheral tubular ER. The nuclear envelope consists of apposed membrane sheets with a lumen where the inner and outer membranes only connect at the nuclear pores. The peripheral ER branches out from the nuclear envelope towards the cell periphery and forms a series of sheets and tubules throughout the cell. In muscle cells and also in the yeast *Saccharomyces cerevisiae* large regions of the peripheral ER are tethered to the plasma membrane, which are then referred to as cortical ER. During the last years researchers have described an intimate structure-function relationship between the different ER domains (Shibata, Voeltz et al. 2006).

ER sheets are a rather flat double membrane layers sandwiching a lumen with a constant diameter of 50 nm in animal cells and 30 nm in yeast. It was recently shown in rat neurons that sheets are interconnected by a membrane spiral leading to tight stacking (Terasaki, Shemesh et al. 2013). The curvature in the flat sheets is low which probably favors the association of ribosomes to them. The high ribosome density on the sheets was already appreciated in the early EM studies where it was termed rough endoplasmic reticulum (rER). ER sheets are the primary location for protein translation, translocation and folding. Once secretory proteins are inside the lumen or integral membrane proteins inserted in the ER double membrane they can be modified and subsequently exported to their site of function via the secretory pathway (Shibata, Voeltz et al. 2006, Westrate, Lee et al. 2015).

ER tubules radiate either from the nuclear ER or from ER sheets and are largely ribosome-free and therefore corresponding to the smooth endoplasmic reticulum (sER) (Shibata, Voeltz et al. 2006). Membrane curvature in the tubules is high (in cross section) and they are probably the site of lipid synthesis and signaling. ER tubules also facilitate inter-organelle contacts with mitochondria, Golgi, vacuoles, peroxisomes, late endosomes, lysosomes and the plasma membrane (Westrate, Lee et al. 2015)

The cortical ER, which extensively contacts the plasma membrane in yeast, is formed by highly fenestrated ER sheets resembling a slice of Swiss cheese. In muscle cells these contacts are important for Ca^{2+} storage and signaling. The close apposition of these organelles facilitate the exchange of signals, lipids and small molecules (Phillips and Voeltz 2016).

1.3. Cellular lipids and their function

1.3.1. Membrane structure and function

The smooth tubular ER synthesizes the bulk of structural phospholipids and sterols, as well as non-structural lipids triacylglycerols (TAGs) and sterol esters (SEs) (Bell, Ballas et al. 1981). In the cell, lipids fulfill three general functions: Reduced carbons in triacylglycerols and sterol esters serve as energy and membrane precursor reservoirs, polar lipids form membranes which divide the cell into discrete reaction spaces, and signaling lipids convey signals between membranes and establish organelle identity (van Meer, Voelker et al. 2008, Henry, Kohlwein et al. 2012).

The structure and function of storage lipids will be discussed in detail below. The second group of lipids, polar lipids, make up most membranes in the cell. They consist of a polar head group and hydrophobic moiety. The hydrophobic moiety tends to self-assemble in hydrophilic environment driven by entropy. The polar head groups interact with polar aqueous environment. These chemical properties of amphipathic lipids drive the compartmentalization in the cell. The main lipids in eukaryotic membranes are phospholipids: phosphatidylcholine (PC), phosphatidylethanolamine (PE), phosphatidylserine (PS), phosphatidylinositol (PI), and phosphatidic acid (PA). The relative abundance of these change depending on cell type and organism. The hydrophobic moiety is diacylglycerol with saturated or cis-unsaturated fatty acid chains of different length. The variability of fatty acid chain length and saturation in combination with different head groups generates thousands of different phospholipids in the cell. Size and charge of the head group and the degree of fatty acid saturation influences phospholipid packing, membrane curvature and bilayer thickness (van Meer, Voelker et al. 2008).

Apart from phospholipids, sphingolipids constitute a second group of structural membrane lipids. Their hydrophobic moiety is ceramide and the mayor subclasses are sphingomyelin (SM) and glyceroshingolipids (GSL). Additionally, the major class of non-polar lipids in membranes are sterols (cholesterol in mammals and ergosterol in yeast) (van Meer, Voelker et al. 2008, Klug and Daum 2014).

Apart from structural lipids, membranes also harbor so-called signaling lipids, however in much lower amounts. When phospholipids and sphingolipids are hydrolyzed they can generate a series of messenger lipids with two mayor modes of action: The newly formed molecules can be soluble and readily leave membranes and signal trough related membrane receptors or they remain in the membrane and subsequently can be recognized by cytosolic and membrane proteins. PI and phosphorylated derivatives of PI are especially important in cell signaling and establish organelle identity (Klug and Daum 2014).

All mayor structural lipid classes are synthesized in the ER. The mammalian ER consist of about 55% PC, 27% PE, 13% PI, and 4% PS whereas the numbers differ slightly in yeast (39% PC, 19% PE, 23% PI, and 6% PS) (Zinser, Sperka-Gottlieb et al. 1991, van Meer, Voelker et al. 2008). Although primarily synthesized in the ER, sterols (ergosterol in yeast), are rapidly exported to the plasma membrane and endosomes (Zinser, Paltauf et al. 1993). Thus, their levels in the ER are kept relatively low. SL are synthesized in the ER and the Golgi apparatus and are subsequently enriched in the plasma membrane.

Sterols and sphingolipids accumulation in the plasma membrane leads to denser packing of the lipid bilayer and therefore higher resistance to mechanical stress (van Meer, Voelker et al. 2008).

Significant levels of lipid synthesis also occur in the mitochondria. They synthesize especially Cardiolipin, a lipid unique to mitochondria which highlights their bacterial origin (van Meer, Voelker et al. 2008).

1.4. Lipid transport between organelles

After their synthesis in the ER, cellular lipids need to be distributed to their site of function. Almost all organelles harbor lipids which where synthesized elsewhere and subsequently transported to their final destination. Various ways of lipid transport exist in the cell. In the ER and in other continuous membrane systems, lipids can diffuse laterally. An important lipid transport pathway between organelles is the secretory pathway which is better known to transport proteins from the ER to the Golgi and later to the plasma membrane. Also the endocytic pathway, which serves to internalize proteins and lipids from the plasma membrane, contributes to lipid transport. Mitochondria and peroxisomes however are not connected to the secretory pathway. Here, lipids exchange with these organelles probably occur at membrane contact sites through lipid transfer proteins which shuttle lipid monomers between apposed membranes (van Meer, Voelker et al. 2008, Lev 2010).

1.4.1. Lipid transfer proteins

In humans, 125 genes encoding ten families of lipid transfer proteins (LTPs). LTPs are conserved from yeast to mammals and being also found in plants (Chiapparino, Maeda et al. 2016). These globular, mostly soluble proteins are classified by their very diverse lipid transfer domain (LTD) folds. Although LTPs are very diverse polypeptide chains, they a have striking similarities in their mode of action. LTPs contain a hydrophobic or amphipathic lipid-binding pocket and typically bind a single lipid molecule. A lid-like structure closes the lipid binding pocket once the molecule has been accommodated and shields it during the transfer reaction (Fig. 1.1B, 2B) (Lev 2010, Chiapparino, Maeda et al. 2016). Interestingly LTPs show a very broad range of lipid-binding specificity, varying not only between protein families but also between members of the same. Ligand specificity dependents on the size, shape and charge of the lipid binding pocket, but also on the subcellular location and the membrane interaction motives of the protein (Lev 2010). Consequently, LTPs require a precise subcellular localization to exhibit their functions. Membrane targeting can involve transmembrane helices, the lid domain and specialized lipid targeting domains but is also dependent on membrane fluidity and curvature which can be sensed by some LTPs (Lev 2010, Lev 2012).

LTP catalyzed lipid exchange requires a series of sequential events: interaction with the donor membrane, extraction of the substrate from the membrane, dissociation from the donor membrane, diffusion trough the cytosol, and substrate delivery to the donor membrane (Lev 2010, Lev 2012).

1.4.1.1. Lipid transfer proteins at membrane contact sites

Since the discovery of ER-organelle contact sites, called Membrane Contact Sites (MCS), is has been proposed that these sites are sites of LTP action. At MCS two apposed membranes come close together (≤ 30 nm) which yields optimal conditions for lipid transfer between membranes (Prinz 2014). It has been shown that at least four LTPs are localized to ER-Golgi MCS and accelerate lipid exchange. All of these proteins contain a Pleckstrin homology (PH) domain, which binds to the PI(4)P rich Golgi-membrane, and a FFAT motif that binds to specific ER receptor proteins (Mesmin, Bigay et al. 2013, Selitrennik and Lev 2016). This suggests that LTPs might be able to physically bridge the MCS and thus facilitate lipid exchange (Phillips and Voeltz 2016).

In yeast, the EMES complex (ER-mitochondria encounter structure) mediates lipid exchange between the ER and the mitochondria. For example, PS -which is synthesized at the ER- is modified to PE by the mitochondria-localized phospholipid synthase, and PE subsequently is metabolized by an ER-bound enzyme to PC (Fig. 1.3). These lipids need to be shuttles between the two organelles. Additionally, PA, the precursor for mitochondria-specific cardiolipin, is synthesized at the ER and must be transported to the mitochondria (Fig. 1.3).

Three of four proteins of the ERMES complex contain the putative SMP (*s*ynaptotagmin-like *m*itochondrial-lipid binding *p*rotein) lipid-binding domains and are members of the SMP/TULIP (*tu*bular *lip*id-binding) family of lipid transfer proteins. However, it remains to be clarified weather ERMES directly transfers lipid between mitochondria and ER or rather serves as a theater to facilitate the lipid exchange by other proteins (Prinz 2014, Phillips and Voeltz 2016).

1.4.1.2. Lipid transfer proteins: A theoretical framework

At first glance it is hard to understand how LTPs often move lipids against obvious concentration gradients. There are three concepts that can give an explanation: metabolic trapping, thermodynamic trapping, and heterotypic lipid exchange (Holthuis and Menon 2014).

A good example of a metabolic trap is ceramide transport from ER to Golgi by the CERT proteins. Ceramide can be transported bi-directionally, however fast ceramide metabolization at the Golgi leads to a one-way transport from the ER to the Golgi (Holthuis and Menon 2014).

Thermodynamic trapping has been proposed for sterol transport from the ER to the plasma membrane. Sterols are moved against a concentration gradient from the ER to the plasma membrane. In the plasma membrane fatty acid tails of sphingolipids and phospholipids possess more saturated double bonds than in the ER. Sterol association with these saturated lipids in the plasma membrane is energetically more favorable than association with the less saturated lipids in the ER. This provides a thermodynamic trap driven by the enhanced stabilization and sequestration of sterols by neighboring lipids. At the same time, this also allows for higher sterol concentrations in the PM than in the ER (Holthuis and Menon 2014).

The third conceptual framework, heterotypic lipid exchange, is defined by reciprocal transfer of two distinct lipid species coupling a metabolic trap in one membrane with a thermodynamic trap in the other membrane. This concept is illustrated by the transfer reaction of Oxysterol Binding Protein (OSBP), a member of the ORP (OSB related proteins) family, and its yeast counterpart Kes1, also known as Osh4 and will be outlined in the following paragraphs (Mesmin, Antonny et al. 2013).

1.4.1.3. Oxysterol Binding Proteins: Kes1

S. cerevisiae encodes seven Osh (ORP related homologues) proteins which are divided into four subgroups: Osh1/2, Osh3, Osh4/5, and Osh6/7 (Fig. 1.1A). Osh1-3 contain a lipid bind ORD (OSB related domain) at the C-terminus and a PH (pleckstrin homology) domain at N-terminal which interacts with phosphoinositides. The internal FFAT (two phenylalanines in an acidic tract) motif recognizes specific ER receptors. Osh1-2 also contain ankyrin repeats, a protein-protein interaction motif, whereas Osh3 harbors a GOLD (Golgi dynamics) domain, a specific protein-protein interaction domain mediating Golgi dynamics and secretion. Osh4/5 consist exclusively of the ORD domain and Osh4 was recently described to harbor an amphipathic ALPS (Amphipathic Lipid Packing Sensor) domain at its N-terminus. This amphipathic helix recognizes loosely packed membranes (Drin, Casella et al. 2007). Osh6/7 possess an additional 40 amino acid sequence at the N-terminus (Mesmin, Antonny et al. 2013).

Osh proteins are thought to act as sterol transfer proteins and the deletion of all family members is lethal and induces accumulation of intracellular sterols. Expression of a single family member however rescues viability and sterol distribution (Beh, Cool et al. 2001, Beh and Rine 2004). Osh4 and other family members can also transport sterols *in vitro* between liposomes (Raychaudhuri, Im et al. 2006). Contradictory to previous results, Georgiev, Sullivan et al. (2011) reported transport from ER to the plasma membrane to be independent of Osh proteins. Overall, is unclear if all Osh proteins are *bona fide* LTPs in the cell. Recent data on Osh6 and Osh7 found both proteins at the ER-plasma membrane contact site and involved in reciprocal PS-PI(4)P transfer *in vitro*

(Maeda, Anand et al. 2013, Moser von Filseck, Copic et al. 2015). However, there is intriguing data on the Osh protein family member Osh4 or Kes1 integrating PI(4)P and sterol transport (Fig. 1.1B).

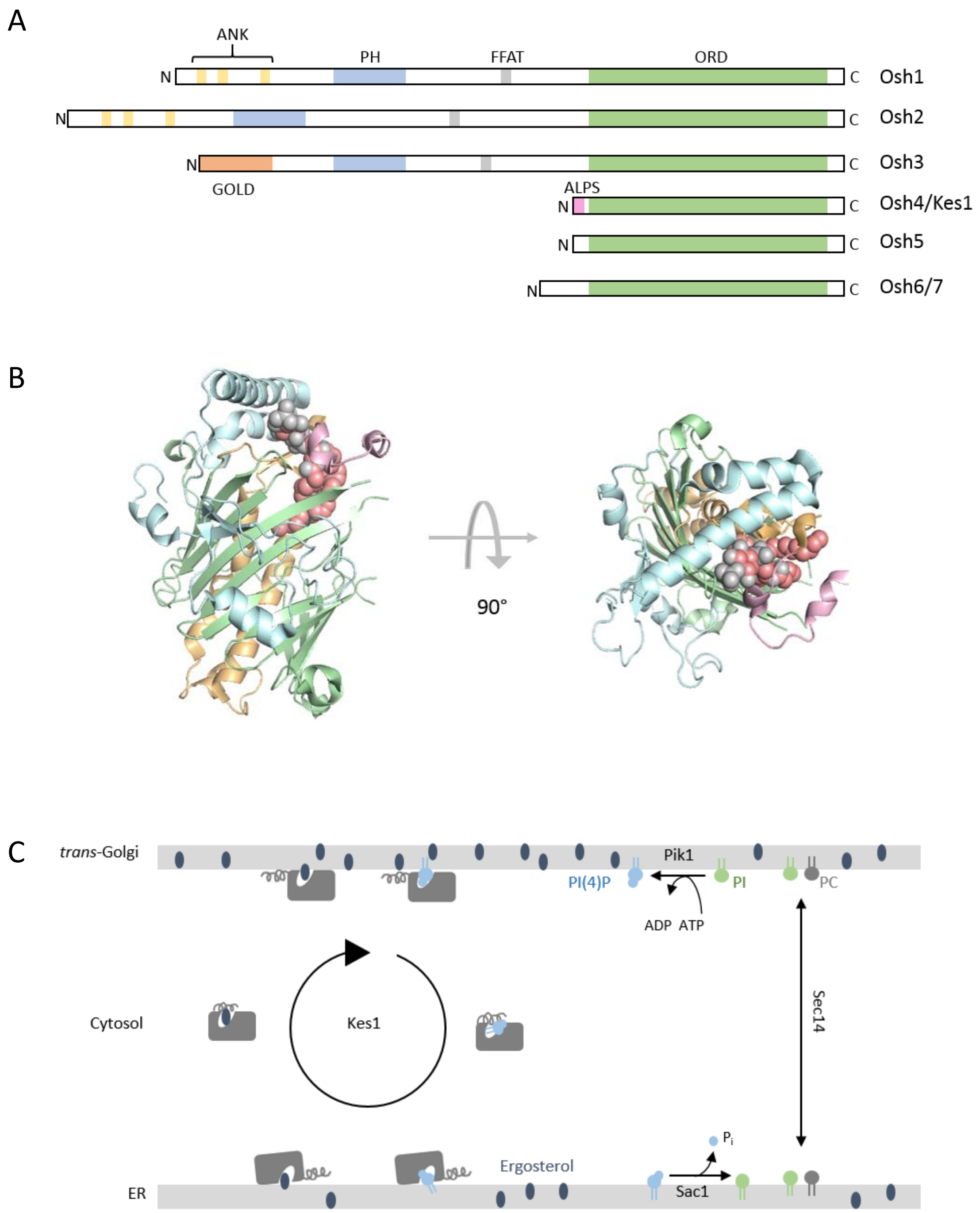

Figure 1.1. Domain organization, structure and function of Oxysterol Binding Proteins.
(A) Domain organization of the Oxysterol Binding protein family of *S. cerevisiae*. ANK= Ankyrin Repeats, PH= PH binding domain, FFAT=two phenylalanines in an acidic tract motif, ORD=OSB related domain, GOLD= Golgi Dynamics Domain, ALPS= Amphipathic Lipid Packing Sensor Domain. Adapted from Beh, McMaster et al. (2012). (B) Crystal structure of Kes1 bound to PI(4)P (PDB:3SPW). The lid region is shown in pink, the N-terminal domain in orange, the β-barrel in green and the C-terminal domain in blue. PI(4)P is shown as spheres with carbon atoms in red, oxygen in grey, and phosphorus in white.(C) Speculative model of Osh4 function (see details in the main text). Adapted from Mesmin, Antonny et al. (2013).

Kes1 was identified as one of seven non-essential genes which rescued cell viability in cells deleted for the essential gene SEC14 (Fang, Kearns et al. 1996, Li, Rivas et al. 2002). Sec14 binds PI and PC, and acts as a coincidence sensor that couples PC metabolism to PI production at the Golgi. Sec14 is essential for Golgi vesicle budding and cell viability. It ensures proper PI level at the Golgi which subsequently is phosphorylated by the Golgi resident kinase Pik1 to PI(4)P. PI(4)P is the master regulator lipid of vesicle budding at the late Golgi (Bankaitis, Mousley et al. 2010).

In other words, deletion of SEC14 in a wild-type background is lethal. Deletion of KES1 is not lethal. Deletion of KES1 in a SEC14 background re-establishes cell viability. But how can the deletion of a non-essential gene product re-establish cell viability? The basic idea is that the non-essential gene product, in this case Kes1, has a lethal activity if a certain regulator, here Sec14, is not present. The lethality in a *SEC14* mutant is therefore not caused by the absence of Sec14 but by the enzymatic activity of Kes1 if Sec14 is not present. Deleting *KES1* removes the cause of death and renders a *SEC14 KES1* double mutant viable (Bankaitis, Phillips et al. 2005).

But what is this lethal activity? Kes1 binds sterol and PI(4)P in a competitive manner. In a proposed model by Mesmin, Antonny et al. (2013), Kes1 recognizes the loose packing of ER membranes with the amphipathic nature of the ALPS domain, docks to the membrane and binds a sterol molecule. Then, it shuttles to the Golgi membranes where the high levels of PI(4)P compete with the bound sterol molecule which is released and enriched in late Golgi membranes. PI(4)P is then shuttled back to the ER and, to maintain low PI(4)P levels at the ER, dephosphorylated rapidly by the phosphatase Sac1. Based on this model Sec14 is essential to shuttle PI back to Golgi membranes where it is converted into PI(4)P. If Sec14 is absent, Kes1 delivers all PI(4)P to the ER where it is dephosphorylated to PI and Golgi secretory function will be abrogated. Viability is rescued if either PI(4)P is no longer extracted from the Golgi by Kes1 or when the PI(4)P phosphatase Sac1 is deleted. In this case, PI(4)P will be shuttled back to the Golgi due to its higher binding affinity to Kes1 (1B, C).

A study by Mousley, Yuan et al. (2012) couples the Sec14/Kes1 antagonism and therefore Golgi function with proliferative signaling and cell-cycle control. Kes1 overexpression lead to a cell-cycle arrest. This was explained by a manipulation of the Golgi sphingolipid homeostasis which in turn controlled cell proliferation and nutrient signaling. In this model, they propose, that Kes1 does not act as a PI(4)P-sterol shuttle itself, but as a sterol sensor which is recruited to membranes bi PI(4)P and released by sterol binding (Villasmil, Bankaitis et al. 2012).

1.4.1.4. Sec14 homologs: Pdr16

In yeast, the Sec14 protein family has more members which shows PI transfer activity: The Sec fourteen homologue proteins (SFHs) which were originally identified by their high sequence identity to Sec14. The Sfh family includes five family members, Sfh1-5, of which none is essential for cell viability in yeast. All family members harbor a SEC14 domain and, except for Sfh1, show PI but no PC transfer activity *in vitro*. If overexpressed Sfh2 and Sfh4 re-establish cell viability in a SEC14 temperature sensitive mutant upon growth under restrictive temperatures, whereas Sfh1 does so to a minor extend. Sfh3 overexpression does not rescue *SEC14* lethality if overexpressed (Li, Routt et al. 2000, Schnabl, Oskolkova et al. 2003). While Sec14, Sfh2, Sfh4, and Sfh5 are mainly localized to cytosol and ER, Sfh1 was detected in the nucleus and Sfh3 on lipid droplets and ER (Schnabl, Oskolkova et al. 2003). Due to its localization Sfh3, also called Pdr16, is of particular interest for this thesis.

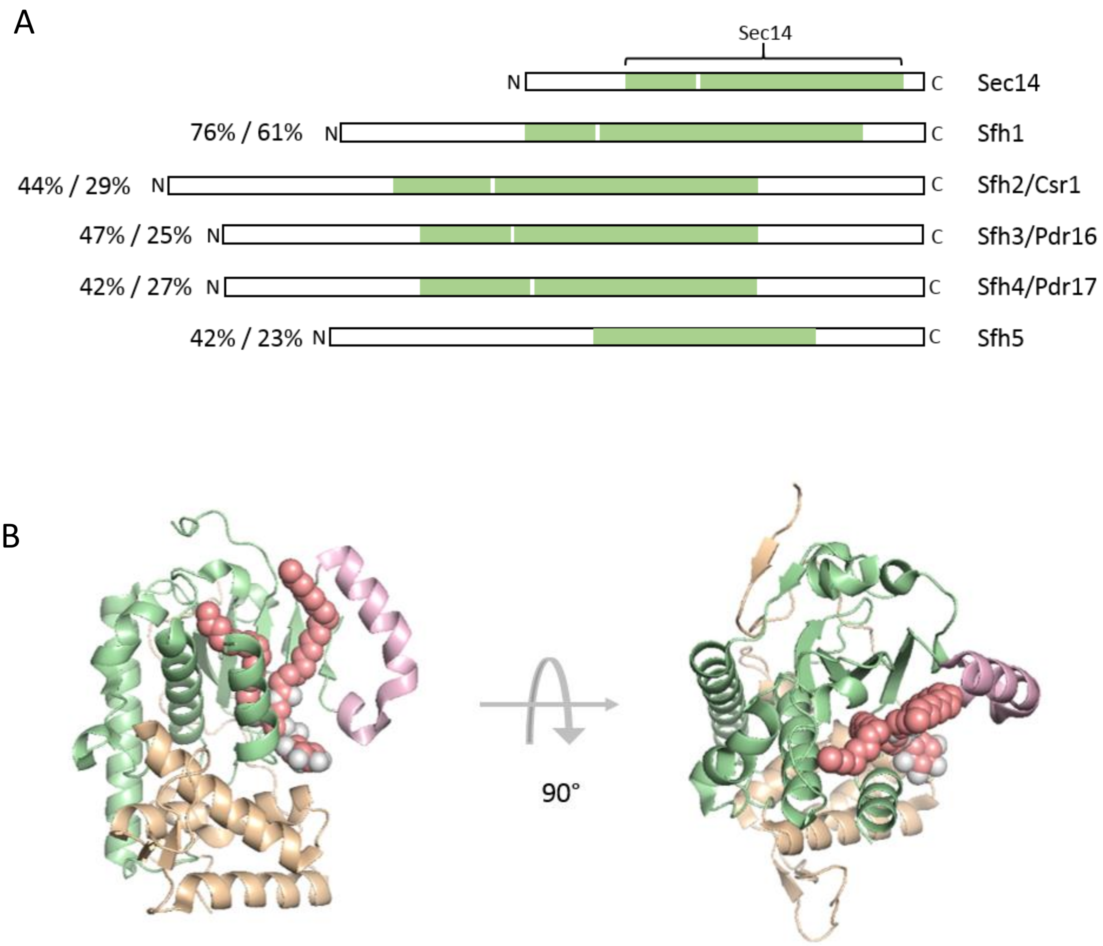

Figure 1.2. Domain organization and structure of the Sfh protein family.
(A) Domain organization of Sec14 and the Sfh protein family. Similarity/Identity based on primary sequence comparisons. The Sec14 domain, also called CRAL-TRIO domain, is depicted in green. The N-terminal portion of the domain, CRAL-TRIO-N is depicted separately, because it is missing in Sfh5. Adapted after Ren, Pei-Chen Lin et al. (2014). (B) Crystal structure of *S. cerevisiae* Pdr16 (PDB:4J7Q) in complex with phosphatidylinositol. The structure consist of an N-terminal domain (orange) and a c-terminal domain (green) that contains a large hydrophobic pocket for ligand binding. The lid domain is depicted in pink. PI is shown as spheres with carbon atoms in red and oxygen in grey.

Pdr16 is 25% identical and 47% similar to Sec14 and structure analysis shows that it adopts the typical Sec14 domain fold (Fig. 1.2B). Most variation can be found in the gating helix and the lipid binding pocket, which is wider and shallower, and also displays an altered charge distribution compared to a classical Sec14 domain. Furthermore, in contrast to Sec14, purified Pdr16 dimerizes. Based on these alterations it was suggested that Pdr16 could bind lipids beyond PI (Ren, Schaaf et al. 2011, Yang, Tong et al. 2013, Ren, Pei-Chen Lin et al. 2014).

Pdr16 was initially identified in a screen searching for targets of the multiple drug resistance regulator Pdr1 and named accordingly Pdr16 (Pleiotropic Drug Resistance). In contrast to Pdr16, most of the Pdr1 controlled gene products are efflux pumps, which are upregulated when yeast cells are exposed to toxic agents and confer a certain level of protection to the cell (do Valle Matta, Jonniaux et al. 2001). *PDR16* deletion mutants display increased sensitivity to azole antifungal drugs which inhibit late steps of the ergosterol biosynthetic pathway, such as fluconazole and miconazole providing a link between Pdr16 and sterol homeostasis (Saidane, Weber et al. 2006).

It was initially reported that *PDR16* deletion caused mayor alterations in sterol and phospholipid composition of the plasma membrane (van den Hazel, Pichler et al. 1999), however this could not be confirmed by Simova, Poloncova et al. (2013). In this last study, changes were only observed if cells were challenged with sub-inhibitory concentrations of azole antifungals. However, these plasma membrane property changes could be responsible for the reported azole sensitivity in *PDR16* deletion strains. Taken together, this data suggested a role of Pdr16 in sterol metabolism. Further support to this idea came from Holic, Simova et al. (2014) showing that Pdr16 binds sterols in an *in vitro* lipid transport assay in permeabilized cells.

A study by Ren, Pei-Chen Lin et al. (2014) reported Pdr16 to be recruited to distinct lipid droplet populations during meiosis. Furthermore, they observed enhanced lipid droplet load in cells overexpressing Pdr16 and enhanced lipolysis in *pdr16Δ* cells. They conclude that Pdr16 localization on lipid droplets regulates lipolysis.

Thus, several studies implicate Pdr16 in lipid homeostasis but its precise functions is still elusive.

1.5. Membrane and neutral lipid synthesis

Cellular processes for lipid synthesis and neutral lipid storage are quite conserved from unicellular organisms such as yeast to multicellular organism such as animals and plant. In the following I will give an overview over lipid biosynthesis in yeast and highlight the differences to the mammalian system.

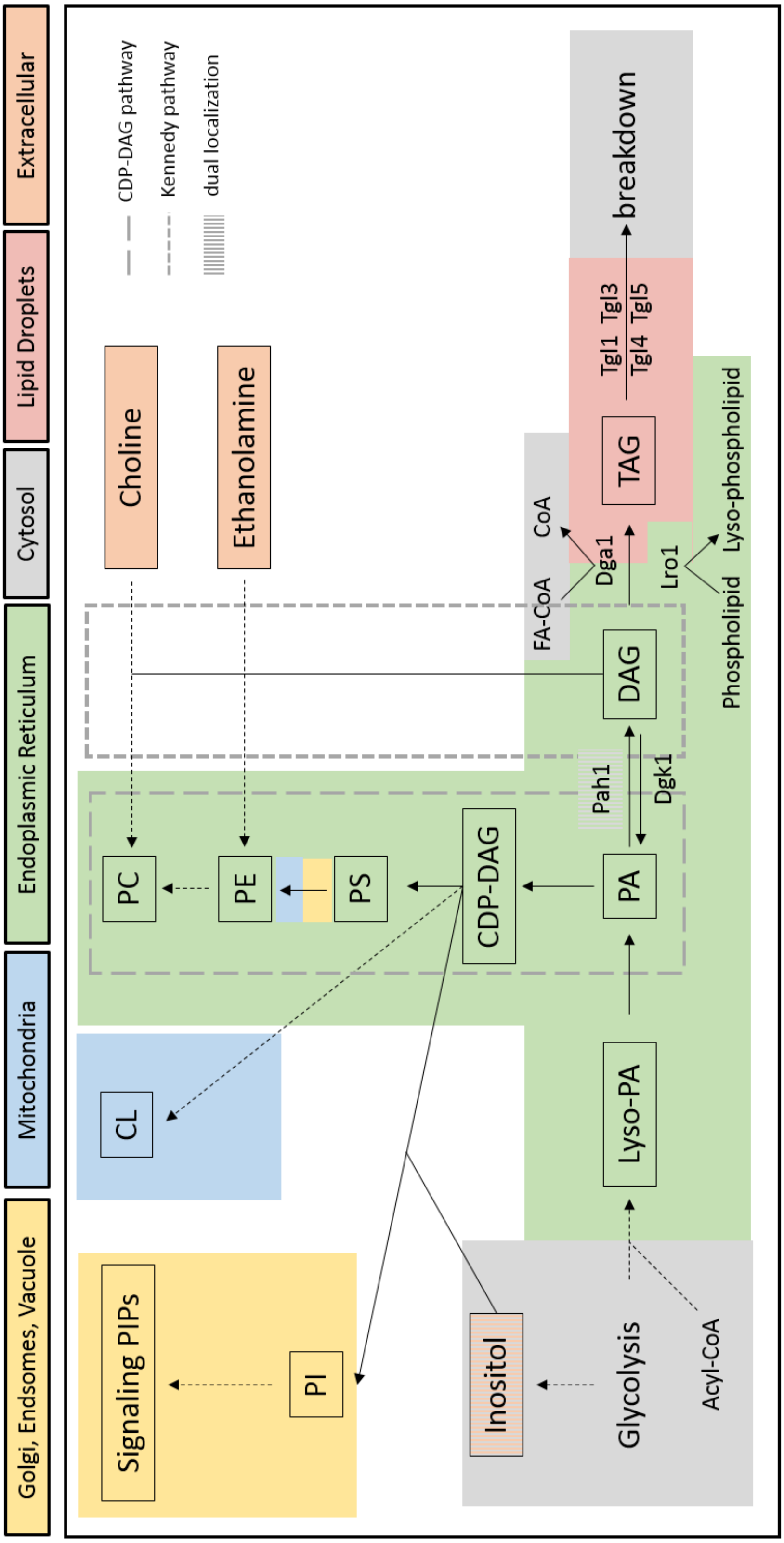

Figure 1.3. Glycerolipid synthesis pathways and their subcellular localization in yeast.
Lipids and intermediates are boxed, enzymes are not. The abbreviations used are: TAG, triacylglycerols; PI, phosphatidylinositol; PA, phosphatidic acid; CDP-DAG, CDP-diacylglycerol; DAG, diacylglycerol; PS, phosphatidylserine; PE, phosphatidylethanolamine; CL, cardiolipin; PC, phosphatidylcholine; Acyl-CoA, Acyl-Co Enzyme A; For details see main text. Modified after Henry, Kohlwein et al. (2012).

1.5.1. Membrane lipid synthesis

The metabolic pathways for membrane and neutral lipid synthesis in the cell are intimately linked (Fig. 1.3). In *de novo* pathways all membrane phospholipids and also neutral lipids are derived from the metabolic hub PA which is formed via two fatty acid CoA-dependent reactions catalyzed in the ER membrane. Here, PA is partitioned between CDP-DAG and diacylglycerol (DAG). The generation of DAG is catalyzed by the PA phosphatase Pah1, a cytosolic enzyme which is recruited to ER membranes (Han, Wu et al. 2006). CDP-DAG and DAG are used by two alternative routes, the CDP-DAG pathway and the Kennedy pathway, to synthesize PE and PC.

In the CDP-DAG pathway, CDP-DAG is converted to PS and further modified to PE and PC. All the enzymatic activities can be found in the ER except for the two PS decarboxylases which catalyze the reaction from PS to PE. These enzymes can be found either in the mitochondria or the Golgi and the vacuole (Henry, Kohlwein et al. 2012). In mammals, PS is synthesized from PC and PE, whereas PC can also be synthesized directly from PE (for a review of mammalian phospholipid metabolism see Fagone and Jackowski (2009), Holthuis and Menon (2014)). In yeast, the CDP-DAG pathway is the major route for PE and PC synthesis whereas mammals preferentially use the Kennedy pathway.

In the Kennedy pathway PC and PE are synthesized from exogenously supplied choline or ethanolamine which enters the cell via a specific transporter. Choline and ethanolamine are activated and finally react with DAG to form PE and PC. Also the mitochondrial lipids, specifically CL, are synthesized in various enzymatic reactions from CDP-DAG. Finally, CDP-DAG donates its phosphatidyl moiety to inositol to form PI. Inositol can be synthesized *de novo* in the cell or imported trough transporters from the medium. Subsequently, PI can be phosphorylated and gives rise to a variety of signaling molecules (Henry, Kohlwein et al. 2012).

PA it is the common precursor for the synthesis of both, membrane phospholipids and neutral storage lipids, as mentioned earlier. The availability of PA in the membrane is coupled with a transcriptional regulation of its synthesizing enzymes (Carman and Henry 2007). PA metabolizing enzymes, such as the PA phosphatase Pah1 which synthesizes DAG has a prominent role as it diverts the precursor flux either to membrane synthesis or lipid storage according to the cell's needs (Fig. 1.3) (Han, Wu et al. 2006). Pah1 is posttranslationally modified and kept soluble by phosphorylation (Choi, Su et al. 2012). Only upon dephosphorylation it is recruited to the ER membrane by the ER resident Nem1/Spo7 complex and gets activated (Santos-Rosa, Leung et al. 2005). Interestingly, activated Pah1 is unstable and degraded rapidly, therefore allowing for a tightly controlled system between membrane synthesis and lipid storage (Pascual, Hsieh et al. 2014).

1.5.2. Triacylglycerol synthesis

As mentioned before, DAG is synthesized by Pah1 from PA. If DAG is not needed for membrane lipid synthesis by the Kennedy pathway, DAG is acylated to triacylglycerol (TAG) (Fig. 1.3). TAG is an inert, non-polar lipid that cannot be accommodated in membranes easily and therefore it is stored in specific neutral lipid storage compartments termed lipid droplets. TAG synthesis occurs at the ER and lipid droplets, and is catalyzed by two enzymes in yeast, Dga1 and Lro1, which use different sources of fatty acids.

Dga1 is an acyl-CoA-dependent diacylglycerol acyltransferase, whereas the Lro1 acylation reaction depends on phospholipids which are converted to Lyso-PLs (Oelkers, Tinkelenberg et al. 2000, Sorger and Daum 2002). Lro1 localization is restricted to the ER, whereas Dga1 moves into the lipid droplet where it can synthesize TAG locally (Oelkers, Cromley et al. 2002, Sorger and Daum 2002, Jacquier, Choudhary et al. 2011).

The contributions of both acyltransferases to the overall TAG pool depend on the growth phase of the cells. During logarithmic phase Lro1 accounts for around 75% of the synthesized TAG, and Dga1 about 25%, respectively. When yeast cells pass through the diauxic shift into stationary growth phase, their metabolism is altered in response to changes in nutrient environment. This alteration includes much increased levels of TAG synthesis. In stationary phase, virtually all TAG synthesis can be attributed to Dga1 and Lro1 only plays a minor role (Oelkers, Cromley et al. 2002).

Also the two sterol acyltransferases Are1 and Are2 catalyze acyl-CoA dependent TAG formation, but contribute only in very minor amounts to the TAG pool (≤ 3 %) (Oelkers, Cromley et al. 2002).

The increase of TAG synthesis in stationary growth phase is due to a change in metabolism from active growth, where lipid precursors are channeled into the CDP-DAG pathway to make membrane lipids, to a quiescence stage where an excess of fatty acids is stored as inert TAG to avoid lipotoxicity.

Remarkably, neutral lipid storage seems not to be an essential process under laboratory growth conditions (Sandager, Gustavsson et al. 2002). Yeast cells lacking *DGA1* and *LRO1* still form lipid droplets comprised exclusively of sterol esters. The other way around, cells lacking *ARE1* and *ARE2* form lipid droplets comprised exclusively of TAG. Only deletion of all four genes *DGA1 LRO1 ARE1 ARE2* leads to lipid droplet-free yeast cells. These quadrupole mutant cells, are viable but display higher sensitivity to a number of stresses including lipotoxic stress due to the missing buffer capacity (Sandager, Gustavsson et al. 2002).

Further evidence for the protective connection between phospholipid and neutral lipid metabolism was provided in a study by Gaspar, Jesch et al. (2008) where Dga1 and Lro1 were required for growth at semi-permissive temperature of a *sec13*^{ts} mutants defective in COPII vesicle budding from the ER. Upon blockage of the secretory pathway, the cell channels PA and DAG membrane lipid precursors into TAG which provides a degree of protection from secretory stress.

TAG degradation provides substrates for phospholipid synthesis upon exit from quiescence and is required for an efficient cell cycle. Degradation is catalyzed by the LD localized lipases Tgl1, Tgl3, Tgl4, and Tgl5 among which Tgl3 and Tgl4 are responsible for the bulk amount (Fig. 1.3). A *tgl3Δ tgl4Δ* double mutant exhibits a delay in re-entering growth when diluted into fresh media (Kurat, Wolinski et al. 2009, Henry, Kohlwein et al. 2012). TAG hydrolysis also depends on the DAG kinase Dgk1 which antagonizes Pah1 activity. *dgk1Δ* cells fail to resume growth if *de novo* FA synthesis is impaired and fail to mobilize TAG upon exit from stationary phase (Fakas, Konstantinou et al. 2011).

1.5.3. Sterol synthesis

Sterols exist in free and esterified form. Free sterols are amphiphilic molecules and are incorporated into membranes, whereas sterol esters are hydrophobic and are stored, just like TAG, in lipid droplets. Excess and lack of free sterols is detrimental for the cell, and therefore sterol biogenesis and homeostasis are tightly controlled in the cell (Espenshade and Hughes 2007, Klug and Daum 2014).

The main sterol of yeast is ergosterol which differs from mammalian cholesterol by two double bonds and a methyl group. Ergosterol synthesis is very complex and involves almost 30 enzymes known as Erg proteins (Klug and Daum 2014). Most activities of later steps (post-squalene) of sterol synthesis are localized exclusively to the ER except for Erg1, Erg7, Erg27, and Erg6 that are also found at lipid droplets. Interestingly, the products of Erg7, Erg27, and Erg6, lanosterol, zymosterol, and fecosterol, respectively, are detectable in the lipid droplet core. Therefore, it seems to be necessary to move sterol precursors repeatedly between ER and LD to synthesize ergosterol (Natter, Leitner et al. 2005).

Sterol esterification form a part of the regulation, detoxification, and storage process of free sterols. In yeast, sterols are esterified by the ER localized acyl-CoA-dependent ergosterol acyltransferases Are1 and Are2 (ACAT related enzymes) (Yang, Bard et al. 1996, Yu, Kennedy et al. 1996). Both enzymes transfer a fatty acid to the hydroxyl group of the sterol. Sterol esterification is completely abolished when both enzymes are deleted, however this does not affect the growth phenotype (Yu, Kennedy et al. 1996, Oelkers, Cromley et al. 2002).

Upon lipid droplet breakdown, SE are hydrolyzed by the SE hydrolases Tgl1, Yeh1, and Yeh2 (Koffel, Tiwari et al. 2005). Whereas Tgl1 and Yeh1 are localized to the lipid droplet, Yeh2 can be found at the plasma membrane. Tgl1 has a dual activity and can also degrade TAG (Jandrositz, Petschnigg et al. 2005, Kohlwein, Veenhuis et al. 2013).

1.6. Neutral lipid storage in lipid droplets

Lipid droplets (LDs) can be found in all eukaryotes including plants and some bacteria and serve as specialized neutral lipid storage compartments in the cell. During many years, LDs were perceived as inert fat storage depots. However, recently they have been recognized as dynamic and metabolically active organelles involved in lipid homeostasis (Pol, Gross et al. 2014).

Apart from neutral lipid storage, which protects the cell from lipid toxicity and provides an energy deposit for times of nutrient shortage, LDs are also involved in a variety of other cellular processes. In *Drosophila*, lipid droplets serve as protein storage depots during embryo development (Cermelli, Guo et al. 2006). In the syncytium of the developing drosophila embryo Li, Johnson et al. (2014) found histones associated to LDs. LDs served as histone storage depots until the histones were needed during rapid nuclear divisions that lead to embryo segmentation. A study published by Moldavski, Amen et al. (2015) found misfolded proteins temporally associated to LDs before being targeted to proteasome degradation. LDs are also involved in viral replication and serve hepatitis C virus as a platform for virion assembly (Herker and Ott 2011).

Deregulation of LD homeostasis also has severe implications in health and disease. Excessive accumulation of LDs occurs in fat related disease, such as obesity and atherosclerosis whereas a lack of LDs is characteristic for lipid storage diseases such as lipodystrophy (Krahmer, Farese et al. 2013).

1.6.1. Lipid droplet structure

The LD is composed of a neutral lipid core enclosed by a phospholipid monolayer decorated by LD-specific proteins (Fig. 1.4). The lipid droplet monolayer is a very unique feature, since organelles in eukaryotic cells are usually enclosed by phospholipid bilayers. The most abundant neutral lipids in the LD core are triacylglycerol (TAG) and sterol esters (SEs). However, also other hydrophobic lipids can be present depending on the cell type and their growth conditions such as retinyl esters in hepatocytes, wax and ether lipids in adipocytes and squalene in yeast (Bartz, Li et al. 2007, Blaner, O'Byrne et al. 2009, Spanova, Zweytick et al. 2012).

Not only composition, but also LD size and number vary greatly among cell types. Whereas white adipocytes have one giant lipid droplet (≥ 100 µm in diameter) that occupies its entire cytoplasm, yeast LDs are much smaller with diameters around 0.4 µm in wild-type cells. LD size varies not only between cell types but also in the same cell. Under conditions of lipid overload the cell can respond in increasing the number of LDs or their volume, or both. Larger LDs have a lower surface-to-volume ratio and are energetically more favorable. However, for the cell a lower surface-to-volume ratio might be crucial to be able to initiate breakdown quickly in times of need. Therefore, the cell regulates not only LD size tightly, but also LD number. However, most mechsnisms underlying this regulation are largely unknown. (Yang, Galea et al. 2012).

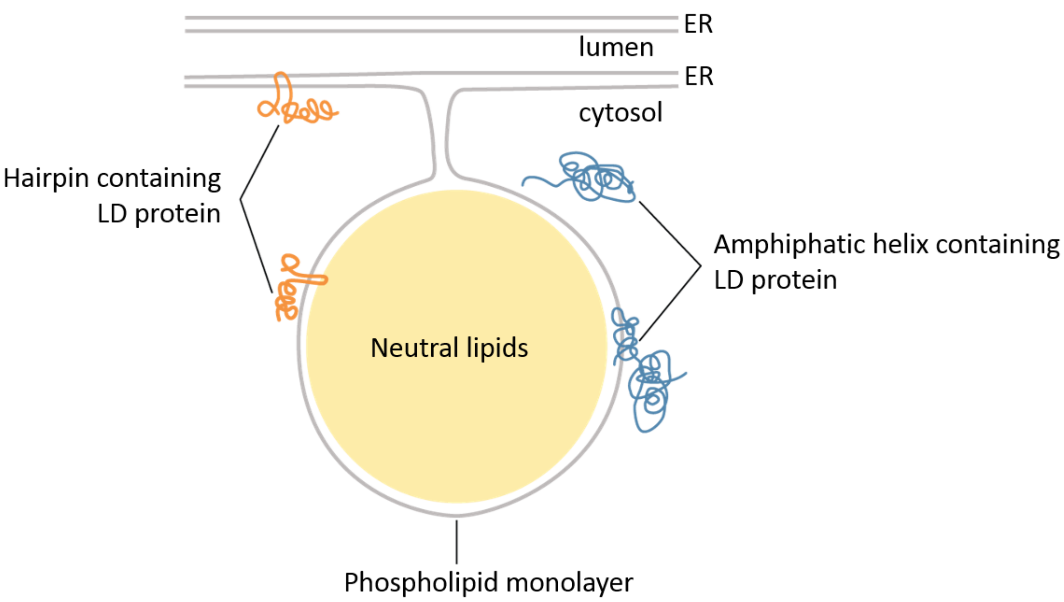

Figure 1.4. Lipid droplet structure.
The cytosolic lipid droplet (LD) is comprised of a neutral lipid core containing mainly TAG and SEs enwrapped by a phospholipid monolayer. LD proteins can be targeted either through an amphipathic helix from the cytosol (blue) or are inserted into the ER and subsequently targeted to the LD via a hairpin motif (red). LDs are formed at the ER membrane and, at least in yeast, stay permanently attached to it.

1.6.2. Lipid droplet biogenesis

1.6.2.1. A biophysical framework

As discussed earlier, neutral lipids are synthesized by ER resident enzymes. Therefore, *de novo* formation of LDs occurs at the ER. The exact mechanism of LD biogenesis is still under debate, but the most widely accepted model involves lipid lens formation between the ER bilayer and subsequent budding into the cytosol (Wilfling, Haas et al. 2014).

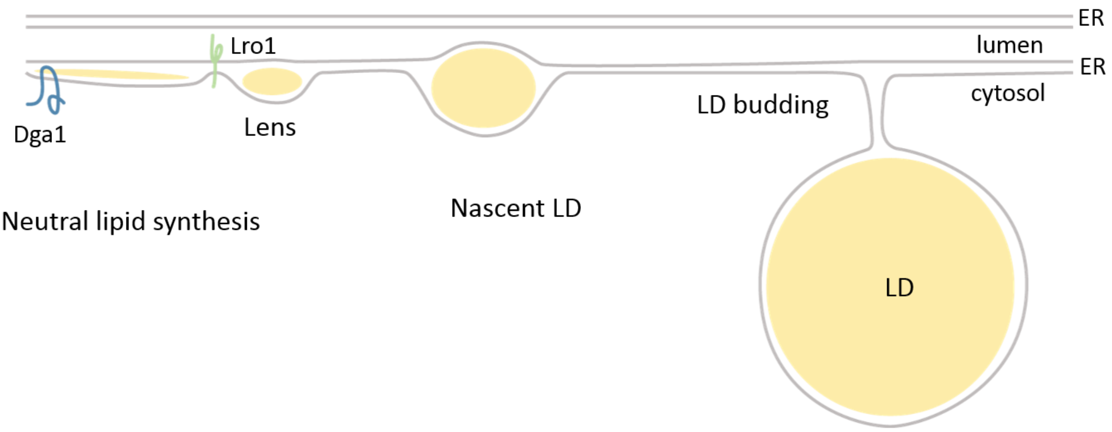

Figure 1.5. The lensing model of lipid droplet biogenesis.
TAG is synthesized at the ER by Dga1 and Lro1. It accumulates between the ER leaflets and forms a lens. Small unstable TAG lenses diffuse freely through the membrane and eventually coalesce into nascent LDs. Reached a certain size, LDs bud out from the ER membrane towards the cytosol carrying with them the cytosolic ER leaflet. In yeast, LDs remain permanently attached to the ER trough membrane bridges.

Although experimental evidence is scares, a widely accepted model states that single fat molecules are encapsulated between the leaflets of the ER bilayer, upon neutral lipid synthesis. These molecules diffuse freely in the membrane, accumulate and form an oil lens. The oil lens can form by a spontaneous de-mixing event that reduces the interactions between the neutral and the phospholipids. Lipid lenses are unstable in the membrane and subsequently coalesce and nucleate nascent lipid droplets. A recent highly debated study by Choudhary, Ojha et al. (2015) gives first visual evidence of nascent LDs by electron microscopy. Nevertheless, what determines the sites of nucleation is unclear.

It has been suggested that special membrane properties, such as high curvature, high local neutral lipid synthesis rates or presence of specific proteins, such as Perilipins, fat storage inducing transmembrane proteins (FIT) or Seipin, could favor LD nucleation. It is also possible that the de-mixing event itself changes the bilayer properties, such as curvature or packing, and therefore favors LD nucleation itself (Thiam and Foret 2016). Once the LD reaches a critical size, either through accumulation of freely diffusing neutral lipids in the membrane or local synthesis, it is predicted to become unstable in the bilayer again. Therefore it buds, mostly into the cytosol, in a mechanism similar to de-wetting (Fig. 1.6).

De-wetting describes the rupture of a thin film on a substrate to form a droplet, as known by water on a hydrophobic surface. In the case of LD budding towards the cytosol, the oil phase de-wets from the ER phospholipid monolayer. This process depends on the surface tension of the interfaces, meaning the surface energy cost for generating an interface between phospholipids and neutral lipids, and the surface tension itself depend on the phospholipid composition of the membrane. In other words, the shape of a forming LD (and the completeness of budding) can be described by the contact angle α which is determined by surface tension. Small values of α, for example close to 0°, correspond to budding. The contact angle determines if a droplet remains in contact with the ER membrane, as it seems to be the case in yeast (Jacquier, Choudhary et al. 2011). Proteins implicated in LD budding could influence α or modulate membrane surface tension and therefore favor budding (Thiam, Farese et al. 2013, Thiam and Foret 2016).

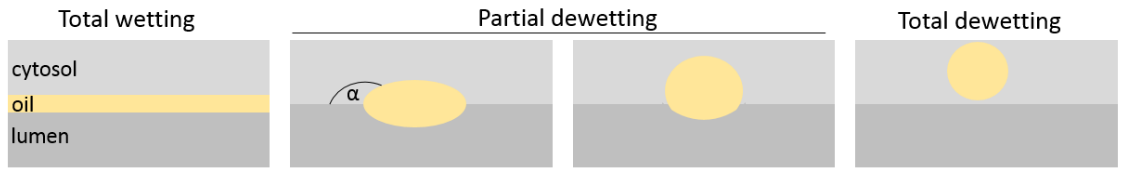

Figure 1.6. Biophysics of a three fluid phase wetting situation.
The shape of the yellow liquid in between two fluids is determined by the tensions of the interfaces between the different phases. Depending on the values of each surface tension total wetting, partial de-wetting and total de-wetting can happen. In case of partial de-wetting, the shape is determined by the angle α determined of the value of the two surface tensions. A nascent LD can be considered an oil phase between the cytosol and the ER lumen. Adapted after Thiam and Foret (2016).

LDs are usually found in the cytosol of the cell. Directional LD budding by de-wetting could originate from different membrane tensions in the ER monolayers. If the tension in the cytosolic leaflet is lower than the one of the luminal one, de-wetting from the luminal leaflet is favored and the LD buds into the cytosol. The asymmetry in the leaflets could be introduced by enzymes which favor local PL synthesis or structural or cytosolic proteins that induce positive curvature in the outer ER leaflet (Thiam, Farese et al. 2013, Thiam and Foret 2016).

1.6.2.2. Proteins regulating lipid droplet biogenesis

There are several protein classes suggested to regulate the various steps of LD biogenesis. The mammalian genome encodes five perilipin (Plin) genes and additional mRNA splice variants. These proteins are expressed tissue specific and differ in their sub-cellular pattern. Plin proteins are recruited from the cytosol to LDs and are involved in shielding the neutral lipid core from lipases and/or promoting LD formation (Sztalryd and Kimmel 2014). In plants, Oleosins were suggested to have similar functions. Oleosins are small integral proteins with a hairpin motif for LD targeting and are abundant on oil bodies, especially in seeds (Hsieh and Huang 2004). Interestingly, Plin proteins and oleosins are absent in lower eukaryotes, in particular yeast. Two recent studies from the Schneiter lab expressed Oleosin1, Plin1-3, and Plin5 in *S. cerevisiae*. All proteins were properly targeted to LDs. When expressed in cells without LD (quadruple mutant; *dga1Δ* *lro1Δ are1Δ are2Δ*) the proteins were either cytosolic or targeted to the ER. However, if in the same background intramembranous TAG levels in the ER were elevated by genetic manipulation or if extracellular diacylglycerol was administrated, these proteins were able to sequester neutral lipids in the ER bilayer and promote LD formation (Jacquier, Mishra et al. 2013, Mishra and Schneiter 2015). Therefore, it is very likely that these proteins assist LD budding in the mammalian system. In yeast however, other mechanisms have to exist.

A second protein class was recently found to be involved in LD budding (Choudhary, Ojha et al. 2015). Fat storage inducing transmembrane (FIT) proteins are conserved transmembrane proteins localized to the ER. Humans have two FIT proteins, FIT1 and FIT2, whereas yeast has no homolog of FIT 1 but two of FIT2 called Scs3 and Yft2. FIT proteins bind TAG and overexpression leads to LD accumulation, thus FIT proteins were initially thought to play a role in early steps of LD biogenesis by concentrating TAG between the ER leaflets (Kadereit, Kumar et al. 2008, Moir, Gross et al. 2012, Goh and Silver 2013). However, a recent study in yeast by Choudhary, Ojha et al. (2015) finds early steps of LD biogenesis undisturbed in a *SCS3 YFT2* deletion strain, but vectorial budding towards the cytosol is altered. LDs are formed, but bud towards the luminal side of the ER. At the same time they stay connected with the cytosolic leaflet of the ER since TAG breakdown by cytosolic lipases is not altered in these cells.

Another protein essential for normal LD biogenesis and assembly is Seipin, which function will be discussed in detail below.

1.6.3. Lipid droplet growth and shrinkage

1.6.3.1. Lipid droplet growth through fusion and ripening

LDs in the cytoplasm provide a biological example of an oil-in-water emulsion. The phospholipid monolayer acts as surfactant stabilizing the LD. LDs are formed at the ER and ER and LD membrane composition are quite similar. The major phospholipid in the LD monolayer in yeast and mammals is PC (50-60%), followed by PE (20-30%) and PI (Tauchi-Sato, Ozeki et al. 2002). Due to its cylindrical shape PC provides excellent coverage of the LD surface area, lowers surface tension and stabilizes the LD (Thiam, Farese et al. 2013).

LD stability in the cell depends on the surface properties of its monolayer. Surface properties are influenced by two processes: Coalescence and ripening.

Coalescence or fusion of two LDs depends on their surface tension and phospholipid composition. It can only occur if the surface tension is high and the phospholipids of both LDs stabilizes a pore that is formed between the LDs upon close apposition. If the pore is stabilized, LDs fuse and form a new larger LD (Thiam, Farese et al. 2013, Thiam and Foret 2016). *In vivo*, LD fusion is thought to happen rarely, except under certain conditions, such as PC deficiency (Guo, Walther et al. 2008, Krahmer, Guo et al. 2011).

Ripening describes a process where smaller droplets disappear and bigger droplets grow at the same time. The direction of the transfer is determined by the difference in Laplace pressures in the droplets, which is the pressure difference between the inside and the outside of a curved liquid surface. The Laplace pressure in a small LD is higher than in a large LD and the mismatch drives the ripening process. It was suggested that the protein FSP27 forms channels between droplets and is involved in ripening processes by allowing for the transfer of lipid molecules from the smaller to the larger droplet (Gong, Sun et al. 2011). Ripening seems to be a process especially important in adipocytes, however it is not clear if it occurs in other systems. Comparing timescales, the ripening transfer process takes several minutes, whereas coalescence is extremely fast (Thiam, Farese et al. 2013, Thiam and Foret 2016).

1.6.3.2. Lipid droplet growth and shrinkage through neutral lipid synthesis and degradation

More direct ways of mediating growth or shrinkage of LDs are either local TAG synthesis by Dga1 on the droplet or neutral lipid degradation by LD localized lipases (Jacquier, Choudhary et al. 2011, Klein, Klug et al. 2016). The acyl transferase Dga1 was found to relocalize to LDs and facilitate local TAG synthesis (Jacquier, Choudhary et al. 2011). Local growth of LDs requires a coordinated growth of the sourrounding phospholipid monolayer. It was found in Drosophila, that the CTP:phosphocholine cytidyltransferase α isoform (CCTα), a PC synthesizing enzyme, can sense the lack of PC on expanding LDs, bind to its surface and locally synthesize PC to meet the demand of an expanding neutral lipid core (Krahmer, Guo et al. 2011).

In lipolysis lipids are hydrolyzed to liberate fatty acids to generate energy or membrane lipids. In adipocytes, TAG is hydrolyzed sequentially by adipose triglyceride lipase (ATGL), hormone sensitive lipase (HSL) and monoacylglycerol lipase. Lipolysis is triggered by a hormonal signal that activates protein kinase A (PKA). PKA phosphorylates perilipin 1, a very abundant LD protein that shields LDs and protects them from lipolysis. Upon phosphorylation, perilipin 1 releases the ATGL lipase activator CGI-58 which binds to ATGL and targets the lipase to the LD. PKA also phosphorylates HSL which is also recruited trough perilipin 1 to LDs. There is no evidence that monoacylglycerol lipase is recruited to LDs or dependent on a hormonal signal (Walther and Farese 2012).

Lipolysis in non-adipose tissue is not as well understood. In yeast, TAG is hydrolyzed by TAG lipases Tgl1, Tgl3, Tgl4, and Tgl5 and SE by the SE lipases Tgl1, Yeh1, and Yeh2, as mentioned earlier. Lipolysis in yeast is most active during growth resumption after stationary phase when cells are transferred into fresh glucose-containing media. Tgl3 and Tgl4 both reside on the LD and are responsible for the bulk amount of TAG hydrolysis (Henry, Kohlwein et al. 2012, Kohlwein, Veenhuis et al. 2013). Interestingly, Tgl4 phosphorylated by the cyclin dependent kinase Cdk1/Cdc28 at the G1/S transition of the cell cycle (Kurat, Wolinski et al. 2009). This suggests, that lipolysis-derived metabolites might be important to drive cell cycle progression. Regulation of mechanisms of SE breakdown are nor understood, which is surprising since about 50% of the LD is made up of SEs (Kohlwein, Veenhuis et al. 2013).

1.6.4. Lipid droplet protein targeting

Phospholipid composition of the LD monolayer can influence size and behavior of LD. However, also LD monolayer associated proteins play an important role in LD homeostasis. Proteomics and cell biology have revealed many LD associated proteins, but methodological issues complicated the interpretation of some of these studies. Recently, a study by Krahmer, Hilger et al. (2013) identified 111 LD proteins in *D. melanogaster* by mass spectrometry and protein correlation profiles. Another study by

Currie, Guo et al. (2014) published 30 high confidence LD proteins in *S. cerevisiae*, most of them involved in lipid metabolism. Grillitsch, Connerth et al. (2011) showed that the LD proteome in yeast is very dynamic and strongly depends on the carbon source cells were grown on. They suggest that this could be due to changes in the LD phospholipid monolayer.

As mentioned before, the LD is enclosed by a phospholipid monolayer. All other organelles in the cell feature bilayers. Therefore, most integral membrane proteins are accommodated in bilayers. The LD phospholipid monolayer thus imposes special requirements on proteins targeted to the LD. Proteins containing multi-spanning transmembrane domains and loop domains are excluded from LDs because hydrophilic segments would be placed in the oil phase which is energetically unfavorable. Instead, LD proteins must interact with the PL monolayer or be embedded in the hydrophobic core. General targeting mechanism or signals for LD proteins are unknown, however two properties are emerging: amphipathic α-helices and hydrophobic hairpins (Fig. 1.4) (Thiam, Farese et al. 2013, Kory, Farese et al. 2016).

1.6.4.1. Lipid droplet protein targeting by amphipathic helices

Protein containing amphipathic α-helices are targeted directly to LD surface from the cytosol. Membrane binding mediated by amphipathic helices is not exclusive to LD but has been characterized for proteins binding to lipid bilayers and targeting is well-studied. In this model, amphipathic helices are unfolded in solution but fold into a helix upon membrane binding. The hydrophobic surface of the helix is then embedded into the membrane, in the case of LDs into the hydrophobic core, and the hydrophilic residues face the aqueous environment. Electrostatic interactions of surrounding residues with the membrane surface may also play a role (Terzi, Holzemann et al. 1997, Hristova, Wimley et al. 1999). The amphipathic lipid packaging defect sensor (ALPS) motif, an amphipathic helix type found for example in Kes1, is known to binds preferentially highly curved bilayers with membrane packaging defects in which the helix can be accommodated (Drin, Casella et al. 2007). What causes some amphipathic helix proteins to target lipid bilayers and others LDs, is not understood. However, while lipid bilayers are a relative fluid and continuous surface, LDs monolayers can have much higher surface tension exposing the hydrophobic core and possible packaging defects (Kory, Farese et al. 2016).

This model is supported by the finding that in *Drosophila* the CTP:phosphocholine cytidyltransferase α isoform (CCTα) is recruited to PC poor lipid droplets who are likely to have higher surface tension. CCTα gets activated on the LD surface and synthesizes PC to counterbalance the deficit (Krahmer, Guo et al. 2011). Another prominent example of proteins recruited from the cytosol to the LD are perilipins, a class of highly abundant LD proteins mediating lipid droplet breakdown in mammalians. Perilipins are targeted to LDs via a combination of amphipathic and hydrophobic sequences (Bickel, Tansey et al. 2009).

1.6.4.2. Lipid droplet protein targeting by hydrophobic hairpins

In contrast to proteins targeting the LD from the cytosol, a number of LD proteins first insert into the ER and subsequently move to the LD. These proteins show a dual localization and can be found in the ER in the absence of LDs. They are embedded in the ER double- as well as LD monolayer via a hydrophobic hairpin. The hairpin motif consists of two α-helices forming a V (Kory, Farese et al. 2016). The kink is often achieved by one or more proline residues in the midpoint of the two helices as it was shown for plant Oleosines (Abell, Holbrook et al. 1997, Abell, High et al. 2002). In yeast, one prominent example for this protein class is the diacylglycerol acyltransferase Dga1. Interestingly, Jacquier, Choudhary et al. (2011) showed that Dga1 moves freely between ER and LD independent of energy. This suggests that, at least in yeast, ER and LD stay connected via membrane bridges. Interestingly, FRAP experiments showed, that these proteins prefer the LD over the ER localization (Jacquier, Choudhary et al. 2011, Ruggiano, Mora et al. 2016). However, it remains unclear what drives enrichment of these proteins on LDs over the ER.

In mammals, it was shown by Wilfling, Thiam et al. (2014) that LD targeting of GPAT4, an enzyme involved in TAG synthesis, also occurs through ER-LD bridges. Their study showed that the mechanism of GPAT4 targeting depends on Arf1/COP1 activity. Arf1 guanine-nucleotide exchange factor (Arf1GEF) binds to LDs and locally activates Arf1.

Arf1 then buds nano-droplets off the LD reducing its phospholipid content and increasing the surface tension. The increased surface tension enables the LD to transiently reattach to the ER via membrane bridges which allows for GPAT4 targeting. Arf1/COP1 is also required for LD targeting of other proteins (Beller, Sztalryd et al. 2008, Soni, Mardones et al. 2009).

1.6.5. Lipid droplet deregulation and disease

Accurate lipid storage is of vital importance for the cell, since over- and understorage interfere with normal cell function. Many metabolic diseases are characterized by lipid storage deregulation. In obesity for example adipose tissue exceeds its maximum lipid storage capacity and leads to lipid deposition in non-adipose tissues which causes lipotoxicity or tissue dysfunction. Obesity is often accompanied by a range of symptoms, such as diabetes and hepatic steatosis which are directly linked to LD storage capacities in macrophages and hepatocytes (Walther and Farese 2012). On the contrary, absence of white adipose tissue, or lipodystrophy, is caused by LD storage deficiency. Genetic causes for lipodystrophy include mutations in the human genes BCSL1-4.

1.6.5.1. Lipodystrophy and seipinopathies

Lipodystrophy in humans is characterized by the loss of adipose tissue and accumulation of ectopic fat in non-adipose tissues, especially in the liver. There are two forms of lipodystrophy: acquired and inherited. Here, I will introduce the latter one. Inherited lipodystrophies arise from mutations in specific genes. Berardinelli-Seip congenital lipodystrophy (BSCL) type 1-4, is a rare autosomal recessive disorder discovered by Berardinelli and Seip in 1954 and 1959, respectively.

Each BSCL is characterized by mutation in either 1-Acylglycerol-3-Phosphate O-Acyltransferase 2 (AGPAT2 or BSCL1), Seipin (BSCL2), Calveolin 1 (CAV1 or BSCL3), or Polymerase I and Transcript Release Factor/Cavin (PTRF or BSCL4). In the following I will characterize the phenotype caused by mutations in Seipin (BSCL2) (Wee, Yang et al. 2014).

Berardinelli-Seip congenital lipodystrophy (BSCL) type 2 caused by loss-of-function mutations in Seipin exhibit the most severe phenotype of the four lipodystrophy phenotypes. It is characterized by a loss of metabolic and mechanic white adipose tissue which usually serves protective and supportive functions in the body, e. g. in joints, palms and soles. It was first mapped to the gene in 2001 (Magre, Delepine et al. 2001). Interestingly, in the same year it was discovered that gain-of-function mutations in the same gene do not lead to lipodystrophy but to motor neurophaties collectively named seipinophaties (Patel, Hart et al. 2001, Windpassinger, Wagner et al. 2003, Windpassinger, Auer-Grumbach et al. 2004). Notably, most Seipin mutations are nonsense and lead to truncations, whereas only few are missense (Wee, Yang et al. 2014).

1.6.5.2. Seipin structure and function

The Seipin gene was originally discovered in mammals and flies and later described in worms, yeast and plants (Magre, Delepine et al. 2001, Szymanski, Binns et al. 2007, Fei, Shui et al. 2008). Seipin is an ER integral membrane protein with a luminal loop and both termini facing the cytosol. All species share the conserved core region of Seipin including two transmembrane helices and the loop. The N- and C- termini vary considerably between species. In humans, there are three Seipin splicing isoforms with no difference in function reported. Most mutations leading to lipodystrophy truncate the C-terminal domain, however, there are also some point mutations in the conserved loop (Cartwright and Goodman 2012, Wee, Yang et al. 2014). It was shown that Seipin homo-oligomerizes to a complex of about nine subunits (Binns, Lee et al. 2010) and several interactions with other proteins have been reported.

Two studies from the same group report a Seipin interaction with the PA phosphatase lipin and the 1-acylglycerol-3-phosphate O-acyltransferase 2 (APGAT2) in human cell lines. They suggest that the interaction recruits lipin to the membrane and modulates PA pools (Sim, Dennis et al. 2012, Talukder, Sim et al. 2015). Another study finds Seipin in complex with 13-3-3β that mediates the interaction with cofilin-1 in adipocytes and is involved in actin skeleton remodeling during adipocyte differentiation (Yang, Thein et al. 2014). Lastly, a study by Bi, Wang et al. (2014) in Driophila and human cell lines links Seipin to Ca^{2+} homeostasis by a direct interaction with the sarco/endoplasmic reticulum Ca^{2+}-ATPase (SERCA). However, it is unclear how relevant for LD regulation any of these interactions are.

In multicellular organisms Seipin is implicated in two processes related to lipid metabolism: adipogenesis and lipid storage. Adipogenesis is the differentiation process of a pre-adipocyte to a mature adipocyte that stores large amounts of TAG. If Seipin is deleted in mouse embryogenic fibroblasts (MEF cells) they initiate adipogenesis and LD formation but are not able to finish the developmental program and fully mature into functional adipocytes (Chen, Chang et al. 2012). In this process, the C-terminus of Seipin was shown to interact with various factors to remodel the actin cytoskeleton of the cell during adipocyte development (Yang, Thein et al. 2014). This explains why C-terminal truncations, but not point mutations in the loop, lead to lipodystrophy. Unlike adipogenesis, lipid storage and lipid droplet formation can happen in many cell types. Seipin knockout in non-adipocytes leads to increased TAG amounts and aberrant LDs in yeast, pre-adipocytes and mice (Wolinski, Kolb et al. 2011, Chen, Chang et al. 2012, Prieur, Dollet et al. 2013). However, it is unclear, if Seipin function in adipogenesis and LD storage are mechanistically linked.

1.6.5.3. Few lipid droplets 1 (Fld1), the yeast homolog of human Seipin

Yeast harbors the smallest Seipin orthologue of all species. It displays only 20% sequence homology with its human homolog and consists almost exclusively of the conserved core domain lacking both extended cytosolic termini (Yang, Thein et al. 2013). Fld1, just as human Seipin, is an ER integral membrane protein and localizes to ER-LD contact sites (Szymanski, Binns et al. 2007, Grippa, Buxo et al. 2015).

Fld1, the homolog of human Seipin in yeast, was first identified by two independent genome wide screens by Szymanski, Binns et al. (2007) and Fei, Shui et al. (2008) searching for genes causing aberrant LD phenotypes. The latter one identified 17 few lipid droplet (Fld) phenotypes of which Fld1 was identified as the yeast homolog of human Seipin. They reported two distinct LD phenotypes in these cells: Some cells had very large and few LD, whereas others contained an amorphous aggregation of very small LDs. A third screen by Fei, Shui et al. (2011) searching for mutants producing giant "supersized" lipid droplets (SLDs) also identified FLD1. Most of the genes identified in the latter screen could be placed in phospholipid pathways, especially PC synthesis, and the observed LD phenotype was due to phospholipid imbalances which lead to coalescence of smaller LD into SLDs (Szymanski, Binns et al. 2007). The SLD phenotype was rescued in all mutants, except fld1Δ, by the addition of the PC precursor choline. This suggested that FLD1 could not be placed in a phospholipid synthesis pathway.

Most yeast cells have about 5 to 7 LDs with a diameter of 0.3 to 0.5 µM. *fld1Δ* cells grown in rich medium either show few LDs larger than 1 µm (SLDs) or small aggregated LDs as described by Fei, Shui et al. (2008). When grown in minimal medium, the number of cells with SLDs increases significantly. These cells also showed slightly increased TAG levels due to impaired lipolysis, most likely caused by a significantly lower droplet surface area accessible to lipases (Fei, Shui et al. 2011). Fei, Shui et al. (2011) reported *fld1Δ* cells to display slightly elevated PA levels, however other studies were unable to reproduce this. Addition of inositol to the growth media reduces the cellular PA pool due to increased PI synthesis and indeed, transforms the SLDs in very small and aggregated LD clusters (Szymanski, Binns et al. 2007, Fei, Shui et al. 2011).

Interestingly, in yeast Fld1 exerts its function with a binding partner, low dye-binding protein 16 (Ldb16). Deletion of both genes *FLD1* and *LDB16* at once is rescued by expression of human Seipin indicating that the function of Ldb16 and Fld1 in concert converges on human Seipin. On the same line, deletion of *FLD1* or *LDB16* individually or simultaneously leads to very similar aberrant LD phenotypes: small and clustered or supersized. The prevalence of the cells to form one or the other can be modulated by the addition of phospholipid precursors in the media. If mutant cells are grown in minimal media SLDs are formed. However if inositol, but not choline or ethanolamine are added, LD appear small and aggregates. This suggests an alteration in PL synthesis in *fld1Δ* and *ldb16Δ* cells. However, analysis of neutral and phospholipids in mutant cells showed only subtle differences to wild-type. Curiously, *fld1Δ* and *ldb16Δ* cells are more sensitive to terbinafine, an inhibitor of the sterol synthesis pathway (Wang, Miao et al. 2014).

Wang, Miao et al. (2014) and experiments from our group showed that Fld1 and Ldb16 form a stable complex at the ER-LD contact site. Fld1-Ldb16 interaction was confirmed in immunoprecipitation experiments and also in fluorescence microscopy about 50% of fluorescently tagged Fld1 and Ldb16 co-localized. About 87% of the puncta containing both proteins localized to the ER-LD interface. Ldb16 has two putative transmembrane helices flanked by an N- and C-terminus facing the cytoplasm. The interaction between Fld1 and Ldb16 mapped to the transmembrane domains of both proteins. Ldb16 is unstable in the absence of Fld1, whereas Fld1 self-interaction was diminished in *ldb16Δ* mutants, suggesting that Ldb16 contributes to Fld1 assembly. Sedimentation gradient experiments further suggested a higher order assembly of Fld1-Ldb16 complexes.

Apart from LD morphology, *FLD1* deletion also influences the dynamics of LD biogenesis and vectorial budding, as discussed before for FIT proteins (Choudhary, Ojha et al. 2015). In a recent study, absence of Fld1 lead to a slight delay of LD formation in an inducible LD system and 25% of LD budded into the nucleus. Interestingly, an Fld1 mutant deleted for 14 amino acids in its short N-terminus, displayed already similar LD defects as a *FLD1* deletion, however the SLD phenotype was insensitive to inositol treatment. This means that the mutant missing the N-terminal amino acids always formed SLD and no LD aggregates, although phospholipid precursors were supplemented. Therefore the Fld1 N-terminus seems to be regulating phospholipid access to the LD surface (Cartwright, Binns et al. 2015).

A follow-up study by Han, Binns et al. (2015) addressed the PA imbalances in *fld1Δ* mutant strains. They found a local concentration of PA in spots on ER membranes adjacent to LDs visualized with fluorescent PA-binding probes. These spots were dependent on LD formation, since they were absent in a strain without LDs. These findings were confirmed by two studies who found the yeast lipin homolog Pah1 and the transcriptional repressor Opi1, both containing PA binding motifs, recruited to theses spots (Grippa, Buxo et al. 2015, Wolinski, Hofbauer et al. 2015)

The thesis on hand follows up on a study from Grippa, Buxo et al. (2015) that characterized the role of the Fld1-Ldb16 complex at the ER-LD contact site as a fusion barrier for phospholipids. First, they addressed phospholipid dependence of the LD phenotype caused by *FLD1* and *LDB16* deletion. As reported before, ectopic inositol supplementation lead to a shift of SLDs to small aggregated LDs due to enhanced PI synthesis. Second, PI synthesis was stimulated genetically by overexpressing the CDP-DAG synthase Cds1 which also resulted in the prevalence of small clustered LD aggregates. This suggested that the LD phenotype is indeed caused by phospholipid imbalances and that the Fld1-Ldb16 complex might function as a phospholipid diffusion barrier between ER and LD.

Next, they asked if the aberrant LD phenotype had an impact of the LD proteome. Indeed, 27 LD proteins were strongly reduced or absent from LDs in *fld1Δ* or *ldb16Δ* mutants compared to wild-type. Remarkably, these proteins were either targeted to SLD or aggregates but not to both. This indicates that the phospholipid monolayer of SLDs and small LD aggregates might be different. Additionally, proteins which were not found on LDs in wild-type cells, were targeted to LDs in cells lacking *FLD1* and *LDB16*. This suggests a global LD targeting defect in yeast cells lacking the Seipin complex.

Interestingly, proteins which are usually not found on LD were targeted to aberrant small LD clusters induced by *FLD1* and *LDB16* deletion. Many of these proteins contains amphipathic helices which caused the aberrant targeting in two cases, the CTP:phosphocholine cytidyltransferase Pct1 and the sterol-PI(4)P shuttle Kes1. Both proteins contain amphipathic helices but with different chemistry. According to this, Pct1 was targeted to spots on the ER in close vicinity of the LD aggregates and Kes1 directly onto the aggregate. In the case of both proteins, targeting was mediated by their amphipathic helices since a GFP tagged version alone showed a similar localization pattern. The Kes1 amphipathic helix is a well-characterized amphipathic lipid packaging sensor (ALPS) motif which is known to recognize membranes with phospholipid packaging defects (Drin, Casella et al. 2007).

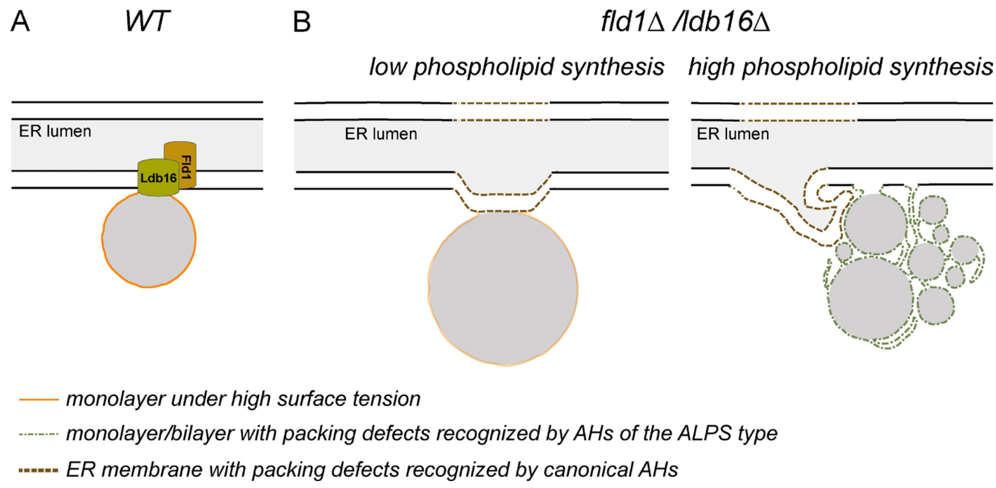

Figure 1.7. Fld1-Ldb16 complex acts as a diffusion barrier at the ER–LD contact site.
(A) ER-LD contact site under wild-type conditions. The Fld1/Ldb16 complex at the contact sites prevents the equilibration of the two membrane systems. (B) In cells lacking *FLD1* and *LDB16*, phospholipids freely diffuse between the two organelles. Under low-synthesis conditions, phospholipids can become limiting and LDs coalesce into a supersized one. Under high-phospholipid-synthesis conditions, ER membrane and LDs equilibrate. The low surface tension of these LDs prevents their coalescence. These aggregates display phospholipid packing defects. Both low and high phospholipid synthesis leads to phospholipid defects in membranes adjacent to LDs, which are recognized by proteins containing canonical AHs. Modified from Grippa, Buxo et al. (2015).

In conclusion, these data suggests that phospholipid availability influences the surface-to-volume ratio of LDs directly if the Seipin complex is absent in yeast cells (Fig. 1.7). Under wild-type conditions, LD size and number is independent of the phospholipid availability in the media and phospholipid synthesis and LD biogenesis are independent processes. This independence is lost upon *FLD1* and *LDB16* deletion. When the Seipin complex is missing, phospholipid availability is directly reflected on the LD phenotype. If phospholipids are limited (minimal media), the cell forms SLD with a low surface-to-volume ratio. If phospholipids synthesis is stimulated (minimal media + inositol) membranes overflow small lipid droplets and ER-LD tangles are formed as nicely depicted in ER tomography in this study. Therefore, in a wild-type scenario, the Fld1-Ldb16 complex at the ER-LD contact site acts as a fusion barrier for phospholipids.

In the thesis on-hand we analyze the role of a third binding partner of the Seipin complex in LD formation and homeostasis.

2. Materials and Methods

Reagents

All reagents were purchased from Sigma-Aldrich, Missouri, USA, unless indicated otherwise. Lipid droplet dyes Bodipy493/503 (Invitrogen, California, USA) and monodansyl pentane (MDH; Abgent, California, USA) were used at 1 µg/ml and 0.1 mM, respectively. Anti-HA (rat 3F10 monoclonal) antibody was purchased from Roche, Basel, Switzerland, anti-GFP (rat) from Chromotec, Martinsried, Germany and anti-DPM1 (mouse) from Life Technologies, California, USA. Polyclonal anti-Usa1 antibody was previously described (Carvalho, Goder et al. 2006). Synthetic peptides were used to raise polyclonal antibody anti-Osw5 (amino acids 74-87 and 132-146) in rabbits. The antibody was affinity purified. Fld1 and Ldb16 antibodies were raised as described in Grippa, Buxo et al. (2015).

Yeast Strains and Plasmids

Protein tagging, promoter replacements and individual gene deletions were performed by standard PCR-based homologous recombination (Longtine, McKenzie et al. 1998, Janke, Magiera et al. 2004). Strains with multiple gene deletions were made either by PCR-based homologous recombination or by crossing haploid cells of opposite mating types, followed by sporulation and tetrad dissection using standard protocols (Guthrie and Fink, 1991). The strains used are isogenic either to BY4741 (*MATa ura3Δ0 his3Δ1 leu2Δ0 met15Δ0*) or to BY4742 (*MATα his3Δ1 leu2Δ0 lys2Δ0 ura3Δ0*) and are listed in Table 2.1. Plasmids and primers used in this study are listed in tables 2.1 and 2.3, respectively.

Media and Growth

Cells were grown in Yeast Extract Peptone Dextrose (YPD) media (1 % yeast extract, 2 % bacto peptone, 2% dextrose), YPGal (1 % yeast extract, 2 % bacto peptone, 2% galactose), Synthetic Complete (SC) media (0.17% yeast nitrogen base, 5g/l ammonium

sulfate, 2% glucose, and amino acids), SCGal (0.17% yeast nitrogen base, 5g/l ammonium sulfate, 2% galactose, and amino acids), or Synthetic Drop-out media supplemented with the corresponding amino acids for plasmid selection. Cells were grown at 30°C and assayed in logarithmical growth phase at an optical density at λ = 600 nm (OD_{600}) between 0.5 – 1.2 or in stationary growth phase at 4-6.

For induction of the galactose promoter, cells were de-repressed over night at 30°C in media containing 2% raffinose as carbon source. In the morning the cells were diluted into the corresponding media containing 2% galactose.

Cloning

A complete list of plasmids and primers can be found in table 2.2 and 2.3.

To obtain pRS415-Pdr16-GFP (pPC 1421), Pdr16-GFP was amplified from genomic DNA of strain yPC8693 with primers Pdr16-GFP-SpeI-Frwd (#2398) and Yos9R5 (#185). Insert and empty vector pRS415 were digested with SpeI/XhoI, purified and ligated.

To obtain pRS415-Pdr16(E235A, K267A)-GFP (pPC1422), mutations were introduced into bPC1438 in a two-step protocol based on the Quick Change site directed mutagenesis kit from Agilent, California, USA and Zheng, Baumann et al. (2004).

To obtain pRS316-Ldh1-GFP (bPC1438), Ldh1 was amplified from genomic DNA from wild-type yeast (yPC1505) with primers Ldh1-NotI-F (#2448) and Ldh1-BamHI-R (#2449). Insert and vector pPC1046 (pRS316 backbone and c-terminal GFP) were digested with NotI/BamHI. Digested backbone and insert were isolated from an agarose gel, purified and subsequently ligated.

Western Blot Analysis

Proteins were analyzed on Biorad Criterion^{TM} TGA precast gradient gels 4-15% and subsequently transferred to a PVDF membrane with a semi-dry blotting chamber in

transfer buffer (3 g/l Trizma Base, 14.4 g/l glycine, 20% methanol) for immunoblot analysis. Membranes were blocked in 5% milk or bovine serum albumin (BSA). Primary antibodies were diluted 1:1000 – 1:5000 for detection in PBS-T/1% milk or BSA. Secondary antibodies (goat anti-rat IgG-HRP, donkey anti-mouse IgG-HRP, donkey anti-rabbit IgG-HRP) were purchased from Santa Cruz Biotechnology,Texas, USA and diluted 1:1000 in PBS-T/1% milk or BSA. Enhanced Chemiluminescence (ECL) substrate was purchased from Perkin Elmer, Massachusetts, USA and bands were quantified with the Quantity One software from Bio-Rad, California, USA.

Immunoprecipitation experiments

Membrane solubilisation: 75-100 OD_{600} logarithmic yeast culture were harvested, washed and resuspended in 1.4 ml Lysis Buffer (50 mM TRIS pH 7.4, 150 mM NaCl, 2 mM $MgCl_2$ and Complete protease inhibitor (Roche, Basel, Switzerland)). Cells were lysed with glass beads and lysates cleared by low speed centrifugation at 4°C. Membranes were pelleted at 50 000 rpm, 25 min, at 4 °C in an Optima Max Tabletop Ultracentrifuge in a TLA 100.3 rotor (Beckmann Coulter, California, USA). The supernatant was aspirated and the membrane pellet resuspended in 600 µl Lysis Buffer. 700 µl Lysis Buffer with 2% Digtonin were added and membranes were solubilized 2-3 hrs on a rotating wheel at 4°C. Solubilized membranes were cleared 15 min, 4°C at full speed in a tabletop centrifuge and 1.1 ml used for the IP.

Immunoprecipitation: Protein carrying a human influenza hemagglutinin (HA) tag were precipitated with 15 µl/sample Pierce^{TM} anti-HA magnetic beads (Pierce, California, Usa). Beads were washed twice with Lysis Buffer + 1% Digitonin, resuspended, added to the solubilized membranes, and the mixture was incubated over-night at 4°C on a rotating wheel. Beads were washed 5 times with Lysis Buffer + 1 %Digitonin and the proteins were eluted with 120 µl SDS sample buffer.

Protein carrying a tandem affinity purification (TAP) tag were precipitated with 30 µl/sample Calmodulin Sepharonse^{TM} 48 (GE Healthcare, Little Chalfont, UK). Beads were washed thrice with Lysis Buffer and blocked with Lysis Buffer + 1% BSA for 1hr at 4°C on a rotating wheel. Beads were washed once with Lysis Buffer and resuspended in Lysis Buffer + 0,1M $CaCl_2$ + 1% Digitonin and added to the solubilized membranes. The mixture was incubated 4 hrs at 4°C on a rotating wheel. Beads were washed 5 times with Lysis Buffer + 0,1M $CaCl_2$ + 1 % Digitonin and the proteins were eluted with 120 µl SDS sample buffer.

Fluorescence Microscopy

Fluorescence microcopy was performed at room temperature with a Zeiss Cell Observer HS with a Hamamatsu CMOS camera ORCA-Flash4.0 controlled by 3i Slidebook 6.0 software. A 100x 1.40 oil immersion objective was used. GFP and Bodipy493/503, mCherry, and MDH signals were detected using GFP filter, RFP filter cube and DAPI filters, respectively, with standard settings.

Data analysis

Lipid droplet size was measured manually with the circle tool in Fiji (Schindelin, Arganda-Carreras et al. 2012) on the Z-stack of the lipid droplet channel (Bodipy).

Lipid Droplet Isolation

LD purification was carried out as previously described (Leber, Zinser et al. 1994, Connerth, Grillitsch et al. 2009) with minor modifications. Briefly, cells were grown in 1l YPD to stationary phase and 3000 ODs of cells were harvested, washed in water, preincubated in 0.1M Tris-HCl pH 9.5, 10 mM DTT for 10 minutes at 30°C, washed, and resuspended to 50 OD600/ml in Spheroplasting Buffer (1.2 M sorbitol, 50 mM TRIS, pH

7.4). For spheroplast preparation Zymolyase (Seikagaku Biobusiness, Tokyo, Japan) 20T from 10mg/ml stock was added (10 µg/OD600 unit cells) followed by incubation in waterbath (30°C, 1h). Spheroplasts were recovered by centrifugation (1000g, 4°C) washed with Spheroplast Buffer and resuspended in Breaking Buffer (10 mM MES-Tris pH 6.9, 12% (w/w) Ficoll400, 0.2mM EDTA) to a final concentration of 0.3g of cells (wet

weight)/ml. PMSF (1mM) and Complete (Roche) were added before homogenization (loose-fitting pestle, 40 strokes) in a Dounce homogenizer on ice. The homogenate was diluted with 1 volume of Breaking Buffer and centrifuged (5000g, 5 min) using rotor JS13.1 (Beckman, California, USA) The resulting supernatant was transferred into 38ml Ultra-Clear™ centrifuge tubes (Beckman, California, USA), overlaid with an equal volume of Breaking Buffer and centrifuged (45 min, 30000rpm) in an SW-32 swinging bucket rotor (Beckman, California, USA). The floating layer was collected from the top of the gradient and following purification steps were performed as described in Connerth, Grillitsch et al. (2009).The recovered high purity top LDs fraction was snap frozen in liquid nitrogen and stored at -80°C.

Lipid Analysis

Steady state lipid labeling for neutral lipid quantification: Cultures in YPGal were diluted to OD_{600} 0.1 and grown for 24 hours at 30°C in presence of 1 µCi/ml [1-14C] acetate (45-60 mCi/mmol) purchased from Perkin Elmer, Massachusetts, USA.

Lipid extraction: Lipids from whole cells (lysed with glass beads) were extracted with chloroform:methanol 2:1 v/v by the single-step modification of Folch, Lees et al. (1957) described by Atkinson, Jensen et al. (1980)by vortexing the sample 3 min at RT, extracting 2-3 hrs at 4°C and washing with 0.9% NaCl. The extracts were dried under a N_2 stream, dissolved in chloroform:methanol 2:1 v/v, resolved by TLC with hexane:diethylether:acetic (80:20:1 v/v) on a Silica plate (Merck, New Jersey, USA), and scanned on a Typhoon Trio phosphorimager (Amersham Biosciences, California, USA) and quantified with Quantity One (Biorad, California, USA).

Microsome preparation

Cells were grown in YPGal to OD_{600} = 0.8 and 400 OD were harvested by a centrifuging 3000 g, 5 min, RT. Cells were washed in ddH2O and resuspended to 30 OD_{600}/ml in Reducing Buffer (0.1M Tris-HCl pH 9.5, 10 mM DDT) and incubated at RT for 10 min. Cells were washed in 10 ml Spheroplasting Buffer (0.7M sorbitol, 0.5% glucose, 10 mM Tris-HCl pH 7.4, 1% yeast eαtract, 2% bacto peptone) and resuspended to 50 OD/ml. For spheroplast preparation Zymolyase (Seikagaku Biobusiness) 20T from 10mg/ml stock was added (10 µg/OD600 unit cells) followed by incubation in waterbath (30°C, 1h). Spheroplasts were recovered by centrifugation 1000g, 5min, 4°C and washed 3 times. Cells were resuspended in 10 ml Lysis Buffer (0.1 M sorbitol, 50 mM KCH_3COO, 2 mM EDTA, 20 mM HEPES-KOH pH 7.4, 1 mM DTT, Complete^{TM} Protease Inhibitor (Roche)) and lysed with 30 strokes in a glass douncer with loose fitting pestle. Lysate was clered by centrifugation 650 g, 5 min, 4°C. Save the supernatant, resuspend the low speed pellet in 5 ml Lysis Buffer, repeat homogenization and low speed spin and combine both supernatants. Layer the combined supernatant on top of 20 ml sucrose cushion (1 M sucrose, 50 mM KCH_3COO 20 mM HEPES-KOH pH 7.4, 1 mM DTT) and spin 6700 rpm 10 min, 4°C in a Beckman Optima L-100K centrifuge in a J 13.1 rotor. Collect the supernatant and adjust to 20 ml and spin in at 15100 rpm, 20 min, 4°C (Type 70 Ti Rotor, Beckman). Discard the supernatant and resuspend the crude microsomal pellet in 20 ml B88 Buffer (20 mM HEPES-KOH pH6.8, 150 mM KCH_3COO, 250 mM sorbitol, 5 mM $Mg(CH_3COO)_2$) and repeat the centrifugation. Resuspend the microsomal pellet in 1 ml B88 Buffer and spin at 200000 rpm, 4°C, 20 min (TLA100.3 rotor in Optima Maα Tabletop Ultracentrifuge (Beckman)). The washed microsomal pellet was resuspended in 100 µl B88 Buffer.

Dga1 enzymatic assay

The assay was modified after Oelkers, Cromley et al. (2002) as follows: All assays were performed in a final volume of 200 µl/reaction at RT for 5, 10 and 25 min. A master mix of 4 reactions was prepared and microsomes were added last to start the reaction. The assay contained B88 Buffer (20 mM HEPES-KOH pH6.8, 150 mM KCH3COO, 250 mM sorbitol, 5 mM Mg(CH3COO)2), 1 mg/ml bovine serum albumin, 125 µM 1,2-Dioleoyl-sn-glycerol in 10 µl ethanol, 50 mM [1-14C]oleoyl-CoA (20,000 dpm/nmol), and 80 g of microsomal protein. Reactions were stopped by the addition of chloroform/methanol (2:1). Lipids were extracted, separated and detected as described above.

Electron Microscopy

Cells were grown in YPD to early stationary phase and cryoimmobilized by high pressure freezing using an EM HPM100 (Leica Microsystems, Vienna, Austria). Samples were freeze-substituted in an automatic freeze substitution system EM AFS-2 (Leica Microsystems, Vienna, Austria), using acetone containing 0.1% of uranyl acetate and 1% water, for 76 hrs at -90°C. On the fourth day, the temperature was risen by 5°C/hr to -45°C and maintained for 5 hrs. Subsequently samples were rinsed in acetone 2 times for 30 min and 3 times for 1 hr and then infiltrated over night with 1:3 HM20/Acetone at -45 °C, 32 hrs with 1:1 HM20/Acetone at -45 °C, and 16 hrs 3:1 HM20/Acetone at -45 °C. Subsequently 100% HM20 was infiltrated two times for 2 hrs at -45 °C and temperature was risen over night to -25 °C and maintained for 8 hrs more. Resin was polymerized with UV light for 24 hrs at -25 °C. Temperature was risen at 5°C/hr to 22°C and maintained for 48 hrs. Ultrathin sections from the resin blocks were obtained using a Leica Ultracut UC6 ultramicrotome and mounting on Formvar-coated copper grids. They were stained with 2% uranyl acetate in water and lead citrate. Thin sections were observed in a Tecnai Spirit (FEI Company, Netherlands).

Mass Spectrometry Analysis

Proteomics: Proteins samples were prepared and analyzed exactly as described in Grippa, Buxo et al. (2015).

Table 2.1. Yeast Strains.

Strain	Genotype
yPC1505 (wt)	*MATa ura3Δ0 his3Δ1 leu2Δ0 met15Δ0*
yPC1506 (wt)	*MATα ura3Δ0 his3Δ1 leu2Δ0 met15Δ0*
yPC3389	*MATa ura3Δ0 his3Δ1 leu2Δ0 met15Δ0 FLD1-TAP-HIS5*
yPC3421	*MATa ura3Δ0 his3Δ1 leu2Δ0 met15Δ0 LDB16-TAP-HIS5*
yPC3541	*MATα ura3Δ0 his3Δ1 leu2Δ0 met15Δ0 ymr147w::KANR*
yPC3546	*MATα ura3Δ0 his3Δ1 leu2Δ0 met15Δ0 ymr147-148w::KANR*
yPC4060	*MATa ura3Δ0 his3Δ1 leu2Δ0 met15Δ0 dga1::KANR*
yPC4069	*MATa ura3Δ0 his3Δ1 leu2Δ0 met15Δ0 pdr16::KANR*
yPC4086	*MATa ura3Δ0 his3Δ1 leu2Δ0 met15Δ0 lro1::KANR*
yPC4114	*MATa ura3Δ0 his3Δ1 leu2Δ0 met15Δ0 ERG6-mCHERRY-KANR*
yPC4278	*MATa ura3Δ0 his3Δ1 leu2Δ0 met15Δ0 HIS3-GAL1-OSW5*
yPC4288	*MATa ura3Δ0 his3Δ1 leu2Δ0 met15Δ0 OSW5-3HA-HIS3*
yPC4289	*MATa ura3Δ0 his3Δ1 leu2Δ0 met15Δ0 FLD1-TAP-HIS5 ldb16::KANR*
yPC4292	*MATa ura3Δ0 his3Δ1 leu2Δ0 met15Δ0 OSW5-GFP-KANR*
yPC4420	*MATa ura3Δ0 his3Δ1 leu2Δ0 met15Δ0 OSW5-3HA-HIS·fld1::NAT*
yPC4695	*MATa ura3Δ0 his3Δ1 leu2Δ0 met15Δ0 LDB16-TAP-HYGB fld1::NATR*
yPC4842	*MATa ura3Δ0 his3Δ1 leu2Δ0 met15Δ0 NAT-ADH-yeGFP-YMR147W*
yPC4843	*MATa ura3Δ0 his3Δ1 leu2Δ0 met15Δ0 NAT-CYC1-yeGFP-YMR147W*
yPC4844	*MATa ura3Δ0 his3Δ1 leu2Δ0 met15Δ0 NAT-TEF-yeGFP-YMR147W*
yPC4845	*MATa ura3Δ0 his3Δ1 leu2Δ0 met15Δ0 NAT-GPD-yeGFP-YMR147W*
yPC4858	*MATa ura3Δ0 his3Δ1 leu2Δ0 met15Δ0 NAT-GAL1-YMR147W*

yPC4888	*MAT? ura3Δ0 his3Δ1 leu2Δ0 met15Δ0 NAT-GAL1p-YMR147W ERG6-mCHERRY-URA*
yPC4890	*MAT? ura3Δ0 his3Δ1 leu2Δ0 met15Δ0 NAT-GAL1-YMR147W fld1::HYGB*
yPC4906	*MAT? ura3Δ0 his3Δ1 leu2Δ0 met15Δ0 NAT-GAL1-YMR147W ldb16::HYGB*
yPC4927	*MATa ura3Δ0 his3Δ1 leu2Δ0 met15Δ0 NAT-GAL1-YMR147W osw5::KANR*
yPC5042	*MATa ura3Δ0 his3Δ1 leu2Δ0 met15Δ0 PET10-mCHERRY-HIS*
yPC5043	*MATa ura3Δ0 his3Δ1 leu2Δ0 met15Δ0 NAT-GAL1p-YMR147W PET10-mCHERRY-HIS*
yPC5045	*MATa ura3Δ0 his3Δ1 leu2Δ0 met15Δ0 TGL3-mCHERRY-HIS NAT-GAL1-YMR147W*
yPC5058	*MATa ura3Δ0 his3Δ1 leu2Δ0 met15Δ0 TGL3-mCHERRY-HIS*
yPC6932	*MATa ura3Δ0 his3Δ1 leu2Δ0 met15Δ0 AYR1-GFP-HIS2*
yPC7249	*MATa ura3Δ0 his3Δ1 leu2Δ0 met15Δ0 NAT-ADH-DGA1-GFP-HIS2*
yPC8693	*MATa ura3Δ0 his3Δ1 leu2Δ0 met15Δ0 PDR16-GFP-HIS2*
yPC9243	*MATa ura3Δ0 his3Δ1 leu2Δ0 met15Δ0 NAT-GAL1p-YMR147W lro1::HIS*
yPC9245	*MATa ura3Δ0 his3Δ1 leu2Δ0 met15Δ0 NAT-GAL1p-YMR147W lro1::HIS dga1::KANR*
yPC9247	*MATa ura3Δ0 his3Δ1 leu2Δ0 met15Δ0 NAT-GAL1-YMR147W dga1::KANR*
yPC9530	*MATa ura3Δ0 his3Δ1 leu2Δ0 met15Δ0 NAT-GAL1p-YMR147W KAN-ADH-DGA1-GFP-HIS*
yPC 9638	*MATa ura3Δ0 his3Δ1 leu2Δ0 met15Δ0 PDR16-GFP-HIS2 fld1::NAT*
yPC9639	*MATa ura3Δ0 his3Δ1 leu2Δ0 met15Δ0 PDR16-GFP-HIS2 Ymr147-148::KanR*
yPC9658	*MATa ura3Δ0 his3Δ1 leu2Δ0 met15Δ0 OSW5-3HA-HIS3 fld1::HYGB*
yPC9695	*MATa ura3Δ0 his3Δ1 leu2Δ0 met15Δ0 NAT-GAL1p-YMR147W PDR16-GFP-HIS*
yPC9700	*Mat? ura3Δ0 his3Δ1 leu2Δ0 met15Δ0 PDR16-GFP-HIS ldb16::HYGB*

yPC9702	*Mat? ura3Δ0 his3Δ1 leu2Δ0 met15Δ0 PDR16-GFP-HIS ldb16::HYGB ymr147w-148w::KANR*
YPC9755	*MATa ura3Δ0 his3Δ1 leu2Δ0 met15Δ0 ymr147w::KANR PDR16-GFP-HIS*
yPC9770	*MATa ura3Δ0 his3Δ1 leu2Δ0 met15Δ0 NAT-GAL1-YMR147W PDR16::KANR*
YPC9782	*Mat? ura3Δ0 his3Δ1 leu2Δ0 met15Δ0 PDR16-GFP-HIS ymr147-148w::KANR fld1::NAT*
yPC9874	*MATa ura3Δ0 his3Δ1 leu2Δ0 met15Δ0 HIS-GAL-OSW5 pdr16::KANR*
yPC9977	*MATa ura3Δ0 his3Δ1 leu2Δ0 met15Δ0 NAT-GPD-YMR147W*
yPC9978	*MATa ura3Δ0 his3Δ1 leu2Δ0 met15Δ0 NAT-GPD-YMR147W ldb16::HYGB*
yPC9987	*MATa ura3Δ0 his3Δ1 leu2Δ0 met15Δ0 HIS-GAL-OSW5 Pdr16-GFP-KANR*
yPC10034	*MATa ura3Δ0 his3Δ1 leu2Δ0 met15Δ0 PDR16-GFP-HIS2 ymr147-148w::KANR [pRS315]*
yPC10064	*MATa ura3Δ0 his3Δ1 leu2Δ0 met15Δ0 NAT-GPD-YMR147W [pRS415-Pdr16-GFP]*
yPC10065	*MATa ura3Δ0 his3Δ1 leu2Δ0 met15Δ0 KAN-GPD-OSW5 [pRS415-Pdr16-GFP]*
yPC10123	*MATa ura3Δ0 his3Δ1 leu2Δ0 met15Δ0 [pRS415-Pdr16-GFP]*
yPC10124	*MATa ura3Δ0 his3Δ1 leu2Δ0 met15Δ0 ymr147-148w::KANR [pRS415-Pdr16-GFP]*
yPC10163	*MATa ura3Δ0 his3Δ1 leu2Δ0 met15Δ0 KAN-GPD-OSW5 [pRS415-Pdr16(E235A, K267A)-GFP]*
yPC10164	*MATa ura3Δ0 his3Δ1 leu2Δ0 met15Δ0 NAT-GPD-YMR147W [pRS415-Pdr16(E235A, K267A)-GFP]*
yPC10165	*MATa ura3Δ0 his3Δ1 leu2Δ0 met15Δ0 ymr147-148::KANR [pRS415-Pdr16(E235A, K267A)-GFP]*
yPC10166	*MATa ura3Δ0 his3Δ1 leu2Δ0 met15Δ0 [pRS415-Pdr16(E235A, K267A)-GFP]*

yPC10167	*MAT? ura3Δ0 his3Δ1 leu2Δ0 met15Δ0 NAT-GAL1-YMR147W are1::KANR are2::HYGB [pRS415-Pdr16-GFP]*
yPC10168	*MATa ura3Δ0 his3Δ1 leu2Δ0 met15Δ0 NAT-GAL1-YMR147W [pRS415-Pdr16-GFP]*
yPC10169	*MAT? ura3Δ0 his3Δ1 leu2Δ0 met15Δ0 lro1::His NAT-GAL1-YMR147W dga1::KANR [pRS415-Pdr16-GFP]*
yPC10189	*MATa ura3Δ0 his3Δ1 leu2Δ0 met15Δ0 PDR16-GFP-HIS2 ymr147-148w::KANR [pRS315-YMR147w-YMR148w]*
yPC10190	*MATa ura3Δ0 his3Δ1 leu2Δ0 met15Δ0 PDR16-GFP-HIS2 ymr147-148w::KANR [pRS315-YMR147W-YMR148WΔBP]*
yPC10191	*MATa ura3Δ0 his3Δ1 leu2Δ0 met15Δ0 PDR16-GFP-HIS2 ymr147-148w::KANR [pRS315-YMR147W-YMR148WΔStemLoop]*
yPC 10192	*MATa ura3Δ0 his3Δ1 leu2Δ0 met15Δ0 are1::KANR are2::HYGB [pRS415-Pdr16-GFP]*
yPC10195	*MATa ura3Δ0 his3Δ1 leu2Δ0 met15Δ0 [pRS316-Ldh1-GFP]*
yPC 10248	*MATα ura3Δ0 his3Δ1 leu2Δ0 met15Δ0 dga1::NAT lro1::KANR*
yPC10241	*MATa ura3Δ0 his3Δ1 leu2Δ0 met15Δ0 ymr147w::KANR [pRS316-Ldh1-GFP]*
yPC10321	*MATa ura3Δ0 his3Δ1 leu2Δ0 met15Δ0 PDR16-GFP-HIS2 [pRS315]*
yPC10409	*MATa ura3Δ0 his3Δ1 leu2Δ0 met15Δ0 AYR1-GFP-HIS2 ymr147-148::KANR*

Table 2.2. Plasmids.

Number	Name	Source
pPC900	pRS315-YMR147w-YMR148w	Gift from F. Posas
pPB901	pRS315-YMR147W-YMR148WΔStemLoop	Gift from F. Posas
pPC910	pRS315-YMR147W-YMR148WΔBP	Gift from F. Posas
pPC 1421	pRS415-Pdr16-GFP	This study
pPC 1422	pRS415-Pdr16(E235A, K267A)-GFP	This study
pPC1438	pRS316-Ldh1-GFP	This study

Table 2.3. Primers.

Number	Primer	Sequence (5'-3')
185	Yos9R5	CTATTGTACTCGAGCGAGGCAAGCTAAACAGATC
2398	Pdr16-GFP-SpeI Frwd	AATACGGCAATTAactagtTACGAAATGCCGGATCTGA CGGAGATAGTTTT
2398	Pdr16-GFP-SpeI	AATACGGCAATTAactagtTACGAAATGCCGGATCTGA CGGAGATAGTTTT
2399	Pdr16-E235A-GFP	TATTCTACAAACTCATTATCCAGcAAGACTAGGAAAA GCACTTTTGA
2340	Pdr16-K267A-GFP Frwd	TATTGACCCACTGACCCGTGAAgcGCTAGTTTTTGATG AACCATTTG

3. Results

We and others previously identified the proteins Fld1 and Ldb16 to form a complex, the Seipin complex, at the ER-Lipid droplet contact site (Szymanski, Binns et al. 2007, Fei, Shui et al. 2008, Grippa, Buxo et al. 2015). The Seipin complex regulates the organelle contact site and is essential for accurate lipid droplet (LD) assembly. Preliminary experiments in our group showed, that the Seipin complex contained two additional proteins, Osw5L and Osw5S. This study characterizes these additional components of the Seipin complex.

3.1. Osw5L and Osw5S form a complex with Fld1 and Ldb16

Osw5L and Osw5S are encoded by two adjacent predicted open reading frames (ORFs), YMR147W and YMR148W, with a curious relationship (Fig. 3.1A). A large-scale cDNA analysis in yeast identified the transcript of YMR147W to be spliced to its downstream ORF YMR148W (Miura, Kawaguchi et al. 2006). The transcript encoded a fusion protein between YMR147W and YMR148W. This suggested, that YMR147W was not an independent ORF but an upstream exon of YMR148W.

YMR148W therefore has two promoters, the upstream promoter generating the spliced transcript with the upstream exon and a downstream one generating an unspliced transcript called YMR148W/OSW5 (outer spore wall 5) (Suda, Rodriguez et al. 2009). The splicing reaction which generates the fusion protein excluded a 29 amino acid sequence at the C-terminus of YMR147W and included 48 amino acids from the intronic region before the YMR148W start codon. In the following, we call the Ymr147w-Ymr148w fusion protein Osw5L(ong) and the unspliced protein Ymr148/Osw5S Osw5S(hort).

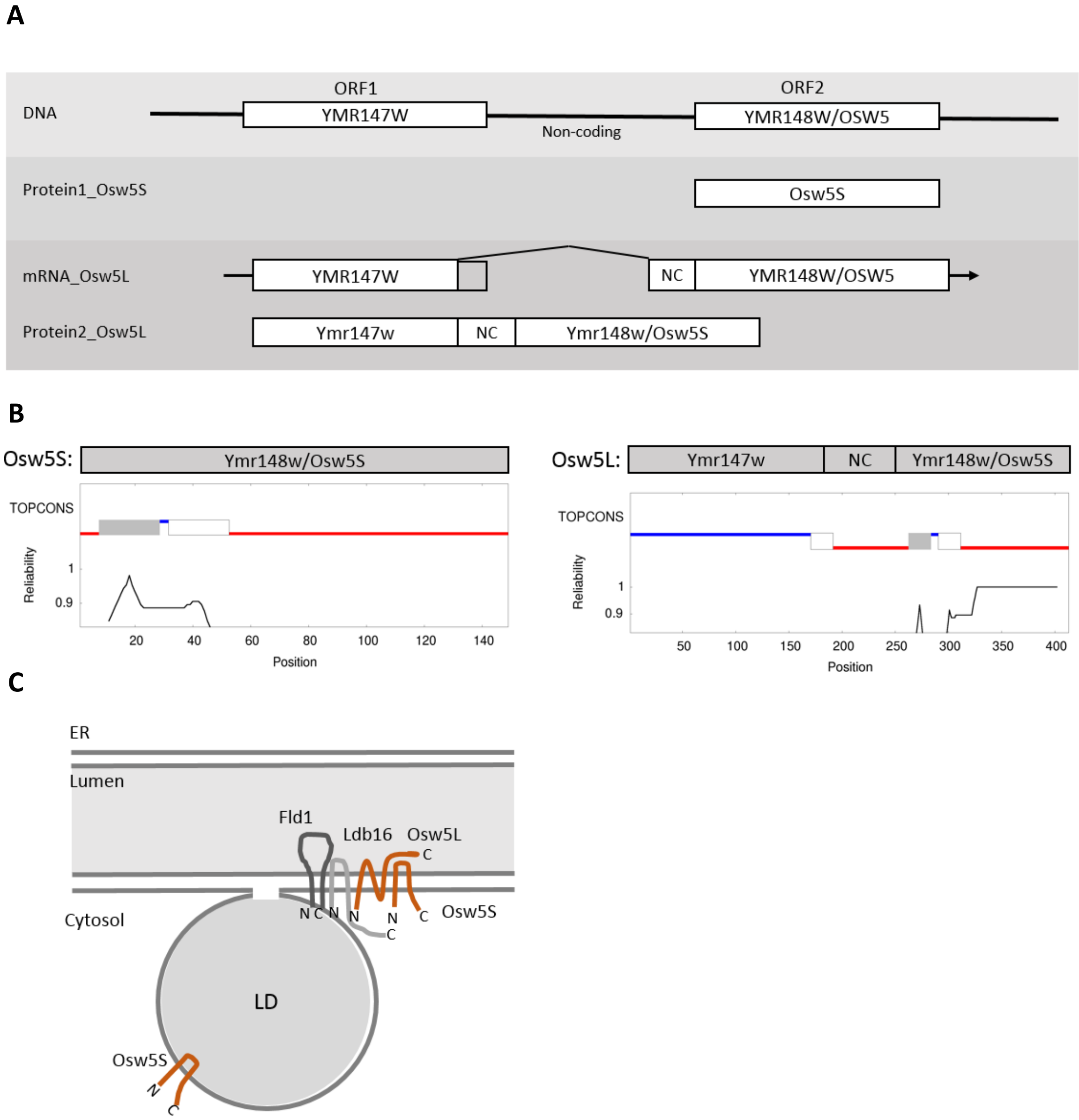

Figure 3.1. Alternative promoter usage gives rise to two protein isoforms: Osw5S and Osw5L.
(A) The transcript of YMR147W is spliced to its downstream ORF YMR148. The transcript encodes a fusion protein between YMR147W and YMR148W. Hence, Ymr147W is not an independent ORF but an upstream exon of YMR148W. YMR148W therefore has two promoters, the upstream promoter generating the spliced transcript with the upstream exon and a downstream one generating an unspliced transcript called YMR148W/OSW5. The splicing reaction which generates the fusion protein excludes a 29 amino acid sequence at the C-terminus of YMR147W and includes 48 amino acids from the intronic region before the YMR148W start codon. In the following we call the Ymr147w-Ymr148w fusion protein Osw5L(ong) and the unspliced protein Ymr147/Osw5S Osw5S(hort). (B) TOPCONS (http://topcons.cbr.su.se) predicts two short transmembrane helices for Osw5S. This would allow the protein to adapt a hairpin conformation which accommodates the protein in both ER double membranes and LD phospholipid monolayers. The fusion protein Osw5L is predicted to have 3 transmembrane helices. The additional domain would exclude it from the LD but is consistent with an ER localization. (C) The Seipin complex proteins Fld1 and Ldb16 are localized at the LD-ER contact site. Osw5L and Osw5S interact with Ldb16. Whereas Osw5L is exclusively located in the ER, Osw5S can move from the ER into the LD.

To validate the preliminary results from our group, we added a tandem affinity purification (TAP) tag to Fld1 and Ldb16 and generated an antibody against the Osw5S. This antibody detects the fusion protein Osw5L as well as Osw5S. In immunoprecipitation experiments two proteins co-precipitated with the Seipin complex as previously detected by mass spectrometry: Osw5L and Osw5S (Fig. 3.2A). We generated a chromosomally C-terminal human influenza hemagglutinin (HA) tagged version of Osw5L and Osw5S by adding three HA tags to the C-terminus of the OSW5 ORF. When we pulled on Osw5L-HA and Osw5S-HA, Ldb16 and Fld1 co-precipitated, suggesting that the interaction of both proteins with the Seipin complex was specific (Fig. 3.2B). Moreover, abundant ER proteins, such as Usa1 and Kar2, did not co-precipitate. Taken together, this data suggests that Osw5S and Osw5L are *bona fide* interactors of the Fld1-Ldb16 Seipin complex.

Interestingly, the interaction of Osw5L and Osw5S with the Seipin complex depended on the presence of Ldb16, but not FLd1 (Fig. 3.2A). This indicates that both proteins are recruited to the Seipin complex through Ldb16. In the absence of Fld1, Ldb16 is rapidly degraded, therefore reduced Osw5L/Osw5S levels in the Ldb16-Tap *fld1Δ* strain were rather attributed to reduced amounts in Ldb16-TAP and not a loss of interaction (Fig. 3.2A). Reciprocally, Fld1 and Ldb16 were only co-precipitated when both components of the Seipin complex were present (Fig 3.2B).

We observed that only a small fraction of Osw5L and Osw5S associated with the Seipin complex and *vice versa* (Fig 3.2A, B). So, the interaction of Osw5L and Osw5S with Fld1 and Ldb16 seems to be much weaker than the one between Fld1 and Ldb16 itself. In these experiments, protein complexes were solubilized in the mild detergent digitonin. If stronger detergents were used, such as NP40, Osw5L and Osw5S interaction with Fld1-Ldb16 was strongly diminished (data not shown). This also argues for a rather loose association between the two proteins and the Seipin complex.

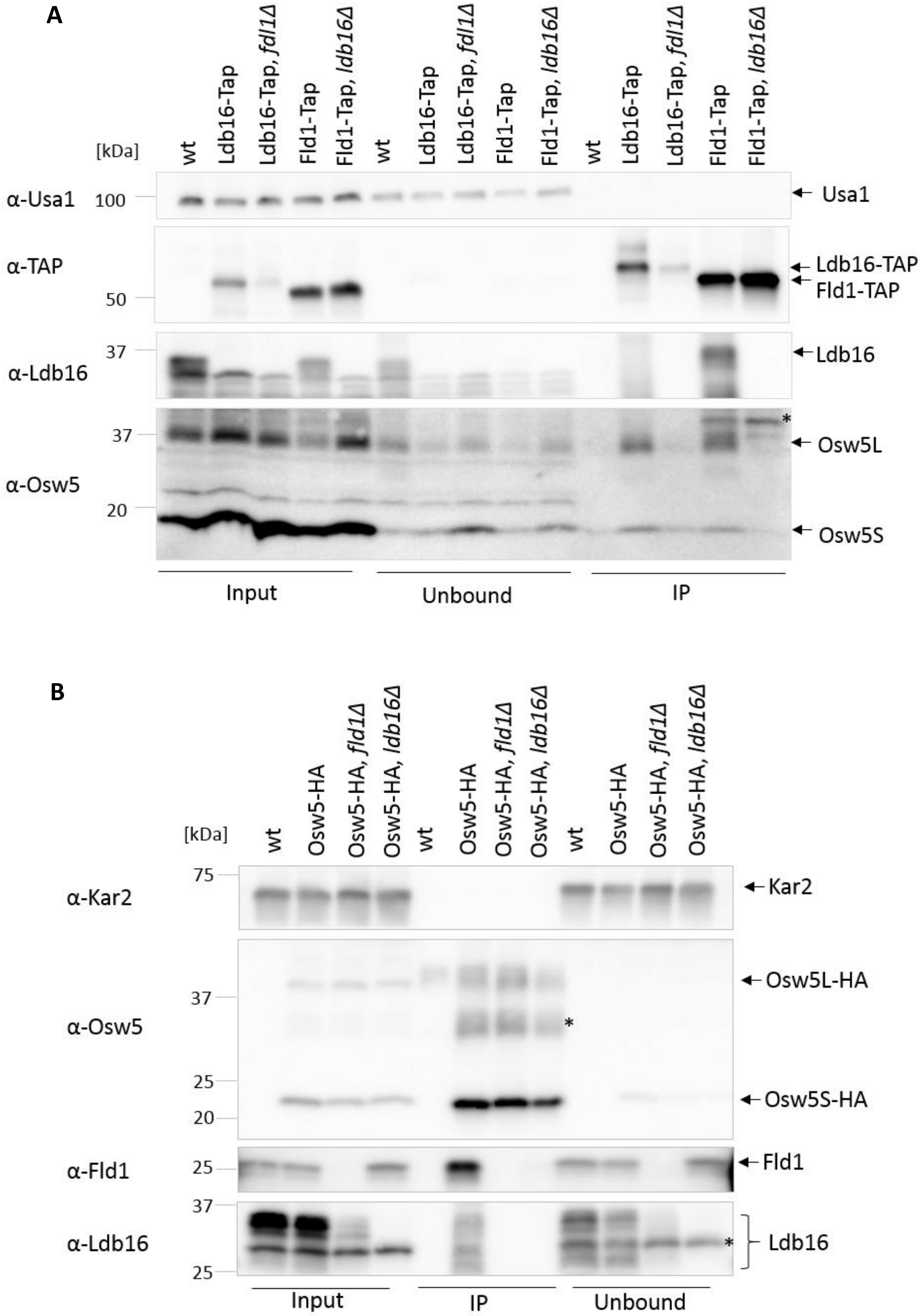

Figure 3.2. Osw5S and Osw5L form a complex with the Seipin complex proteins Fld1 and Ldb16.
Cells of the indicated genotypes were grown to logarithmic phase in minimal medium, lysed and membranes were isolated. Fld1-TAP and Ldb16-TAP (A) and Osw5-HA (B) were precipitated from solubilized membranes with 1% digitonin. * unspecific band

3.2. Cellular metabolism regulates Osw5L and Osw5L isoform abundance

Next, we wanted to understand how isoform abundance was regulated. Therefore, we looked at isoform abundance under different conditions. We grew cells harboring the HA tagged version of Osw5L and Osw5S from logarithmic to stationary phase in minimal medium and analyzed the expression pattern of both proteins over time by western-blot. Interestingly, protein abundance of Osw5L and Osw5S were dependent on the growth phase of the cell (Fig. 3.3). Osw5S was always more abundant than Osw5L. Osw5S was present in both logarithmic and stationary phase and its abundance slightly increased in stationary phase. However, Osw5L was more abundant in logarithmic growth phase and strongly decreased in stationary phase.

Concluding, both proteins behaved inversely: As the cell went from logarithmic to stationary growth phase, Osw5S abundance slightly increased whereas Osw5L abundance strongly decreased.

The absence of Osw5L in stationary phase could serve as a switch to convey metabolic information to the lipid droplet biogenesis machinery.

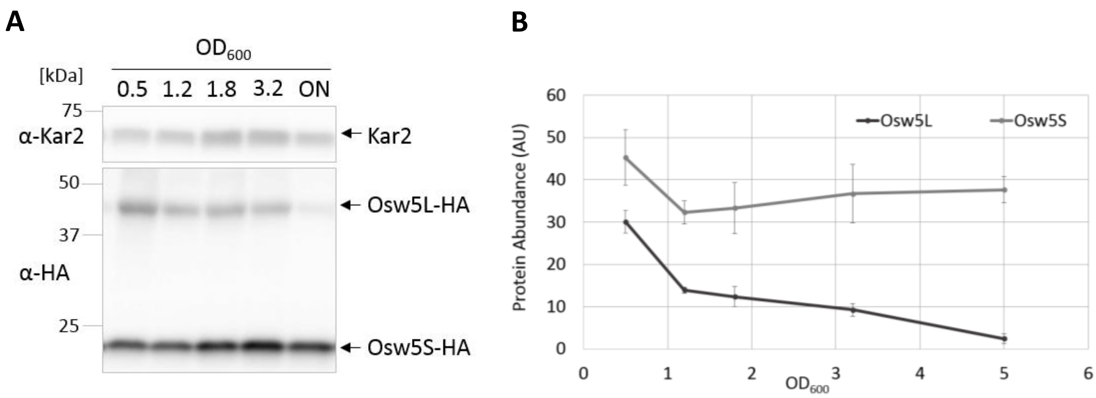

Figure 3.3. Osw5S and Osw5L isoform abundance change over time.
(A) Cells were grown in SC medium, a sample was taken at the indicated OD_{600} values and after over-night growth. Samples were analyzed by western blot and quantified. (B) Quantification of Osw5S and Osw5L protein abundance from (A) with Quantity One software. The average of three independent experiments normalized to Kar2 as loading control is displayed. Error bars indicate standard deviation.

3.3. Osw5S is a bona fide lipid droplet protein, whereas Osw5L is restricted to the ER bilayer

We wanted to know, where the two isoforms could be found in the cell. To analyze the subcellular localization of Osw5S, we GFP tagged Osw5S C-terminally. We saw Osw5S-GFP co-localizing with LDs in light microscopy (Fig. 3.4A). LD size increased when cells reached stationary phase and Osw5S formed rings around LDs, which is typical for proteins localizing to the LD surface (data not shown). Furthermore, in biochemical fractionation experiments Osw5S co-fractionated with the *bona fide* LD protein Erg6 in LD and ER fraction (Fig 3.4B). Here, cells were lysed, membranes isolated and fractionated into LDs and ER.

In agreement with the localization data, the structure prediction server TOPCONS (Tsirigos, Peters et al. 2015) predicted Osw5S to have two transmembrane domains with only few amino acids separating them. This configuration fits with the secondary structure of a hydrophobic hairpin domain common to many other LD proteins. This fold accommodates the protein in the LD monolayer as well as ER membrane (Fig 3.1B, D) (Kory, Farese et al. 2016).

To visualize Osw5L in light microscopy, we had to exchange its intrinsic promoter for the slightly stronger Cyc-promoter and add a GFP to its N-terminus. GFP-Osw5L showed a web-like distribution reminiscent of an ER localization in the cell (Fig 3.4A). A punctuate LD co-localization was also seen and could be due to its interaction with the Seipin complex that is localized to ER-LD contact sites. However, structures adjacent to or at the LD are hard to resolve with our microscopy setup. Also biochemical fractionation data suggested an ER localization of Osw5L, since it was restricted to the ER fraction and excluded from LDs, just as the ER marker protein Kar2 (Fig. 3.4B).

When we predicted the topology of the fusion protein Osw5L, TOPCONS predicted an additional transmembrane domain. This luminal domain would prevent Osw5L from localizing to LDs since it cannot be accommodated in the neutral lipid core of the droplet (Fig 3.1C). This prediction is in concordance with microscopy and biochemical data (Fig. 3.4)

In summary, Osw5S had a dual localization to the ER and LDs presumably mediated by its hairpin loop, whereas Osw5L was restricted to the ER and excluded from LDs due to the presence of an additional domain (Fig 3.1D).

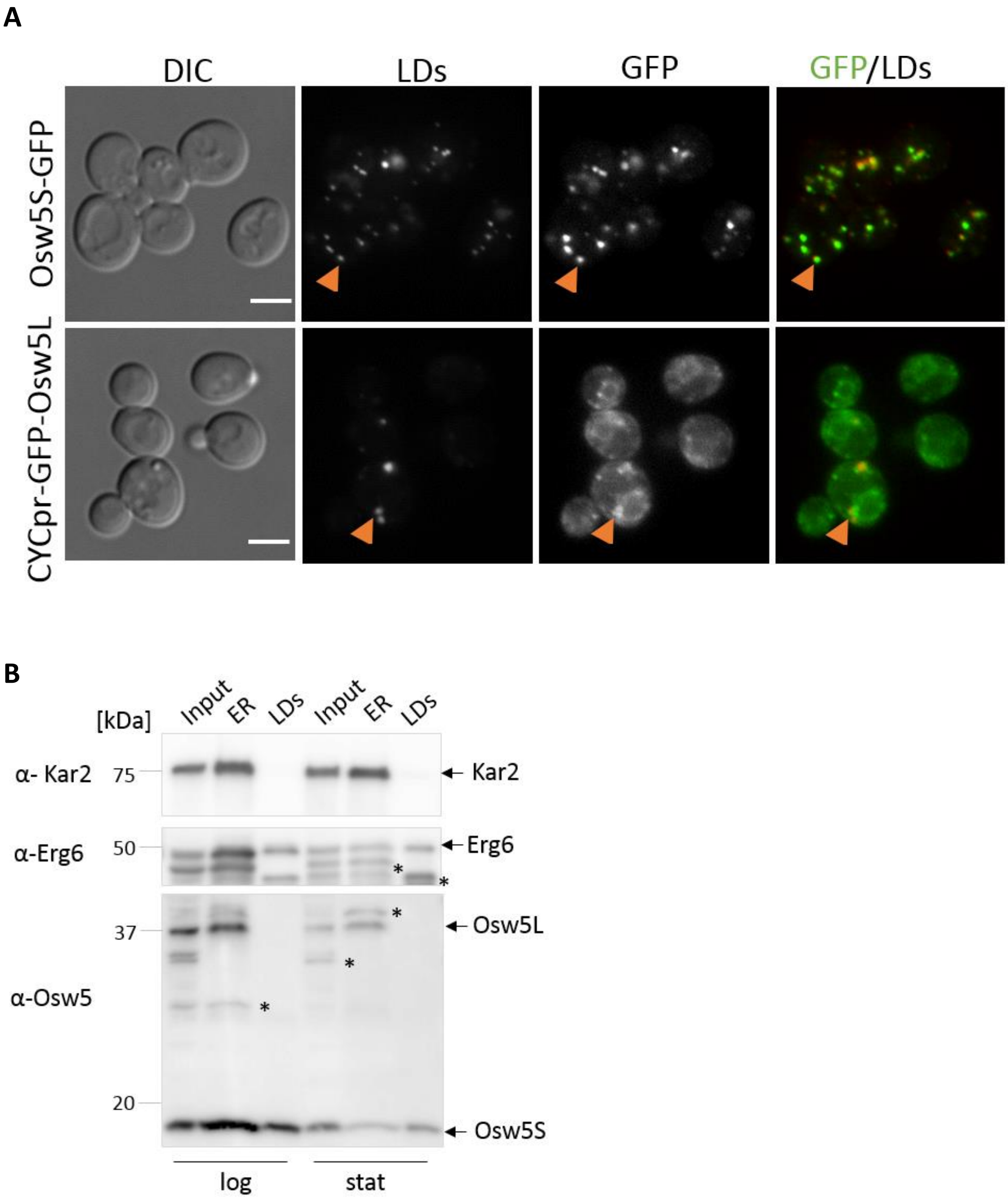

Figure 3.4. Osw5S has a dual localization to LDs and ER, whereas Osw5L is restricted to the ER.
(A) Cells were grown to logarithmic phase in YPD for observation. LDs were stained with MDH. Arrows indicate GFP-Ymr147w/Osw5S-GFP co-localization with LDs. Scale bar is 5 µM.
(B) Wild-type cells were grown to logarithmic or stationary phase and ER and LDs were separated by buoyant density centrifugation. Fractions were analyzed by western blot where Kar2 indicates ER and Erg6 ER and LD contain fractions. * Unspecific band

3.4. Osw5S deletion leads to aberrant lipid droplets

Deletion of the Seipin complex leads to aberrant LD phenotypes in the cell (Szymanski, Binns et al. 2007, Wang, Miao et al. 2014). In minimal media, LDs in *FLD1* and *LDB16* deletion mutants are supersized and reduced in number. We tested, if deletion of any of the Osw5 proteins had a similar phenotype (Fig. 3.5).

We grew wild-type cells to stationary phase, stained LD with the neutral lipid dye Bodipy and imaged and quantified LD size and number (Fig 3.5A). Indeed, in *osw5LΔ osw5SΔ* double deletion cells, we noticed slightly bigger LDs. LDs typically ranged around a size of 0.6 µM in wild-type cells (86%). In *osw5LΔ osw5SΔ* cells however, only 56% ranged around 0.6 µM, 35% around 0.8 µM, and 6% were bigger than 0.8 µM (Fig 3.5B). We wondered, if the size increase could be attributed to deletion of the fusion protein Osw5L or Osw5S alone. Therefore we measured LD size in *ymr147Δ* cells where Osw5S expression was maintained (Fig. 3.5). In these cells, LD size was wild-type like. Therefore the LD phenotype was caused by the lack of Osw5S alone and not the fusion protein Osw5L. We could not observe an additional LD phenotype upon deletion of the fusion protein Osw5L.

To have a better look at LD in an *osw5LΔ osw5SΔ* deletion strain, we prepared samples for electron microscopy (EM). LD, LD-ER contact sites, and the ER itself were similar to control cells (Fig. 3.6). The mild increase in LD size are hard to appreciate by EM, since we are looking at thin slices in a 2D space.

The mild defects upon Osw5S deletion suggest that Osw5S is a peripheral component of the Seipin complex. This is also consistent with the biochemical data presented earlier.

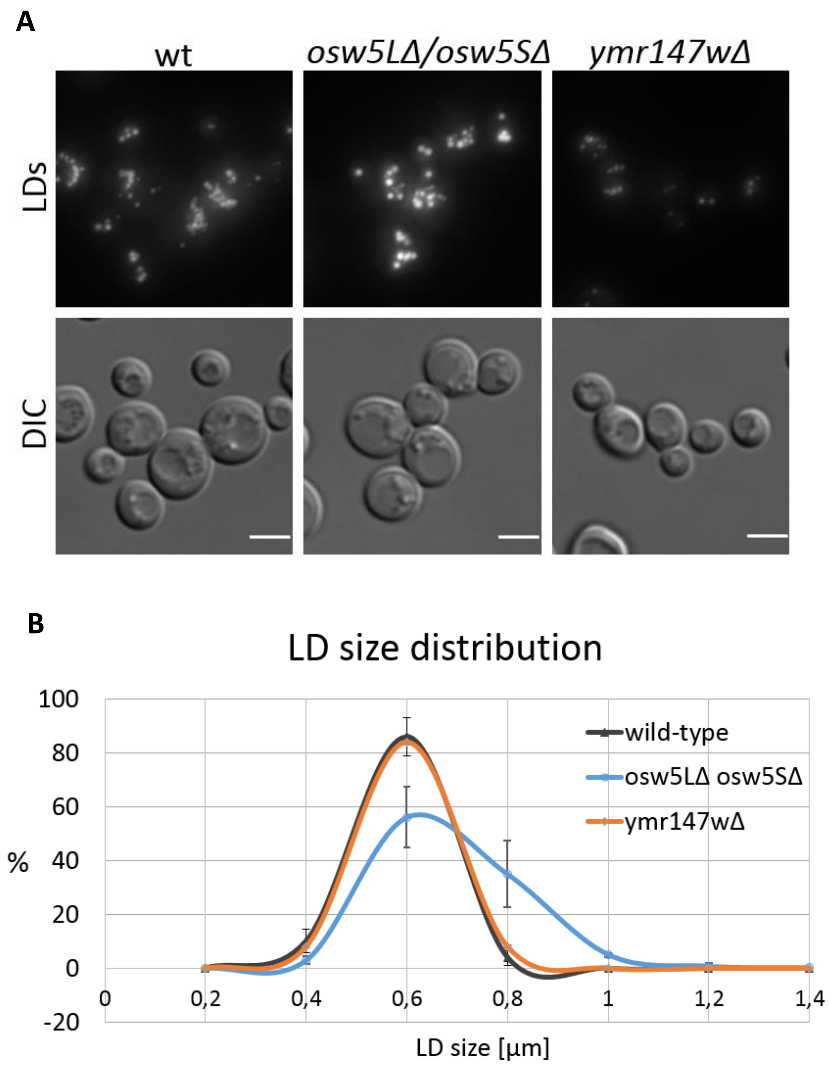

Figure 3.5. Osw5S deletion leads to a LD size increase.
(A) Cultures were inoculated to OD_{600} 0.1, grown for 24 hrs and imaged. LDs were stained with Bodipy. In the LD channel a Z-stack maximum projection is shown. Scale bar is 5 µM. (B) LD size quantification. LD size was quantified manually on Z-stack maximum projections in three independent experiments with more than 200 LDs quantified in each. Error bars show standard deviation.

3.5. Osw5L overexpression leads to massive lipid droplet accumulation and elevated triacylglycerol levels

We were surprised by the lack of phenotype upon Osw5L deletion and therefore decided to force the expression of the fusion protein by overexpression to levels exceeding those of Osw5S. Thereby we inverted their usual expression pattern.

We placed Osw5L under the strong inducible GAL-promoter and imaged the cells in logarithmic and stationary growth phase. This leads to the expression of only Osw5L in the cells (Fig. 3.7E). To visualize LDs, we stained them with the fluorescent neutral lipid dye MDH (Fig. 3.7). Osw5L overexpression lead to more LDs per cell, clustering to few loci in about 45% of the cells (Fig. 3.7A, C, 3.6). As a control, we also overexpressed Osw5S to the same level (Fig. 3.7E). This only had a minor effect on the LD phenotype.

Intrigued by the LD cluster size and the strong lipid signal in microscopy, we analyzed neutral lipid content of Osw5L and Osw5S overexpressing cells. We isolated triacylglycerol (TAG) and sterol ester (SE), the main components of the LD, from those cells and separated the lipids via thin layer chromatography (TLC). Neutral lipid analysis confirmed light microscopy data: Osw5L overexpressing cells accumulated about 3 fold more TAG than wild-type cells, whereas SE levels remained largely unaffected. On the contrary, Osw5S overexpression had only minor effects on the TAG content of the cells (Fig. 3.7B, D).

To analyze if the LD phenotype depended directly on Osw5L overexpression, we placed an N-terminally GFP tagged version of Osw5L under successively stronger promoters (Cyc, Adh, Tef, Gpd, Gal) and analyzed the LD phenotype via microscopy (Fig. 3.8). Overexpression from the Cyc-promoter had no effect on the LD phenotype. However, when we placed Osw5L under the ADH-promoter, or any other stronger promoter, we saw clustering of LDs in the cell. These LD clusters also strongly recruited GFP-Osw5L. The clusters became bigger in a dosage dependent manner, so that when GFP-Osw5L was expressed from the GAL-promoter, clusters were most pronounced. In line with the neutral lipid analysis from cells expressing Osw5L from the GAL promoter (Fig. 3.7D), we supposed that TAG accumulation goes in hand with cluster formation and also increased in a dosage-dependent manner.

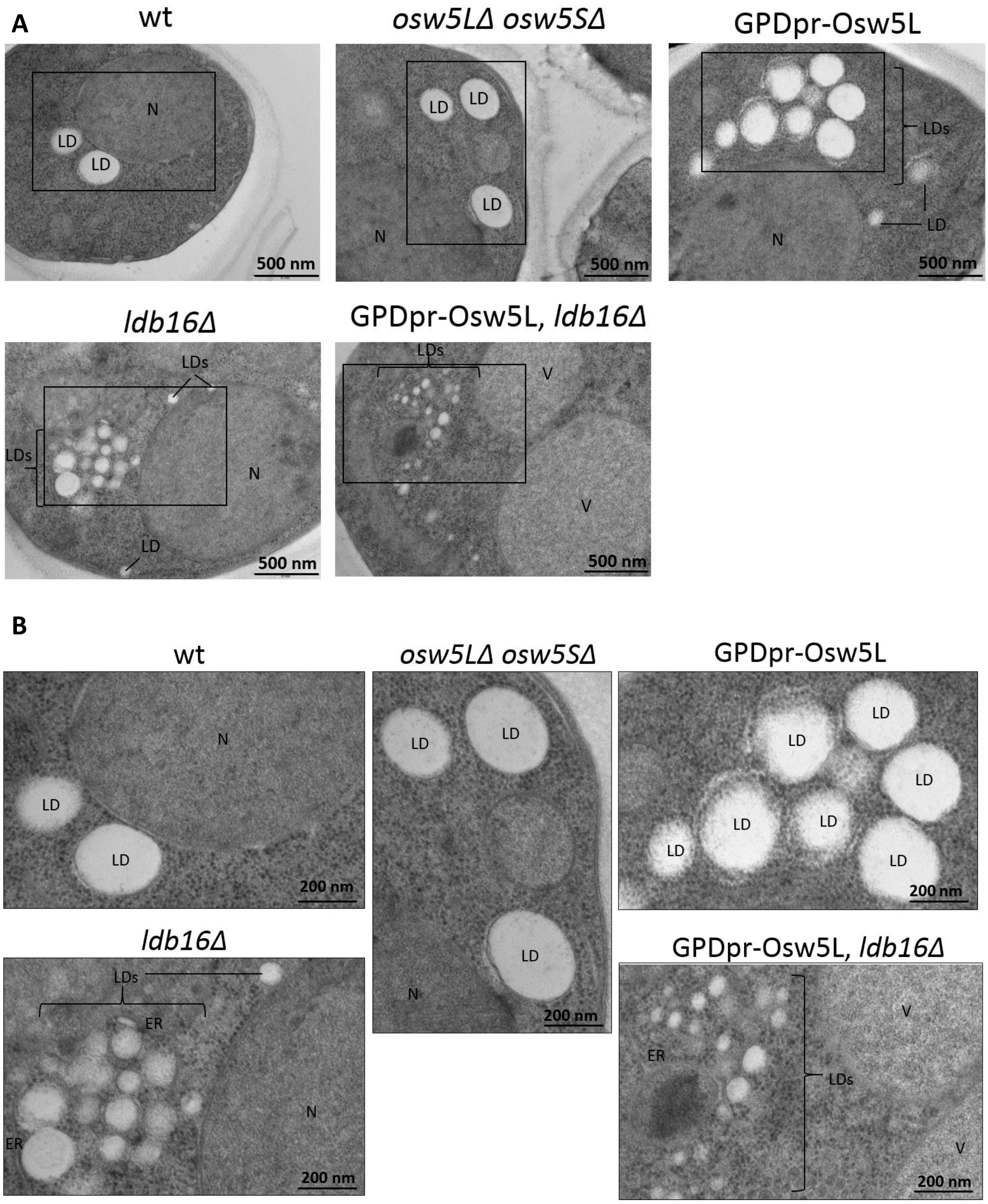

Figure 3.6. Cell and LD ultrastructure in different mutants.
Electron microscopy with cryo-fixation. LD(s)=Lipid droplet(s), N=Nucleus, V=Vacuole, ER=Endoplasmic Reticulum. (A) LD phenotype of the indicated strains. Scale bar indicates 500 nm. (B) Insets show outlined regions in (A) of the corresponding strain. Scale bar indicates 200nm.

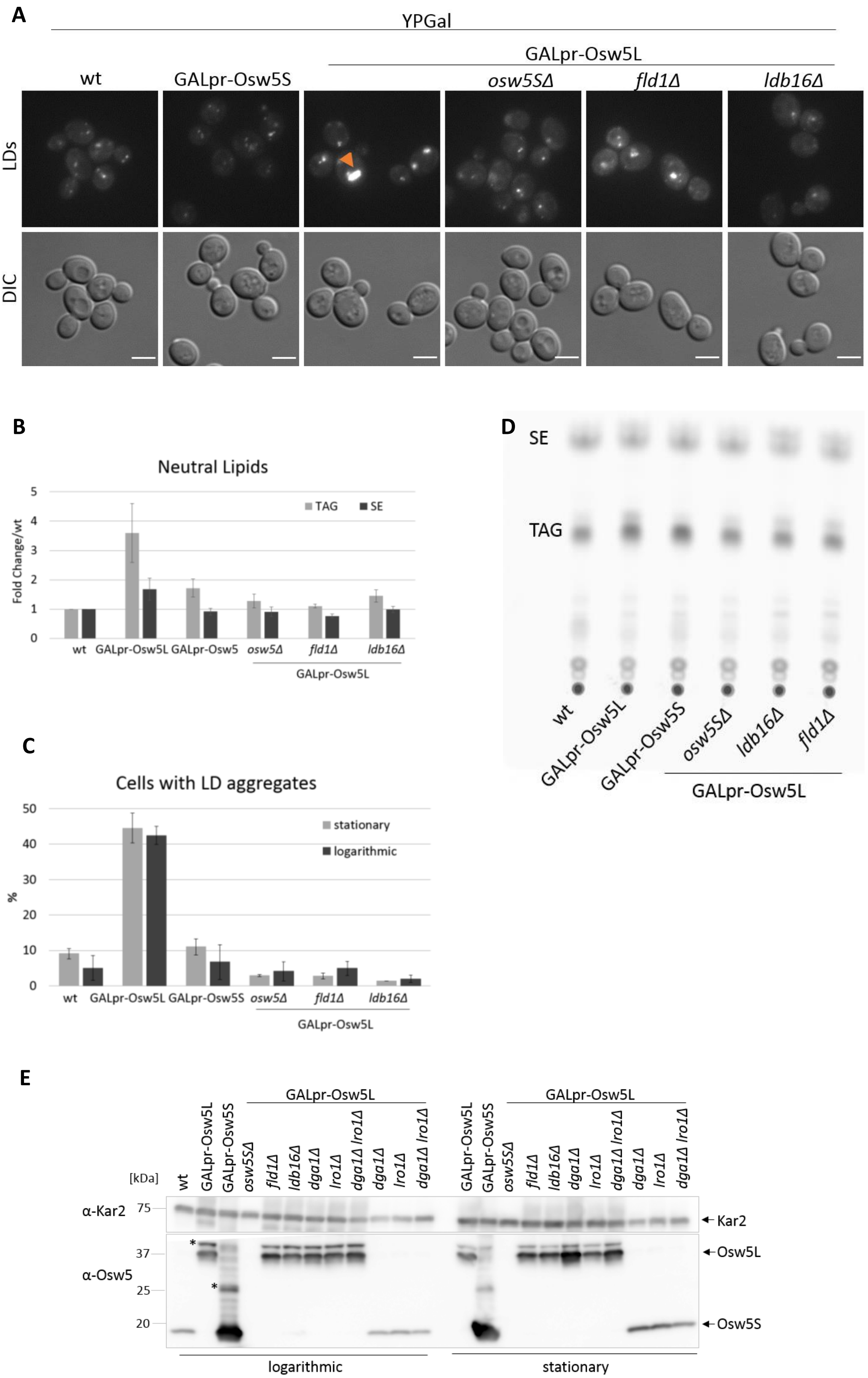

A
YPGal
GALpr-Osw5L
wt
GALpr-Osw5S
osw5SΔ
fld1Δ
ldb16Δ
LDs
DIC
B
Neutral Lipids
TAG
SE
Fold Change/wt
wt
GALpr-Osw5L
GALpr-Osw5
osw5Δ
fld1Δ
ldb16Δ
GALpr-Osw5L
C
Cells with LD aggregates
stationary
logarithmic
%
wt
GALpr-Osw5L
GALpr-Osw5S
osw5Δ
fld1Δ
ldb16Δ
GALpr-Osw5L
D
SE
TAG
wt
GALpr-Osw5L
GALpr-Osw5S
osw5SΔ
ldb16Δ
fld1Δ
GALpr-Osw5L
E
GALpr-Osw5L
GALpr-Osw5L
[kDa]
wt
GALpr-Osw5L
GALpr-Osw5S
osw5SΔ
fld1Δ
ldb16Δ
dga1Δ
lro1Δ
dga1Δ lro1Δ
α-Kar2
α-Osw5
Kar2
Osw5L
Osw5S
logarithmic
stationary

Figure 3.7. Osw5L overexpression leads to TAG accumulation and LD aggregation and is dependent on a functional LD-ER contact site.
(A) Cells were grown to logarithmic phase in YPGal for observation. LDs were stained with MDH. Arrow indicate LD aggregates. Scale bar is 5 µM. (B) Number of LD aggregates was quantified in three independent experiments in 130-386 cells/experiment in the indicated strains in cells in logarithmic and stationary growth phase. Error bars indicate standard deviation. (C) Cells grown in YPGal were diluted to OD_{600} 0.1 and grown for 24 hours in presence of 1 µCi/ml [1-14C]acetate and neutral lipids were extracted and separated by TLC. (D) TAG and SE amounts were quantified in two independent experiments as described in (C) with Quantity One software and normalized to the wt sample. Error bars indicate standard deviation. (E) Western blot analysis of strains with the indicated genotypes. Cells were either grown to logarithmic or stationary growth phase and analyzed. Kar2 serves as a loading control.
* Unspecific band

Notably, when we overexpressed Osw5L, Osw5S expression was shut down simultaneously, as analyzed by western-blot (Fig. 3.7E, 3.8B). This was probably due to strong RNA polymerase occupancy of the YMR147W promoter that did not allow for transcription of OSW5S anymore. Adding back Osw5S from a plasmid did not change the LD phenotype (data not shown), so LD clustering and TAG accumulation seem to be a direct effect of Osw5L overexpression.

Next, we wanted to characterize the LD aggregates more in depth. Therefore, we performed electron microscopy on cells overexpressing Osw5L. LD clusters observed by light microscopy in Osw5L overexpressing cells were confirmed by electron microscopy (Fig. 3.6). LDs were bigger than in wild-type cells and tightly clustered. The ER seemed normal.

In conclusion, overexpression of Osw5L strongly stimulated TAG synthesis and LD formation in a dosage dependent manner, both in logarithmic and stationary phase cells.

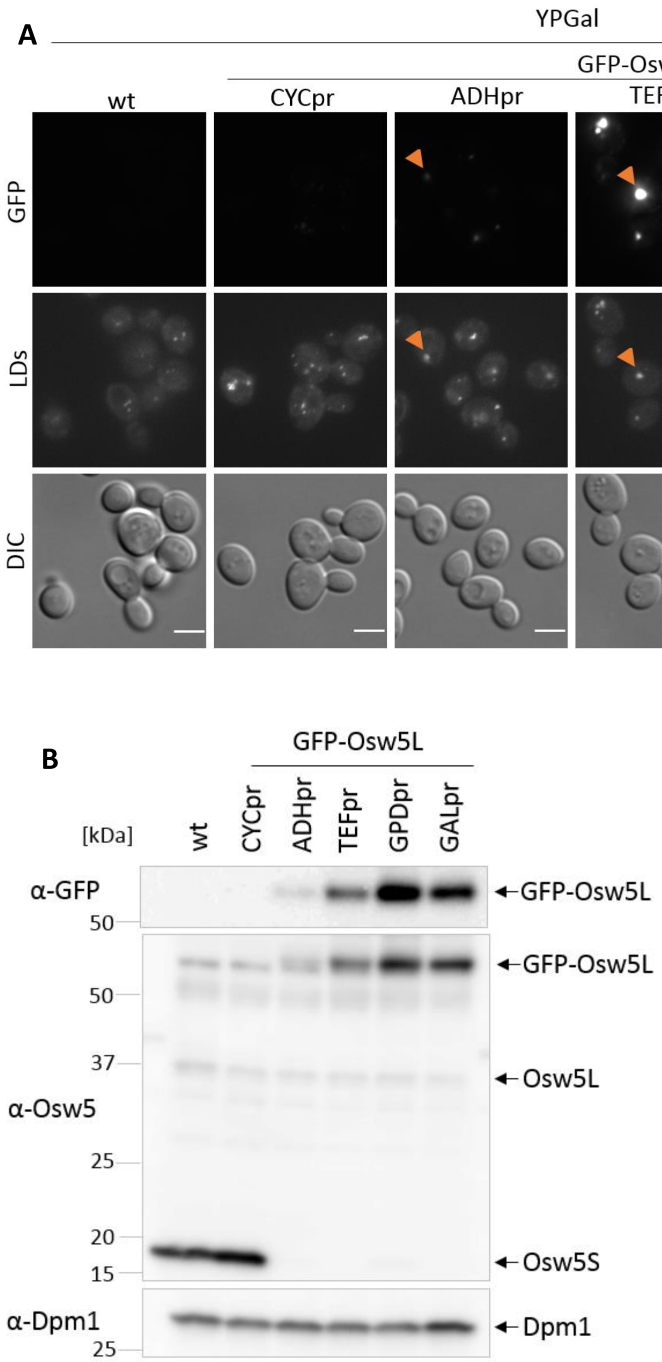

Figure 3.8. Enhanced YMR147W promoter usage leads to Osw5L expression and LD aggregation.
(A) Cells were grown to logarithmic phase in YPGal for observation. LDs were stained with MDH. Arrows indicate GFP-Osw5L co-localization with LD aggregates. Scale bar indicates 5 µM. (B) Logarithmic samples were analyzed by western blot. Dpm1 was used as a loading control.

3.6. LD accumulation and elevated triacylglycerol levels depend on a functional LD-ER contact site

To confirm that the LD phenotype was specific and dependent on the interaction with the Seipin complex, we imaged cells overexpressing Osw5L in combination with *FLD1* or *LDB16* deletion (Fig. 3.7A). *FLD1* or *LDB16* deletion did not affect Osw5L expression levels (Fig. 3.7E). Intriguingly, these cells did no longer accumulate large LD aggregates or excessive amounts of TAG (Fig. 3.7A, B, C, D). Their LD phenotype rather resembled the *LDB16* or *FLD1* deletion phenotype (Fig. 3.7A, C).

We analyzed this more in detail by electron microscopy (Fig. 3.6). We looked at *ldb16Δ* in combination with Osw5L overexpression and *ldb16Δ* as a control. The control *ldb16Δ* cells showed small and tightly clustered LD and additionally the ER showed alterations such as aberrant spacing of the ER leaflets, luminal LDs and altered LD-ER contact sites as described in Grippa, Buxo et al. (2015). Curiously, Osw5L overexpression seemed to have an effect on LD clusters in *ldb16Δ* cells which could not be appreciated in light microscopy. Although LD were small and organized in clustered and cells did not seem to accumulate TAG, LDs were more dispersed as in *ldb16Δ* cells alone (Fig. 3.6).

Taken together, these data show that LD clusters and TAG accumulation caused by Osw5L overexpression are depended on the presence of the Seipin complex and a functional LD-ER contact site.

3.7. Diacylglycerol-O-Acyltransferase 1 (Dga1) mediates increased TAG synthesis in Osw5L overexpressing cells

In yeast, two enzymes esterify diacylglycerol (DAG) to triacylglycerol (TAG): Diacylglycerol-O-Acyltransferase 1 (Dga1) and Lecithin cholesterol acyl transferase related open reading frame 1 (Lro1) (Oelkers, Tinkelenberg et al. 2000, Oelkers, Cromley et al. 2002). Both enzymes transfer a fatty acid chain to DAG, however this fatty acid chain is derived from different pools. Dga1 uses activated acyl-CoA, whereas the preferred acyl-donors for Lro1 are phospholipids (Oelkers, Tinkelenberg et al. 2000, Sorger and Daum 2002). Previous work showed that Lro1 is the main source of TAG during logarithmic growth, whereas Dga1 takes over in stationary phase (Oelkers, Cromley et al. 2002). Dga1 was also found to move into LDs upon formation, whereas Lro1 is an ER resident protein (Jacquier, Choudhary et al. 2011). We deleted *DGA1*, *LRO1* or both in cells overexpressing Osw5L and assayed for TAG content biochemically and via microscopy to identify the enzyme mediating increased TAG synthesis (Fig. 3.9A).

As described earlier, cells overexpressing Osw5L accumulated about 3 times more TAG than control cells (Fig. 3.7B, 3.9B). Maintaining Osw5L overexpression, we individually deleted *LRO1* or *DGA1*. Cells overexpressing Osw5L with an individual deletion for *LRO1* accumulated the same amount of TAG, as cell overexpressing Osw5L alone. Therefore, Lro1 was not involved in stimulated TAG synthesis upon Osw5L overexpression.

However, *DGA1* deletion in presence of Osw5L overexpression lead to a significant decrease of TAG below wild-type levels, as previously described for stationary cells (Oelkers, Cromley et al. 2002) (Fig. 3.9B, D). Cells missing both acyltransferases could not synthesize TAG, whereas SE levels were unaffected, as expected (Oelkers, Cromley et al. 2002). Differences were not due to Osw5L levels, which were similar in all strains (Fig. 3.7E). Therefore, synthesis of surplus TAG upon overexpression of Osw5L requires Dga1 and not Lro1.

Upon *DGA1* deletion in Osw5L overexpressing cells TAG levels were much reduced (Fig. 3.9C, D). However, remaining LDs were still clustered (Fig. 3.9C). Therefore, reduced TAG levels and thus altered TAG to SE ratio did not affect LD clustering in Osw5L overexpressing cells. TAG increase and LD clustering seemed to be two independent processes induced by Osw5L overexpression.

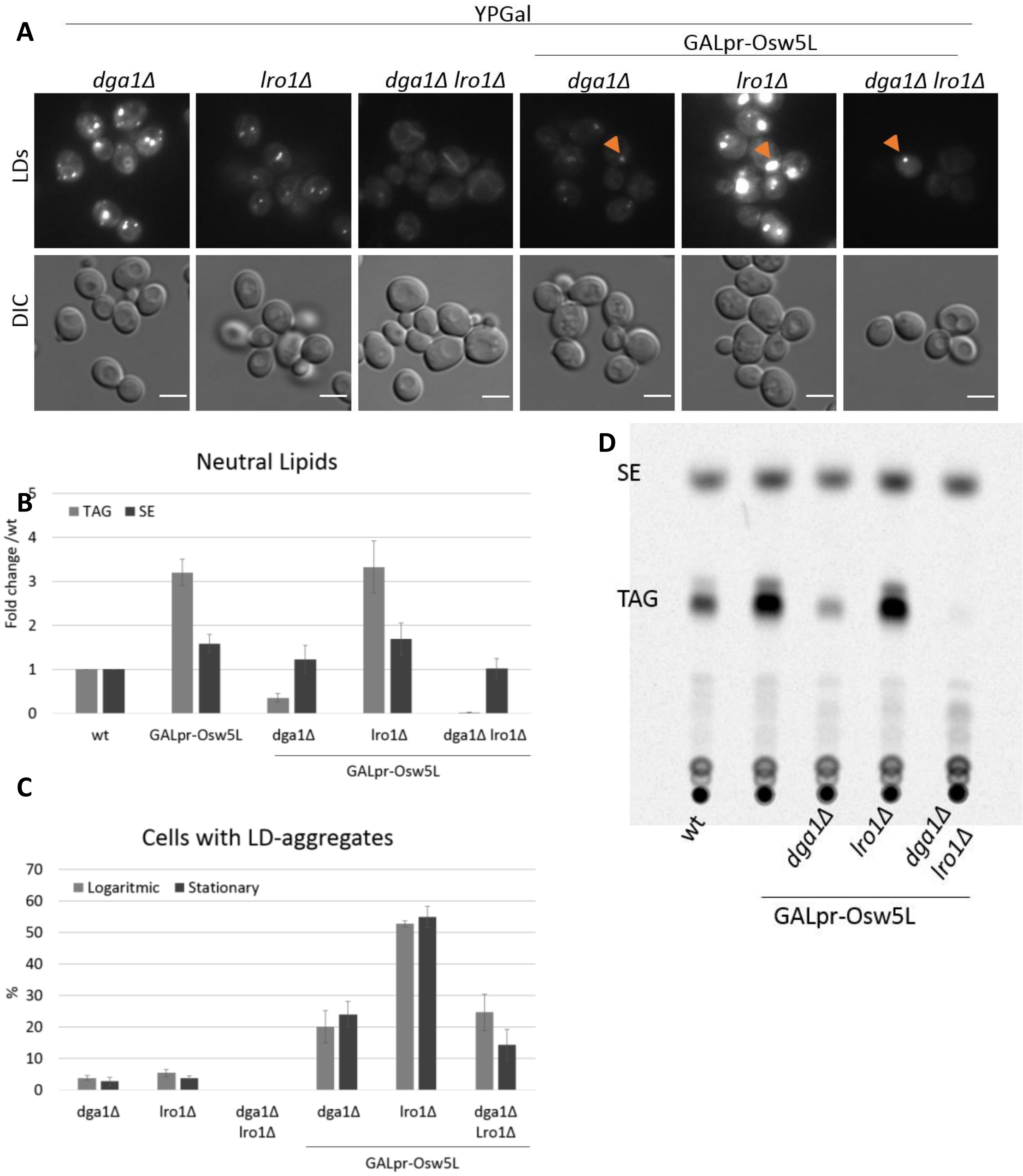

Figure 3.9. Osw5L overexpression dependent TAG accumulation is mediated by the diacylglycerol transferase Dga1.

(A) Cells were grown to logarithmic phase in YPGal for observation. LDs were stained with MDH. Arrows indicate LD aggregates. Scale bar is 5µM. (B) Number of LD aggregates was quantified in three independent experiments in 154-299 cells/experiment in the indicated strains in cells in logarithmic and stationary growth phase. Error bars indicate standard deviation. (C) Cells grown in YPGal were diluted to OD_{600} 0.1 and grown for 24 hours in presence of 1 µCi/ml [1-14C]acetate and neutral lipids were extracted and separated by TLC. (D) TAG and SE amounts were quantified in three independent experiments with Quantity One software and normalized to the wt sample. Error bars indicate standard deviation.

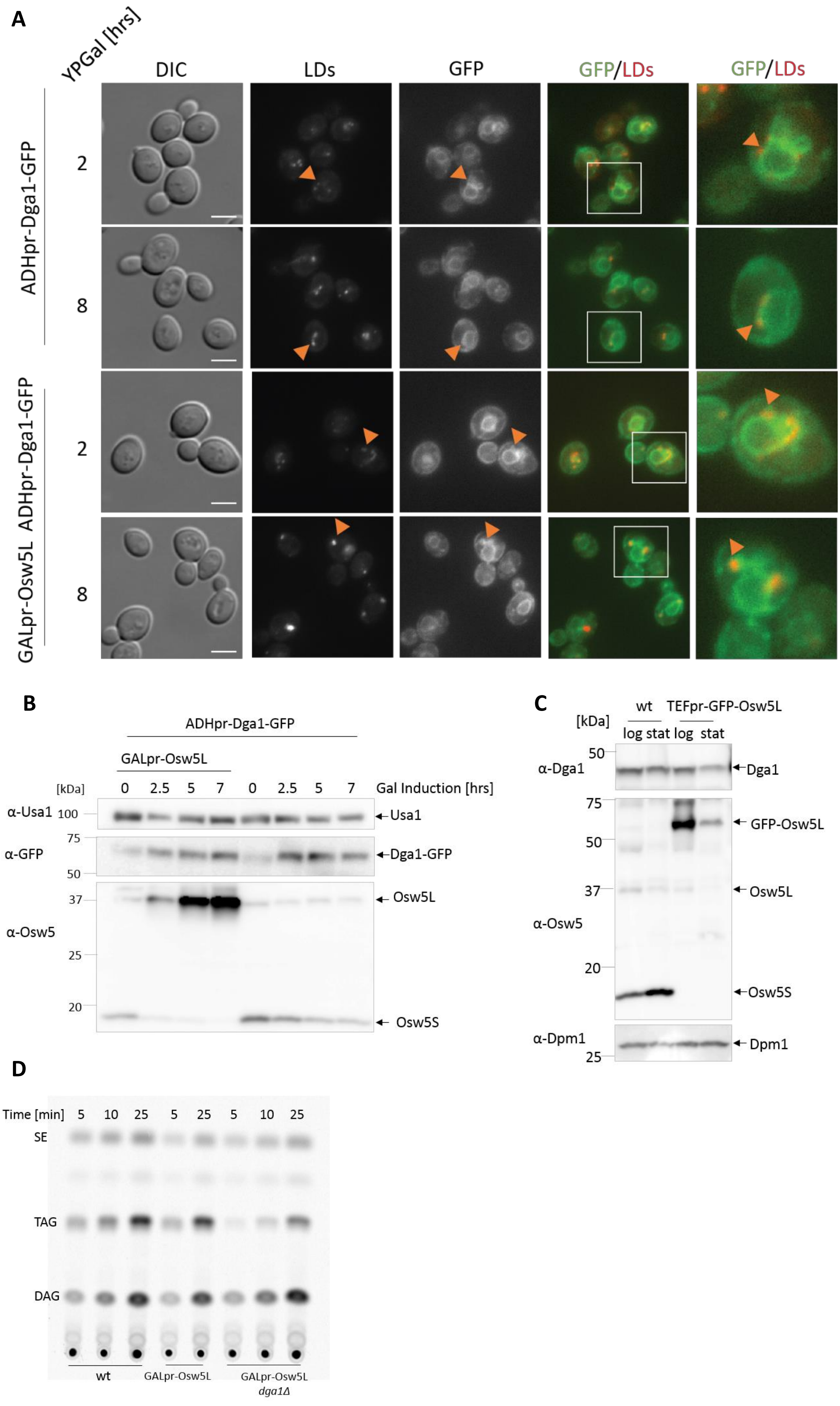

A
YPGal [hrs]
DIC
LDs
GFP
GFP/LDs
GFP/LDs
ADHpr-Dga1-GFP
2
8
GALpr-Osw5L ADHpr-Dga1-GFP
2
8
B
ADHpr-Dga1-GFP
GALpr-Osw5L
[kDa]
0 2.5 5 7 0 2.5 5 7 Gal Induction [hrs]
α-Usa1 100
Usa1
α-GFP
75
50
Dga1-GFP
α-Osw5
37
25
20
Osw5L
Osw5S
C
[kDa]
wt TEFpr-GFP-Osw5L
log stat log stat
α-Dga1
50
Dga1
75
GFP-Osw5L
50
37
Osw5L
α-Osw5
20
Osw5S
α-Dpm1
25
Dpm1
D
Time [min] 5 10 25 5 25 5 10 25
SE
TAG
DAG
wt
GALpr-Osw5L
GALpr-Osw5L
dga1Δ

Figure 3.10. Dga1 is not directly influenced by Osw5L overexpression.
(A) Cells were grown over night in YP + Raffinose and diluted to OD_{600} = 1 in YPGal. Samples were taken after 2 and 8 hrs and imaged. LDs were stained with MDH. Arrows indicate Dga1-LD co-localization. Scale bars indicate 5 µM. Inlay as indicated. (B) Western-blot analysis of cells with indicated genotype grown over night in YP + Raffinose and diluted to OD_{600} = 1 in YPGal. Samples were taken after 2.5, 5, and 7 hrs. Usa1 is the loading control. (D) Cells with the indicated genotype were grown in YPD to logarithmic and stationary phase, a sample was taken and subsequently analyzed by western-blot. (E) Microsomes were prepared from the indicated strains and incubated with DAG and radiolabled Oleyl-CoA to assay Dga1 activity. Samples were taken at 5, 10 and 25 min for wt and Galpr-Osw5L *dga1Δ* strains and at 5 and 25 min for Galpr-Osw5L cells. Neutral lipids were extracted and analyzed by TLC.

3.7.1. Osw5L overexpression does not influence Dga1 abundance, localization, or activity

Based on these findings, we reasoned that Osw5L could act on Dga1 directly in three different ways: Raising Dga1 protein levels, locally concentrating TAG synthesis, or promoting Dga1 activation.

First, we tested by western-blot if Dga1 protein levels were elevated in cells overexpressing Osw5L (Fig. 3.10C). Dga1 levels were not changed, neither in logarithmic nor in stationary growth phase.

Second, we tested if Dga1-GFP concentrated in proximity to LD aggregates upon Osw5L overexpression. To unambiguously detect Dga1, Dga1-GFP was expressed from the constitutive ADH-promoter (ADHpr-Dga1-GFP). Using wide-field microscopy, we followed Dga1-GFP localization upon Osw5L induction from the GAL-promoter over time (Fig. 3.10A, B). In control cells with intrinsic Osw5L levels, Dga1-GFP was distributed throughout the ER and at later time points located to LD as described in Jacquier, Choudhary et al. (2011). When Osw5L was overexpressed, we saw no differences in Dga1-GFP distribution and LD aggregates formed over time as expected. After 8 hours of Osw5L overexpression, Dga1-GFP enclosed the LD aggregates. However Dga1-GFP rather seems to be localized to ER membranes in closed contact to LD aggregates than to the LD aggregates itself (Fig. 3.10A). Therefore, Osw5L overexpression did not induce Dga1-GFP concentration at LD aggregates which argues against enhanced local synthesis at the sites of LD formation.

Last, we analyzed if Osw5L overexpression stimulated TAG synthesis by increasing Dga1 enzyme activity (Fig. 3.10D). We isolated ER microsomes from wild-type cells, Osw5L overexpressing cells and, as a control, cells combining Osw5L with *DGA1* deletion. Microsomes were incubated as described by Oelkers, Cromley et al. (2002) with radioactively labeled ^{14}C-Acyl-CoA and Dga1 activity was assayed after 5, 10, and 25 minutes and lipids were extracted and separated by thin layer chromatography. TAG levels increased over time in all the samples as expected, but no difference between samples could be observed. Hence, Dga1 enzyme activity was not influenced by Osw5L overexpression.

In conclusion, under the experimental conditions tested Osw5L did not seem to influence Dga1 abundance, localization, or activity directly. Possibly the methods used were not sensitive enough to detect changes in localization or activity.

Alternatively, increased precursor levels could lead to increased TAG levels by increasing flux trough the TAG synthesis pathway. In the *in-vitro* assay we provided external DAG, the TAG precursor, which might have masked such differences and prevented their detection (Fig. 3.10D).

As a third possibility which could lead to more TAG in cells, we suggest reduced lipid mobilization from LDs. Impaired lipolysis should be analyzed in future experiments.

3.8. Osw5L overexpression leads to targeting defect of lipid droplet proteins

Next, we asked if overexpression of Osw5L had an effect on the localization of well-characterized LD proteins. By microscopy we imaged the fluorescently tagged LD proteins Pet10, Erg6, Tgl3, and Ldh1. Erg6, Tgl3, and Ldh1 function in lipid biosynthetic pathways (Leber, Zinser et al. 1994, Athenstaedt and Daum 2003, Thoms, Debelyy et al. 2011), Pet10 function is currently unknown, but all are *bona fide* LD protein (Currie, Guo et al. 2014).

When we looked at stationary phase cells, each of the respective proteins localized to the LD, as expected. Upon Osw5L overexpression Pet10, Erg6, Tgl3, and Ldh1 were excluded from most of the LD aggregates (Fig. 3.11). These results suggest a general defect

in protein targeting to LDs induced by overexpression of Osw5L. The proteins tested use different motifs to target LDs. Whereas Erg6 behaves as an integral membrane protein that is first inserted into the ER and subsequently targeted to the LDs (Leber, Zinser et al. 1994), Tgl3 and Ldh1 are a soluble proteins which associated peripherally with the LD (Athenstaedt and Daum 2003, Thoms, Debelyy et al. 2011). Not much is known about Pet10, however it is thought to be soluble and also target from the cytosol to LDs.

What caused these targeting effects is unclear, however there are several possible mechanisms. First, the mistargeting of these four proteins could be due to sterical hindrance by the overexpressed protein localized in close proximity to the LD aggregate itself (Fig. 3.8). Second, an alteration of the LD surface could impede its recognition by Erg6, Tgl3, Pet10, and Ldh1 and thus their targeting. Third, abnormal ER-LD contact sites could also hinder correct LD targeting.

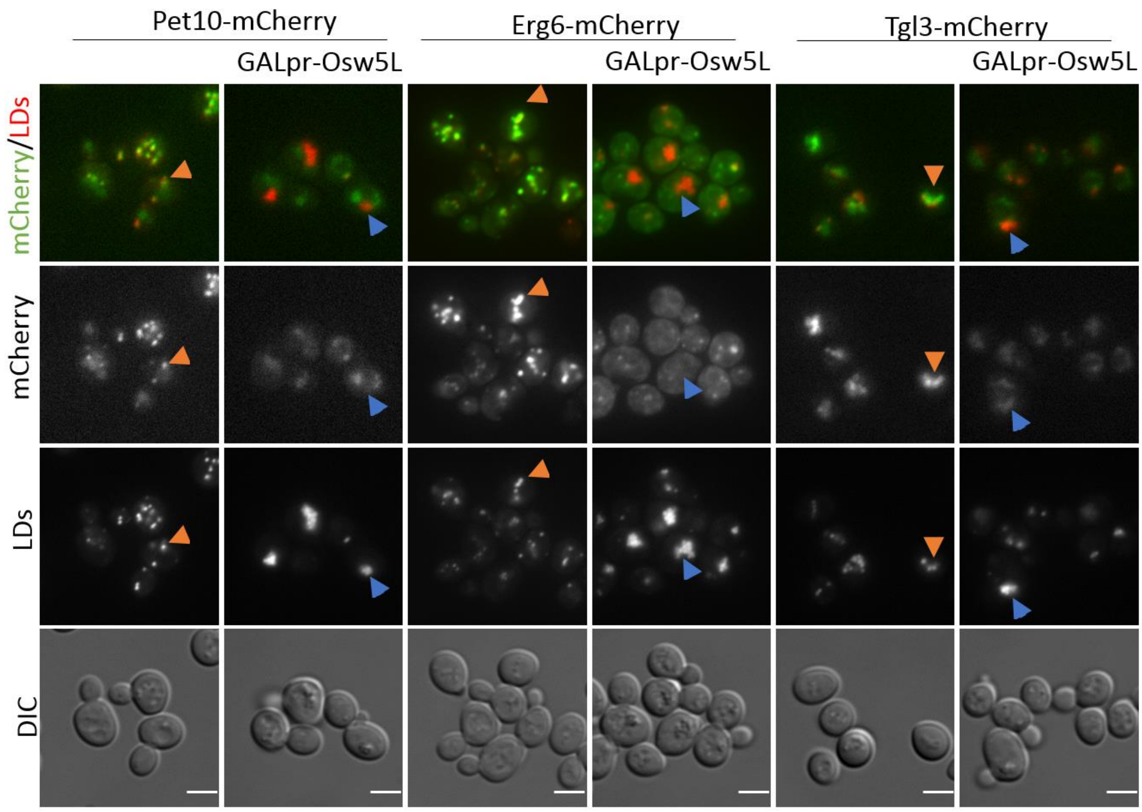

Figure 3.11. LD proteins are excluded from Osw5L overexpression induced LD aggregates.
Cells with the indicated genotype were grown to logarithmic phase in YPGal and imaged. LD were stained with MDH. Orange arrows indicate co-localized proteins with LDs. Blue arrows indicate LD aggregates and LD proteins alone. Scale bar is 5 µM.

3.9. Osw5L /Osw5S deletion cause only minor changes in the lipid droplet proteome

Our group previously showed that mutations in the Seipin core components Ldb16 and Fld1 result in major defects in LD protein targeting (Grippa, Buxo et al. 2015). In this study they isolated high pure LDs from a wild-type strain and strains deleted for either *FLD1* or *LDB16*. LD proteins were isolated, analyzed by quantitative mass spectrometry and subsequently LD proteomes from all strains were compared. In *ldb16Δ* and *fld1Δ* cells, 26 LD proteins were reduced 1.2-8x (log_2) from LDs compared to wild-type LDs (Grippa, Buxo et al. 2015).

Since Osw5L and Osw5S form a complex with Ldb16 and Fld1 we analyzed the LD proteome of *osw5LΔ osw5SΔ* cells by quantitative mass spectrometry. In contrast with LDs isolated from *fld1Δ* and *ldb16Δ*, the proteome of LDs isolated from *osw5LΔ osw5SΔ* cells was mostly similar to the one of LDs from wild-type cells (Table 3.1). Only few proteins were slightly reduced from LDs in *osw5LΔ osw5SΔ* cells. To independently confirm these result, we GFP-tagged most proteins and analyzed their subcellular localization (data not shown). We only found a striking change in the localization of the Sec14 family protein Pdr16 (also called Sfh3), which was lost from LD upon Osw5L/Osw5S deletion (Fig. 3.12A, 3.13A). Pdr16 is a lipid transfer protein and presumably shuttles PI and sterols between membranes. It is also involved in sterol homeostasis (Li, Routt et al. 2000, Yang, Tong et al. 2013, Holic, Simova et al. 2014). Mass spectrometry and target validation was done in cells where both ORFs, *YMR147W* and *YMR148W*, were deleted. Therefore, we next asked the question if Pdr16 mislocalization was due to the absence of Osw5S or the fusion protein Osw5L.

ID	Description	logFC
YBR204C	Ldh1	-1,95
YNL231C	Pdr16	-1,69
*YOR377W	Atf1	-1,20
YIL124W	Ayr1	-1,20
YBR177C	Eht1	-0,98
YMR110C	Hfd1	-0,85
YOR317W	Faa1	-0,84
YML008C	Erg6	-0,79
YKL094W	Yju3	-0,71
YKR046C	Pet10	-0,54
YLL012W	Yeh1	-0,42
*YOR246C	Yor246c	-0,40
YOR081C	Tgl5	-0,21
YKR067W	Gpt2	-0,21
YOR059C	Yor059c	-0,18

Table 3.1. Proteins depleted from LDs upon Osw5L deletion.
LD were isolated from wt and *osw5LΔ osw5SΔ* cells and analyzed by mass spectrometry. The table shows the log_2 –fold change of the indicated protein in the mutant cells respective to the wt sample. Negative numbers indicate depletion in the *osw5LΔ osw5SΔ* cells. Protein LD localization and change were tested by GFP tagging the protein of interest and deleting Osw5L/Osw5S in all strains (except *Atf1-GFP and *Yor246c-GFP due to a lack of GFP signal).

3.9.1. Pdr16 lipid droplet recruitment depends on Osw5L

Pdr16 is a cytosolic protein and usually recruited to LD in logarithmic and stationary cells. Upon Osw5L/Osw5S deletion LD localization was lost and Pdr16 became cytosolic (Fig. 3.12A, 3.13A). This was not due to altered Pdr16 levels, which were maintained in the mutants (Fig 3.11B, 3.12B). To investigate whether loss of Osw5L, Osw5S, or both lead to Pdr16 mislocalization, we tried to rescue targeting in *osw5LΔ osw5SΔ* cells by expressing either Osw5L or Osw5S from a plasmid. Strikingly, only the expression of Osw5L but not Osw5S rescued Pdr16 targeting to LDs (Fig. 3.12A).

To confirm this data, we GFP-tagged the chromosomal copy of Pdr16 in wild-type, *osw5LΔ osw5SΔ*, and *ymr147Δ* cells (Fig. 3.13). Pdr16 LD localization was lost in the double mutant, as described before, and also the presence of Osw5S in the *ymr147Δ* strain did not rescue LD targeting. This confirms our previous finding that Pdr16 recruitment to LDs dependents on the fusion protein Osw5L and not Osw5S.

This was very interesting, since Osw5L is an ER integral membrane protein, as shown before, and therefore it is implausible that Osw5L acts as a receptor for Pdr16 on the LD. However, it is more likely that Osw5L is involved in controlling the surface properties of the LD.

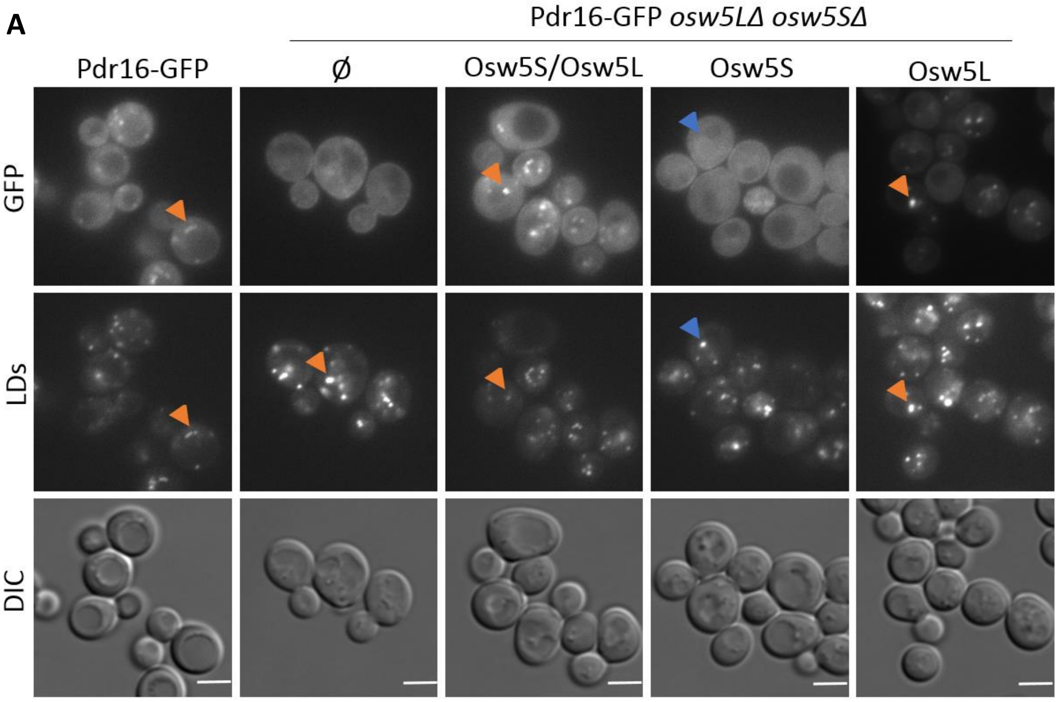

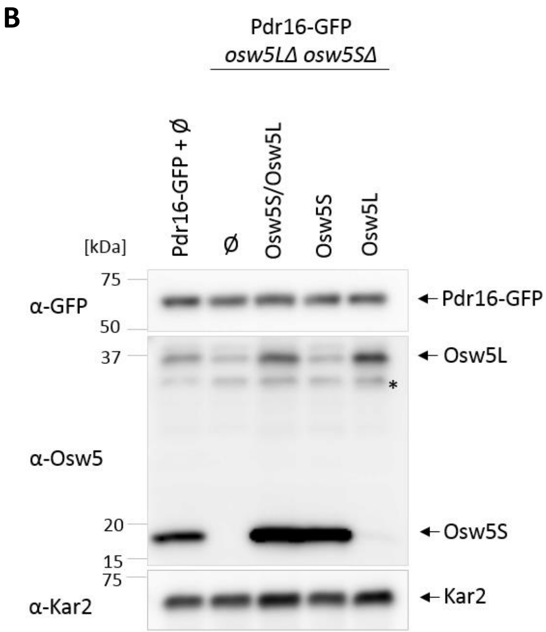

Figure 3.12. Pdr16 LD recruitment depends on Osw5L.
(A) Cells harboring Pdr16-GFP and Pdr16-GFP *osw5LΔ osw5SΔ*, respectively were transformed with a plasmid harboring the Osw5L/Osw5S wt locus or expressing either Osw5L or Osw5S alone. Pdr16-GFP alone was used as control. Cells were grown in SC dropout media to logarithmic phase and imaged. Orange arrows indicate overlapping GFP and LD signal. Blue arrows indicate LDs alone. Scale bar indicates 5 µM.
(B) Samples from (A) were analyzed via western-blot. Kar2 was used as a loading control.

3.9.2. Pdr16 lipid droplet recruitment is mediated trough distinct LD surface properties

Grippa, Buxo et al. (2015) showed, that aberrant LDs in Seipin mutants had altered surface properties which were recognized by certain proteins. Therefore, we assayed Pdr16 localization in cells deleted for Seipin complex mutants alone or in combination with *osw5LΔ osw5SΔ* (Fig. 3.13A). Cells lacking Seipin complex components show very heterogeneous LD sizes. LDs are either supersized or small and clustered. LD proteins which, in wild-type cells, target to LDs evenly, are either recruited to supersized LDs or LD clusters, but not to both in Seipin complex mutants (Wang, Miao et al. 2014, Grippa, Buxo et al. 2015). Upon Seipin complex deletion, Pdr16-GFP targeted LD aggregates and not supersized LDs (Fig. 3.13A). When we deleted *osw5LΔ osw5SΔ* on top of Seipin complex mutants, we saw no change in localization. This again argues against Pdr16 recruitment to LD through a direct interaction with Osw5L. It is more likely that Pdr16 recognizes other features of the LD surface.

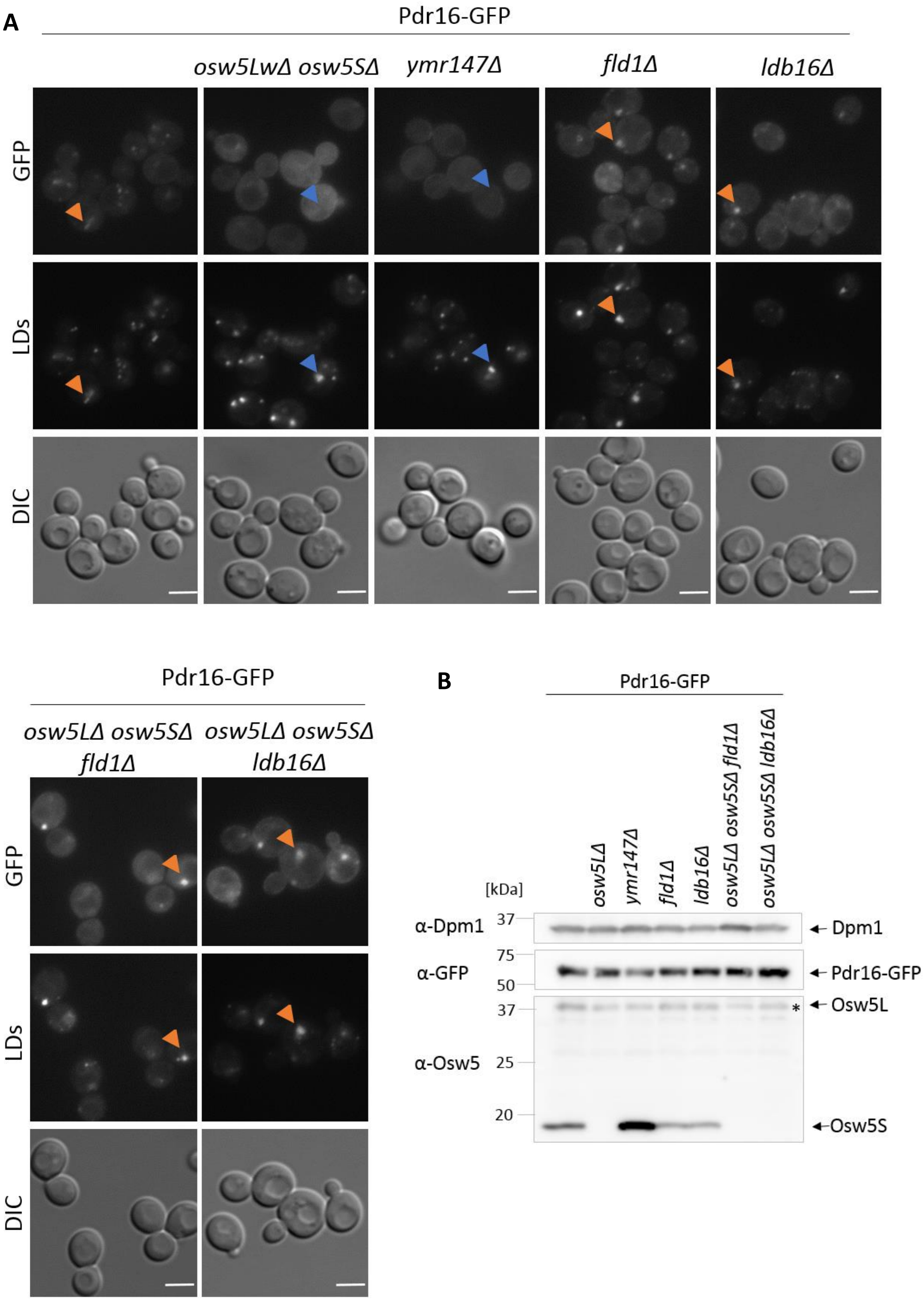

Figure 3.13. Pdr16 LD recruitment is mediated trough distinct LD surface properties.
(A) Cells were grown in YPD to early stationary phase and imaged. LDs were stained with MDH. Orange arrows indicate co-localizing GFP and LD signal. Blue arrows indicate LDs alone. Scale bar is 5 µM. (B) Cells of the indicated genotypes were grown in YPD to logarithmic phase and analyzed by western blot. Dpm1 was used as a loading control. Below the specific Osw5L band lies an unspecific signal. *unspecific band

3.9.3. Pdr16 lipid droplet recruitment is not responsible for increased TAG levels in Osw5L overexpressing cells

If Osw5L has a direct role in recruiting Pdr16, than its overexpression should lead to increased concentration of Pdr16 on Osw5L induced LD aggregates. We tagged Pdr16 with GFP in a strain overexpressing Osw5L, and Osw5S as control, and imaged the cells. Indeed, Pdr16 was heavily recruited to LD aggregates upon Osw5L overexpression (Fig 3.14A). Osw5S overexpression did not promote Pdr16 recruitment. This was not due to increased Pdr16 levels which were maintained in all strains (Fig. 3.14B).

As mentioned earlier, Osw5L overexpression leads to LD accumulation and elevated TAG levels. Now we tested whether the extensive Pdr16 recruitment to the LD aggregates was responsible for these increased TAG levels in these cells. Deleting *PDR16* in Osw5L overexpressing cells did neither affect TAG content nor LD clustering as shown by microscopy and biochemistry (Fig. 3.14 A, C). Therefore, Pdr16 recruitment was caused by Osw5L overexpression but did not contribute to the LD phenotype.

In summary, under wild-type conditions Pdr16 localizes to LDs (Fig 3.12A, 3.13A). Recruitment to LDs was abolished upon Osw5L/Osw5S deletion (Fig 3.12A, 3.13A). In rescue experiments in this strain, expression of Osw5L but not Osw5S re-established LD targeting (Fig. 3.12A). On the same line, Osw5L overexpression induced strong Pdr16 recruitment to LDs (Fig. 3.14A). In Seipin complex mutants LDs are altered as described before (Szymanski, Binns et al. 2007). In these mutants, Pdr16 localized to LD clusters and this localization was independent of the presence of Osw5L/Osw5S (Fig. 3.13A). Altogether, our data suggests that Pdr16 LD recruitment depends on, but was not directly mediated by, Osw5L. Osw5L could alter surface properties of the LDs itself. Consequently, we propose that Osw5L is involved in modulating the LD surface.

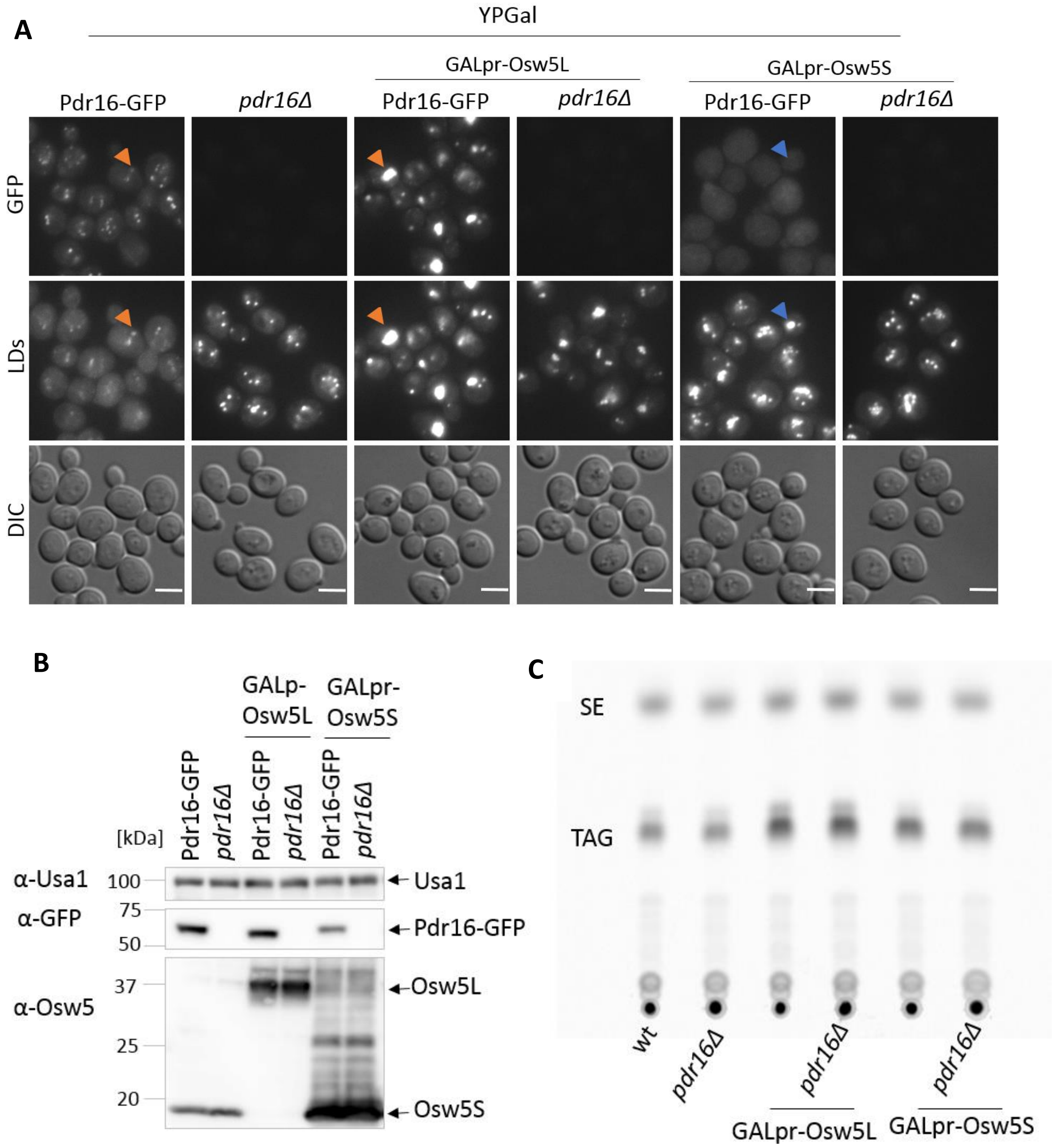

Figure 3.14. Pdr16 LD recruitment is an effect of Osw5L overexpression.

(A) Cells were grown in YPGal to logarithmic phase and imaged. LDs were stained with MDH. Orange arrows indicate overlapping GFP and LD signal. Blue arrows indicate LDs alone. Scale bar is 5 µM. (B) Cells of the indicated genotypes were grown in YPGal to logarithmic phase and analyzed by western blot. Usa1 was used as a loading control. (C) Cells of the indicated genotype were grown in YPGal, diluted to OD_{600} 0.1 and grown for 24 hours in presence of 1 µCi/ml [1-14C]acetate and neutral lipids were extracted and separated by TLC.

3.9.4. Pdr16 lipid droplet recruitment is not mediated by its PI binding capacity

Pdr16 is a lipid transfer protein and thought to bind and shuttles sterols and PI between membranes (Holic, Simova et al. 2014). To understand which molecule or membrane feature Pdr16 could recognize on the LD surface, we made use of the Pdr16$^{E235A, K267A}$ mutant (Holic, Simova et al. 2014). The point mutation in the protein interferes with its PI binding capacity and therefore this Pdr16 mutant binds exclusively sterols and no PI.

To test whether it is still recruited to Osw5L induced LD aggregates, we assayed its localization in the cell via microscopy. Pdr16-GFP and its derivatives were expressed from the endogenous PDR16 promoter in a low copy plasmid and its localization analyzed by live cell microscopy.

In wild-type cells, most Pdr16 localized to LDs, however some of plasmid born Pdr16-GFP also localized to the plasma membrane (Fig. 3.15A). These changes can be due to increased levels of plasmid born Pdr16-GFP (Fig. 3.15C). In *osw5LΔ osw5SΔ* cells, LD localization of plasmid born Pdr16-GFP was greatly reduced but, in contrast with the chromosomally expressed Pdr16, not completely abolished (Fig. 3.12A, 3.13A, 3.15A). As well as the chromosomally tagged Pdr16, plasmid born Pdr16-GFP was strongly recruited to LD aggregates in Osw5L overexpressing cells. Osw5S overexpression did not promote recruitment. PI defective Pdr16$^{E235A, K267A}$-GFP showed the same LD localization pattern as wild-type Pdr16-GFP. Thus, loss of PI binding capacity in mutant Pdr16-GFP did not affect its localization.

Hence, Pdr16 LD recruitment to LD aggregates is probably not mediated, at least exclusively, by PI.

A

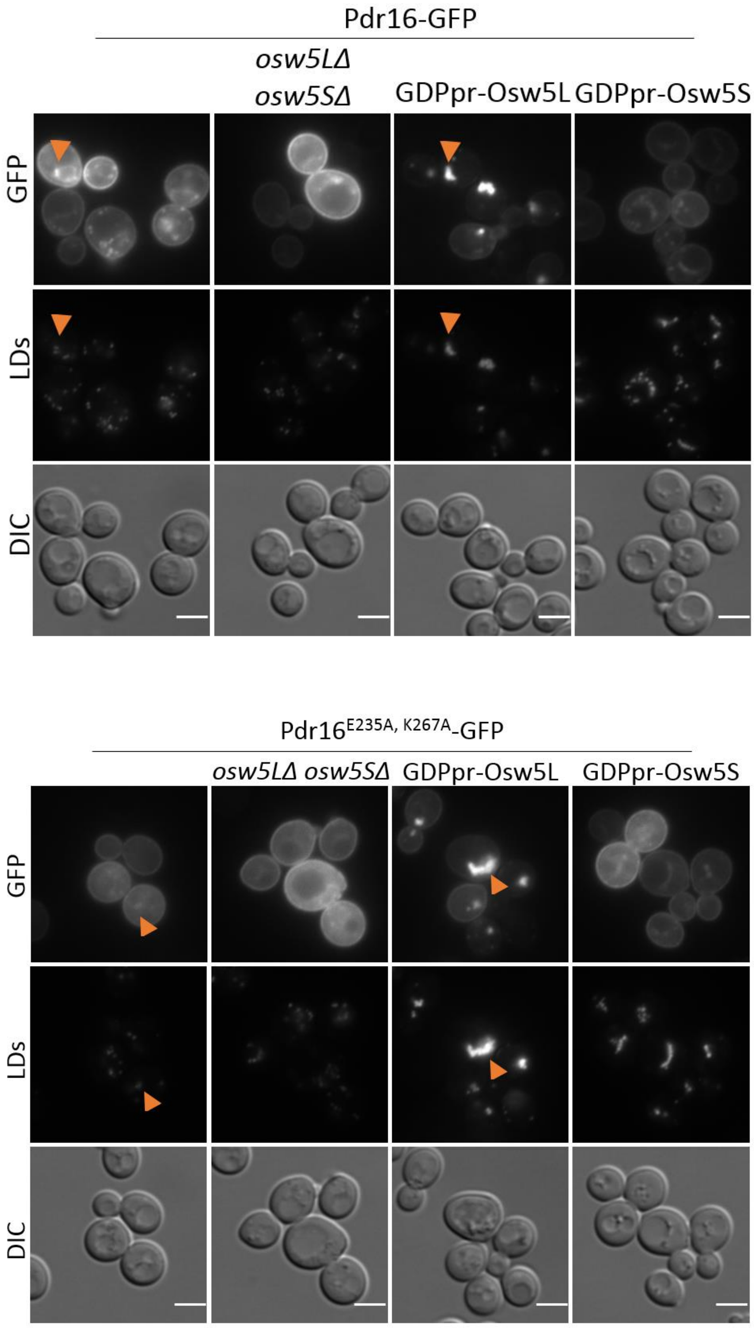
Pdr16-GFP
osw5LΔ osw5SΔ
GDPpr-Osw5L
GDPpr-Osw5S
GFP
LDs
DIC
Pdr16E235A, K267A-GFP
osw5LΔ osw5SΔ
GDPpr-Osw5L
GDPpr-Osw5S
GFP
LDs
DIC

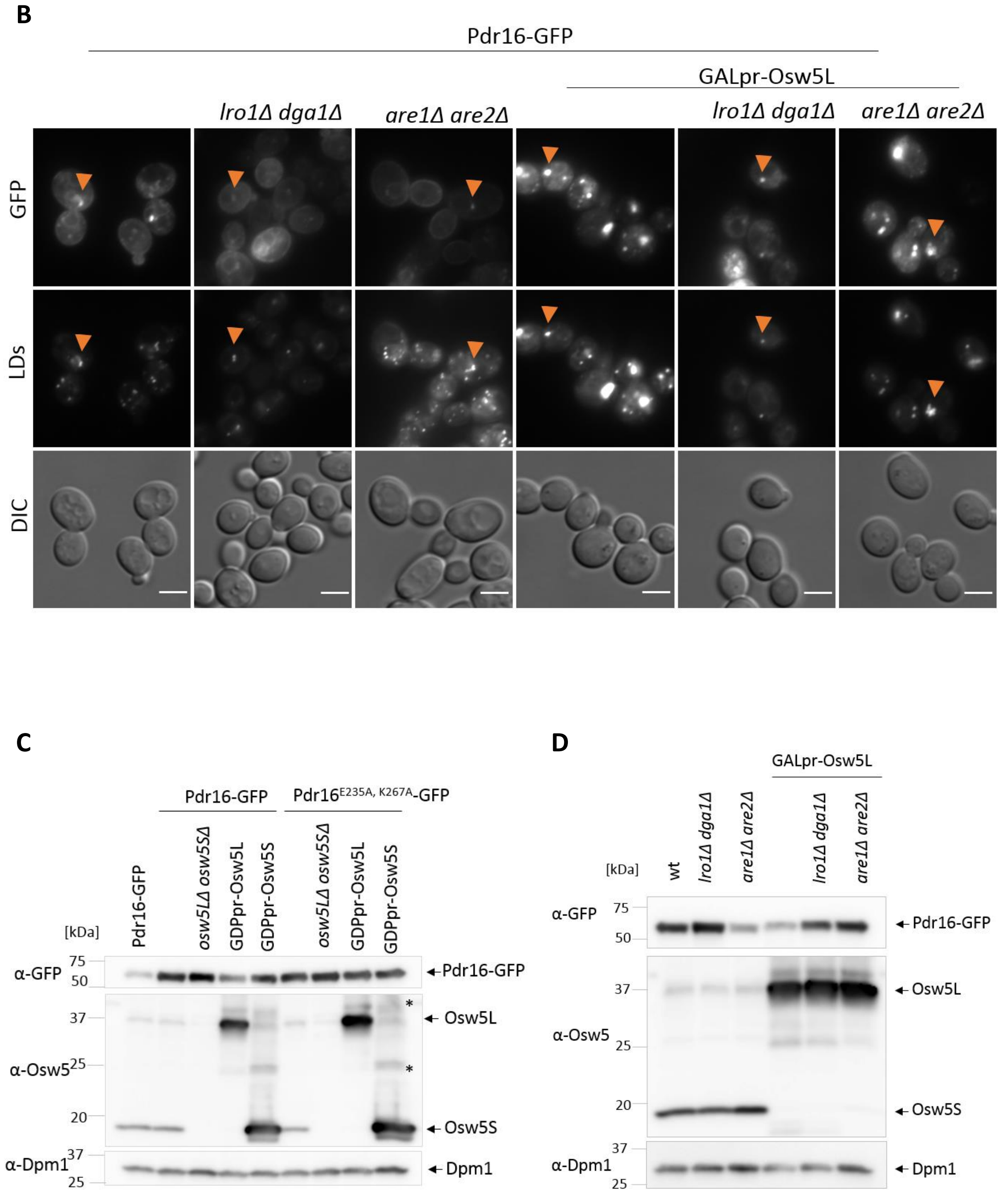

Figure 3.15. Pdr16 recruitment is independent of PI and LD content.

(A) Cells were grown in SC dropout media to logarithmic phase and imaged. Pdr16-GFP is expressed from a plasmid. Orange arrows indicate co-localizing GFP and LD signal. Scale bar is 5 µM. (B) Cells were grown in SC dropout media with galactose to logarithmic phase and imaged. Pdr16-GFP is expressed from a plasmid. Orange arrows indicate overlapping GFP and LD signal. Scale bar in 5 µM. (C) Cells of the indicated genotypes were grown in SCGal dropout media to logarithmic phase and analyzed by western blot. Dpm1 was used as a loading control. (D) Cells of the indicated genotypes were grown in SC dropout media to logarithmic phase and analyzed by western blot. Dpm1 was used as a loading control.

3.9.5. Pdr16 lipid droplet recruitment is independent of lipid droplet content

Pdr16 does not only have the capacity to bind PI, but also sterols (Holic, Simova et al. 2014). Ergosterol synthesis in yeast is a complicated process with about 30 enzymes involved, localized to ER and LD (Natter, Leitner et al. 2005, Klug and Daum 2014). To store sterols, they are esterified by two ergosterol acyl transferases, Are1 and Are2, and subsequently deposited into LDs (Yang, Bard et al. 1996, Yu, Kennedy et al. 1996). Upon deletion of *ARE1* and *ARE2*, no ergosterol esters can be synthesized (Yang, Bard et al. 1996). We deleted *ARE1* and *ARE2* or *DGA1* and *LRO1* in combination and assayed Pdr16-GFP recruitment via microscopy. The LDs of these cells contain exclusively SE or TAG, respectively (Yang, Bard et al. 1996, Oelkers, Cromley et al. 2002).

Plasmid born Pdr16-GFP was recruited to LDs independent of their content (Fig. 3.14B). When we additionally induced Osw5L overexpression, Pdr16-GFP was strongly recruited to LD aggregates. This was also true for cells containing LDs exclusively made of SE (*dga1Δ lro1Δ*) or TAG (*are1Δ are2Δ*), although total LD numbers were reduced in these cells, as expected (Yang, Bard et al. 1996, Oelkers, Cromley et al. 2002, Sandager, Gustavsson et al. 2002). Therefore, neither sterol esters nor TAG composition of LDs were recognized by Pdr16 on the LD surface and thus are probably not involved in Pdr16 LD targeting.

3.10. Kes1 is recruited to lipid droplet aggregates in Osw5L overexpressing cells

As mentioned before, in yeast the Seipin complex at the ER-LD contact site is important to establish organelle identity. Thus, it has been proposed to act as a diffusion barrier for proteins as well as phospholipids (Szymanski, Binns et al. 2007, Wang, Miao et al. 2014, Grippa, Buxo et al. 2015). LD phenotype as well as LD proteome in Seipin complex mutants are highly altered (Grippa, Buxo et al. 2015). Many *bona fide* LD proteins are absent from these aberrant LDs. However, some proteins that in wild-type cells are absent from LD, are also ectopically recruited to LD aggregates from the cytosol in Seipin mutant cells. Some examples are Kes1, Pct1, and Gvp36. These proteins share one common feature, an amphipathic helix. Grippa, Buxo et al. (2015) proposed that the proteins recognize membrane packaging defects on the aberrant LD surface with this amphipathic helix motif.

Since Osw5L and Osw5S are accessory proteins of the Seipin complex, we tested Kes1, Pct1, and Gvp36 localization in *osw5LΔ osw5SΔ* and Osw5L and Osw5S overexpressing cells. Indeed, Kes1 was recruited to LD aggregates in Osw5L overexpressing cells (Fig. 3.16C). This was not due to altered protein levels which were maintained in all strains (Fig. 3.16B). Kes1 harbors an amphipathic helix which senses membrane packaging defects, called ALPS motif (Drin, Casella et al. 2007). In Seipin mutants, this motif is necessary and sufficient to recruit Kes1 to *fld1Δ* and *ldb16Δ* induced LD aggregates (Fig. 3.16C) (Grippa, Buxo et al. 2015). However, this is not true for Kes1 in cells overexpressing Osw5L. Only full length Kes1 was recruited to LD aggregates, and not the amphipathic helix alone (Fig. 3.16C). Therefore, the reason why Kes1 is recruited to LD aggregates in Seipin complex mutants and Osw5L overexpressing cells, seems to be different.

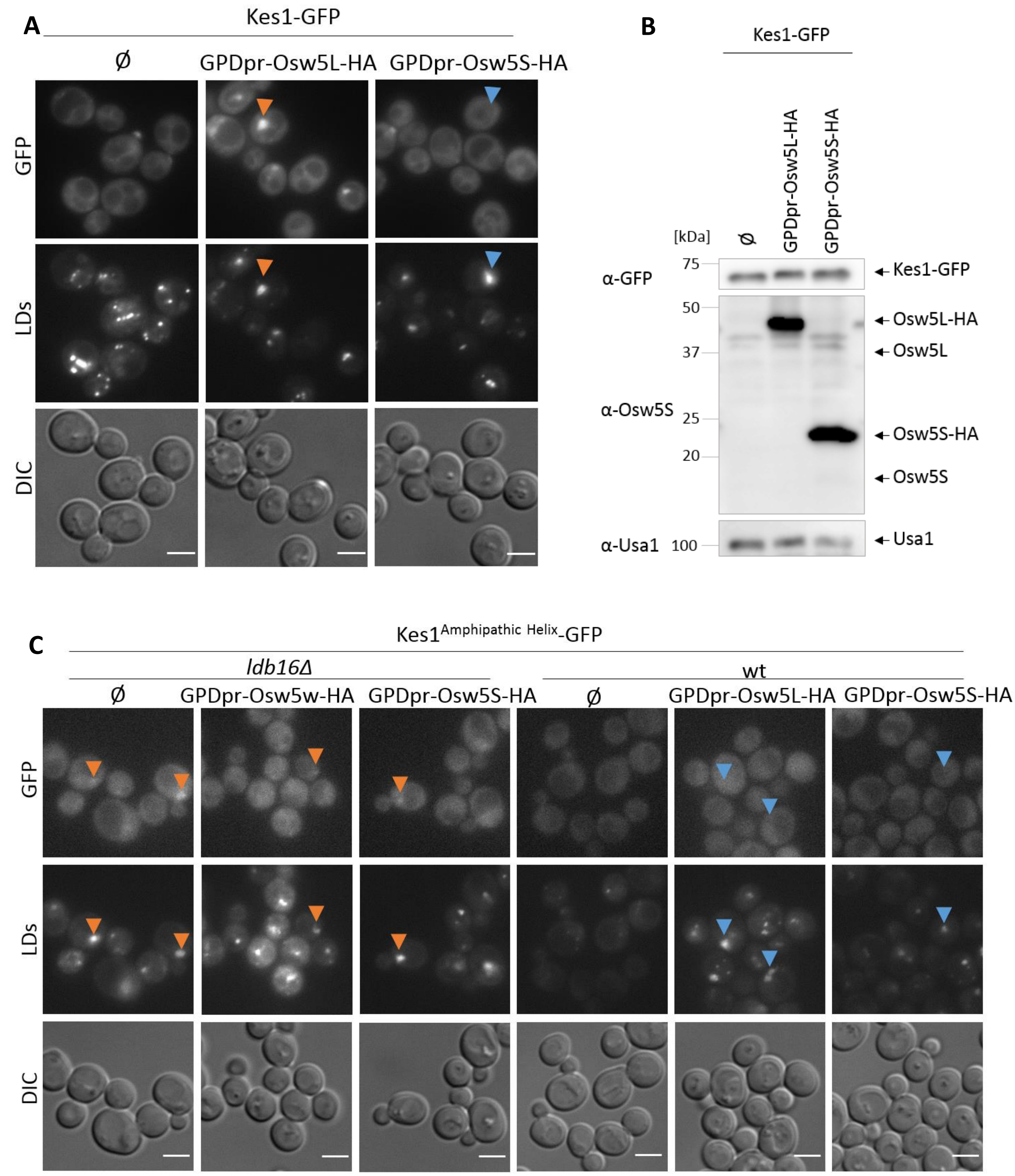

Figure 3.16. Kes1-GFP is recruited to Osw5L overexpression induces LD aggregates.
(A) Cells harboring a chromosomal GFP-tagged Kes1 were transformed with empty plasmid, GPDpr-Osw5L-HA, or GPDpr-Osw5S-HA. Cells were grown in SC dropout media to logarithmic growth phase and imaged. LDs were stained with MDH. Orange arrows indicate overlapping GFP and LD signal. Blue arrows indicate LDs alone. Scale bar indicates 5 µM. (B) Cells harboring a chromosomal GFP-tagged Kes1 were transformed with empty plasmid, GPDpr-Osw5L-HA, or GPDpr-Osw5S-HA. Cells were grown in SC dropout media to logarithmic growth phase and analyzed by western blot. Usa1 was used as a loading control. (C) Cells harboring a chromosomal GFP-tagged amphipathic helix of Kes1 were transformed with empty plasmid, GPDpr-Osw5L-HA, or GPDpr-Osw5S-HA. Cells were grown in SC dropout media to logarithmic growth phase and imaged. LDs were stained with MDH. Orange arrows indicate overlapping GFP and LD signal. Blue arrows indicate LDs alone. Scale bar indicates 5 µM.

3.11. Osw5L overexpression does not influence lipid distribution in the cell

Osw5L deletion dependent loss of Pdr16 LD localization, and Pdr16 and Kes1 recruitment to LD aggregates induced by Osw5L overexpression, argues for a role of Osw5L in modulating surface properties of LDs. Therefore, we analyzed the distribution of various lipid-binding fluorescent probes in Osw5L overexpressing and *osw5LΔ osw5SΔ* cells.

These probes consist of a specific lipid binding protein domain fused to a fluorescent protein and were visualized via light microscopy. We detected Phosphatidylinositol-4-Phosphate (PI(4)P) with the PH domain of Osh2 mCherry-2xPH[Osh2] (Fig. 3.17A) (Roy and Levine 2004, Yu, Mendrola et al. 2004), phosphatidylinositol-3-phosphate (PI(3)P) with the FYVE domain of Eea1 RFP-FYVE[EEA1] (Fig. 3.17B) (Hunyady, Baukal et al. 2002), phosphatidylinositol-4,5-biphosphate (PI(4,5)P2) with the PH domain of Phospholipase C GFP-2×PH(PLCδ) (Fig. 3.17C) (Stefan, Audhya et al. 2002), phosphatidylerin (PS) with the C2 domain of Lactadherin Lact-C2-GFP (Fig. 3.17D) (Yeung, Gilbert et al. 2008), and PA with the amphipathic helix of Spo20 GFP-Spo20 (Fig. 3.17E)(Nakanishi, de los Santos et al. 2004).

Although many results pointed to an imbalance of phospholipids on the LD surface, the distribution of the PI(4)P, PI(3)P, PI(4,5)P2, PS, and PA was not altered neither in cells overexpressing Osw5L, nor in *osw5LΔ osw5SΔ* cells. If there were such differences, we were not able to detect them with our fluorescent lipid binding probes.

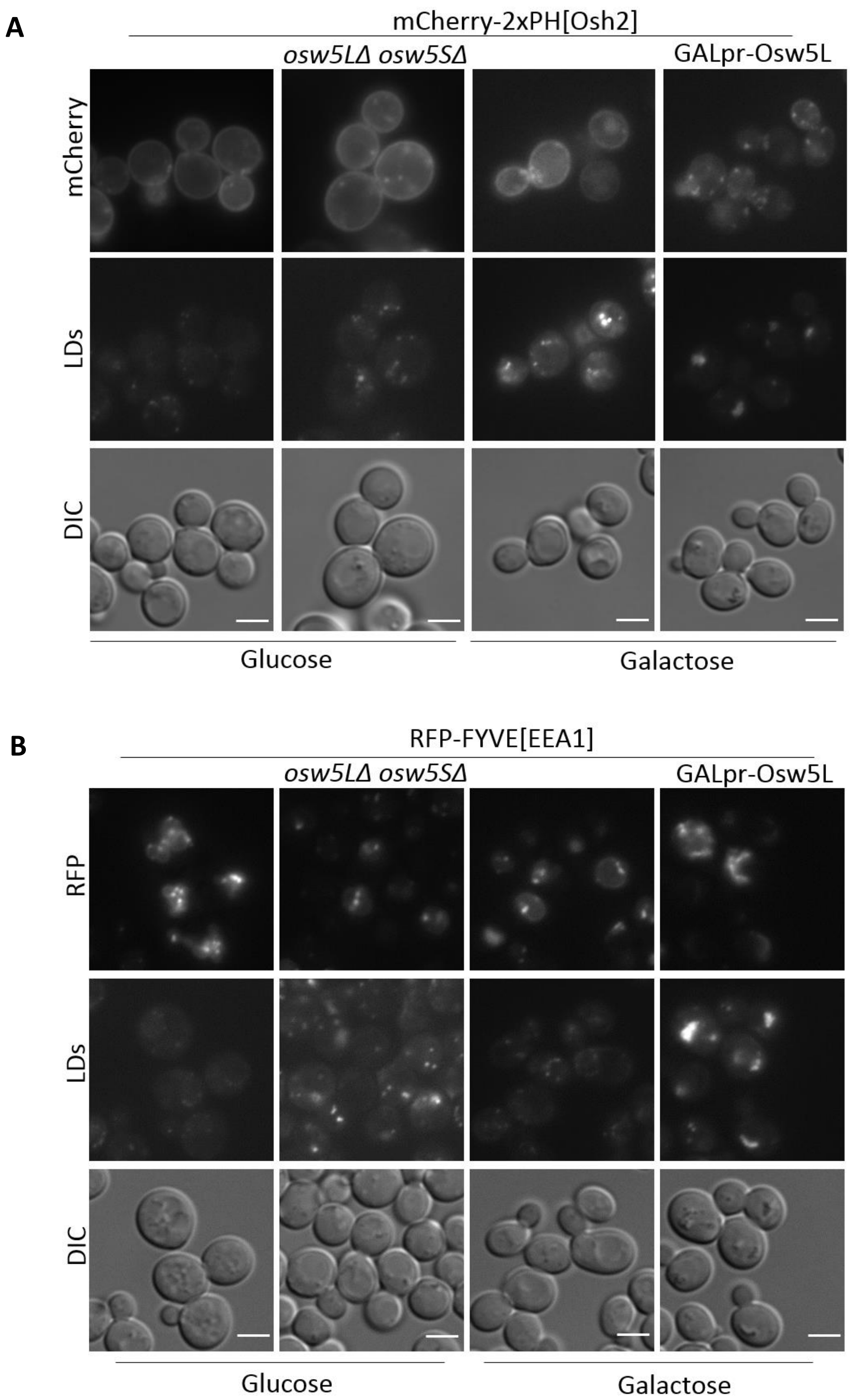
A
mCherry-2xPH[Osh2]
osw5LΔ osw5SΔ
GALpr-Osw5L
mCherry
LDs
DIC
Glucose
Galactose
B
RFP-FYVE[EEA1]
osw5LΔ osw5SΔ
GALpr-Osw5L
RFP
LDs
DIC
Glucose
Galactose

C

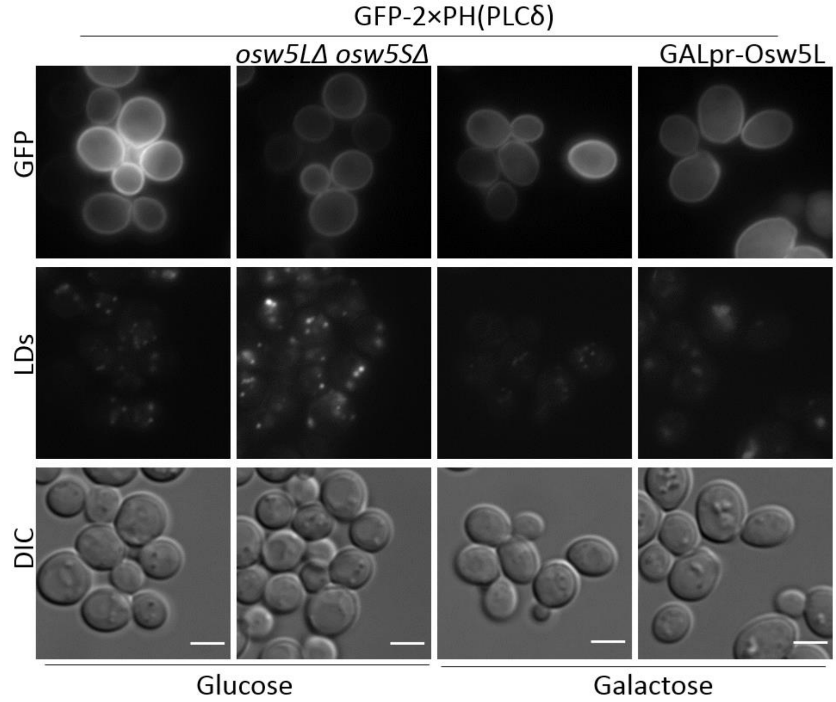
GFP-2×PH(PLCδ)
osw5LΔ osw5SΔ
GALpr-Osw5L
GFP
LDs
DIC
Glucose
Galactose

D

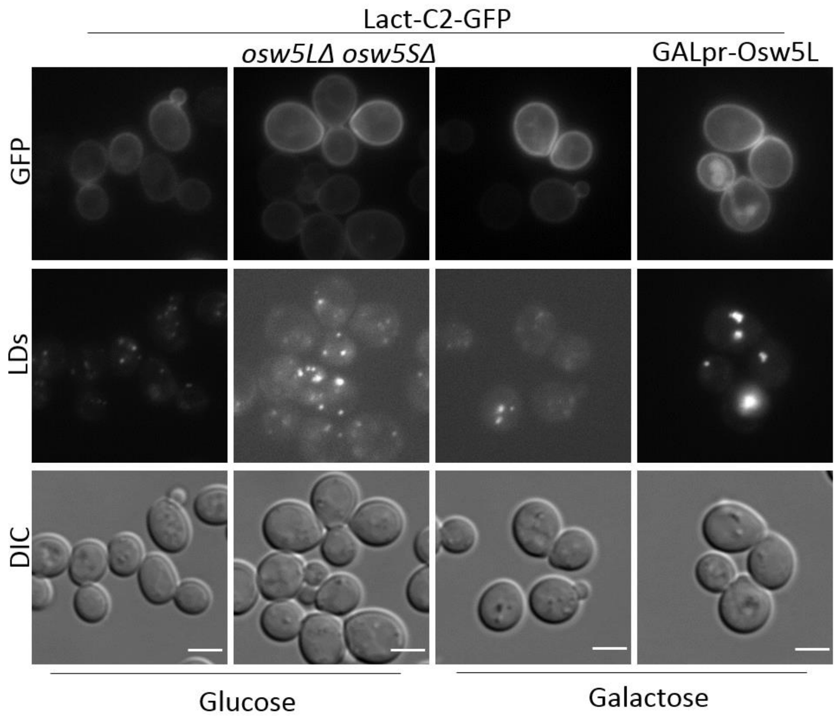
Lact-C2-GFP
osw5LΔ osw5SΔ
GALpr-Osw5L
GFP
LDs
DIC
Glucose
Galactose

E

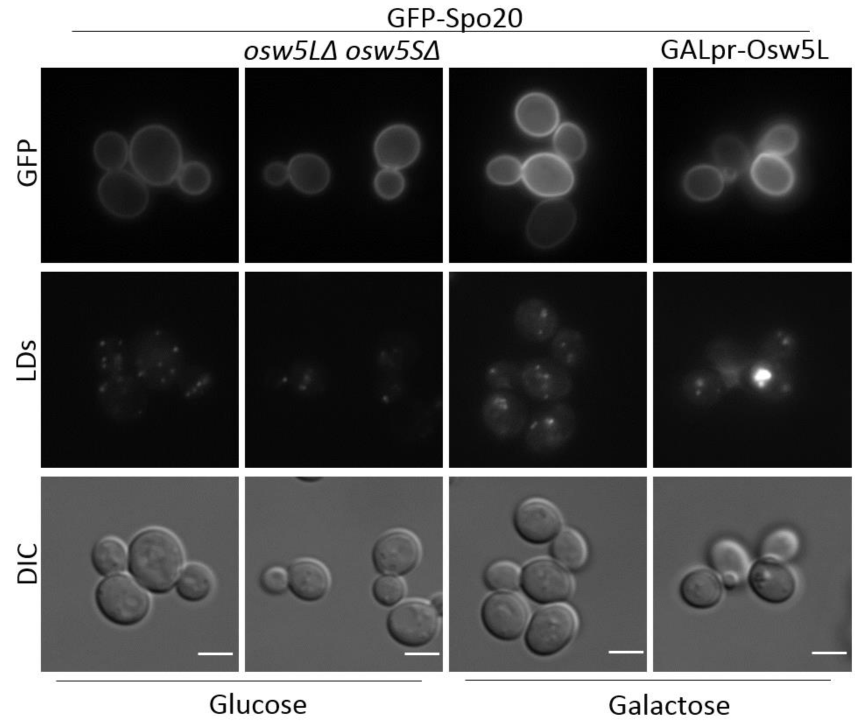

Figure 3.17. Fluorescent lipid binding probes in *osw5LΔ osw5SΔ* and Osw5L overexpressing cells.
Wt cells and cells harboring *osw5LΔ osw5SΔ* and GALpr-YMR147w were transformed with mCherry-2xPH[Osh2] (A), RFP-FYVE[EEA1] (B), GFP-2×PH(PLCδ) (C), Lac1-C2-p416-GFP (D), or GFP-Spo20 (E) and imaged in SC dropout media with glucose or galactose, respectively. Cells were grown to logarithmic growth phase and imaged. LDs were stained with MDH. Scale bar is 5 µM.

4. Discussion

In the cell, lipid droplets (LDs) serve as a general neutral lipid storage organelle. Lipid droplet dynamics, such as formation, breakdown, size and number, are tightly regulated in the cell. Deregulation of fat storage is linked to disease such as overweight, but also lipodystrophies as mentioned earlier. A gene frequently mutated in a Congenital Lipodystrophy Type II encodes for Seipin, a protein involved in LD regulation.

Grippa, Buxo et al. (2015) and others showed, that Seipin localizes to ER-LD contact sites and stabilizes them. Here it may act as a diffusion barrier, controlling the transfer of proteins and lipids between the two organelles. In yeast, Seipin consist of two proteins, Fld1 and Ldb16. Absence of either component of the Seipin complex leads to aberrant LD morphology. LD morphology depends on phospholipid availability. If few phospholipids are available in the cell, supersized LDs with a low surface-to-volume ratio are formed. If phospholipids are readily available, LDs are small and form clusters, overflown with membrane, with a high surface-to-volume ratio. Therefore, phospholipid availability in the cell seems to be directly reflected on the LD monolayer. Additionally, the phospholipid monolayer of these aberrant LDs seems to be altered. This leads to the loss of LD proteins or ectopic recruitment of non-LD proteins (Szymanski, Binns et al. 2007, Wang, Miao et al. 2014, Grippa, Buxo et al. 2015).

In this study, we characterized additional components of the Seipin complex: Osw5L and Osw5S, two isoforms of the same protein. Osw5S is generated from the ORF YMR148W/OSW5, while Osw5L is generated by a splicing reaction which joins the upstream ORF YMR147W with YMR148W/OSW5 and generates a fusion protein (Miura, Kawaguchi et al. 2006).

4.1. Differential regulation of Osw5 isoform suggests a link between cell metabolism and lipid droplet dynamics

Our data showed that the isoform abundance of both protein isoforms fluctuates depending on the metabolic state of the cells. As described earlier, Osw5L is especially expressed in logarithmic phase and its expression is undetectable by western-blot in stationary growth phase. However, Osw5S is expressed constitutively (Fig. 3.3). This switch-like behavior might point to a role in coupling the metabolic state of the cell to LD regulation.

Yeast cell metabolism undergoes extensive changes when glucose as a primary energy source is depleted from its growth media. Here, cells change from fermentative to respiratory growth, stop proliferating and go into quiescence also called stationary phase (Broach 2012). To achieve these changes, the cell needs to integrate and co-regulation various biochemical pathways, such as protein and lipid biosynthesis. A recent study by Casanovas, Sprenger et al. (2015) quantified the proteome and lipidome of a growing yeast cell culture from logarithmic to stationary phase and showed that these metabolic changes are achieved by co-regulating protein and lipid abundance. More specific, enzyme levels of specific lipid metabolic pathways can be correlated well with the abundance of their respective lipid species.

This study also showed, that neutral lipids in LDs undergo cycles of mobilization and storage prompted by growth and quiescence. For example, de-novo sterol synthesis is impeded in stationary phase cells, because they are not needed for cell metabolism. This is achieved by downregulation of sterol synthesizing enzymes (Casanovas, Sprenger et al. 2015). This is in concordance with the finding that protein levels of key enzymes of sterol synthesis pathways are very sensitive to metabolic perturbations. This sensitivity is achieved by their selective degradation by the ER-associated degradation (ERAD) pathway to fine-tune sterol synthesis in the cell (Foresti, Ruggiano et al. 2013).

A tight correlation of protein levels with their respective lipid metabolic pathways was not only described for neutral lipid metabolism, but also for sphingolipids. Thus, this seems to be a more general principle in the cell (Casanovas, Sprenger et al. 2015).

Differential regulation of Osw5 isoform abundance could therefore be linked to their growth stage-dependent cellular function in lipid metabolism and suggests a link between cell metabolism and LD dynamics. Future studies should focus in addressing this very interesting link.

4.2. Osw5 protein isoform abundance could be mediated by transcriptional regulation

Our data suggests, that differences in Osw5L to Osw5S ration are primarily due to changes in transcription. Expression of Osw5L or Osw5S depends on the usage of two different promoters, either before the YMR147W ORF or the YMR148W/OSW5 ORF. The splicing reaction itself, which fuses both ORFs and gives rise to OSW5L, seems not to be regulated (Fig 3.3, 3.8).

In yeast, the preferential use of glucose as carbon source is regulated by a glucose-induced transcriptional repression of genes required for the metabolism of other sugars (Broach 2012). In response to declining glucose levels in the media, the Snf1 kinase complex induces about 400 genes involved in stimulation of glucose uptake and oxidation, stimulation of β-oxidation and inhibition of anabolic reactions. However, Snf1 directly regulates only about 10 % of these genes (Broach 2012). An example of direct regulation is the release of transcriptional repressor Mig1, which regulates genes involved in metabolizing alternative sugars (Schuller 2003). Additionally, Snf1 regulates expression of genes involved in ethanol metabolism and β-oxidation trough the transcription factor Adr1 (Broach 2012). Interestingly, Snf1 also directly regulates lipid metabolism by inactivating an enzyme responsible for fatty acid activation (Woods, Munday et al. 1994) and another enzyme involved in fatty acid de novo synthesis (Hofbauer, Schopf et al. 2014), thereby limiting fatty acid biosynthesis upon glucose depletion.

Since the Snf1 network links carbon and lipid metabolism it might be a good candidate for Osw5 protein transcriptional regulation. Experiments addressing this question would give valuable insight in Osw5 protein function.

4.3. Osw5 proteins act as accessory factors of the Seipin complex and independently

We found Osw5L and Osw5S co-precipitated with Fld1 and Ldb16 in immunoprecipitation experiments, and *vice versa* (Fig. 3.2). However, only a fraction of the proteins seem to be associated with the Seipin complex or the interaction was lost during handling. We found that two pool of Osw5S exist in the cell; one in the ER and a second one on LDs (Fig. 3.4, 3.1B). Therefore, it is not surprising to see only a fraction of Osw5S interacting with the ER-localized Seipin complex. These data point to a rather weak interaction of the Osw5 proteins with Seipin.

However, our experiments suggested that both Osw5 proteins had alternative functions outside of the Seipin complex.

In contrast to Seipin deletion mutants, the deletion of Osw5S had only mild effects on LD size (Fig. 3.5). This suggests, that the *osw5SΔ* LD phenotype could be independent of its function in the Seipin complex. Possibly it could be connected to its function as a LD protein. The absence of Osw5S on the droplet could impede lipolysis and therefore lead to bigger LDs. Further experiments are needed to clarify this.

Osw5L overexpression lead to increased TAG levels and LD clustering (Fig. 3.7). This phenotype was dosage dependent and could be observed already under mild overexpression conditions (Fig. 3.8). This data suggests, that the overexpression phenotype is independent of the physical interaction with Seipin core complex, since the proteins cannot form a stoichiometric complex under this conditions. Notably, the phenotype required the presence of Fld1-Ldb16 and therefore a functional ER-LD contact site (Fig. 3.7). This suggests, that it acts downstream of Seipin.

Taken together, our data suggest an accessory role of Osw5L and Osw5L in ER-LD contact site assembly and function with Seipin and possible functions in LD homeostasis outside of the Seipin complex.

4.4. Dga1 mediates TAG synthesis in cells overexpressing Osw5L

As a result of Osw5L overexpression, yeast cells accumulated more TAGs as control strains (Fig. 3.7). Electron microscopy confirmed that the TAG is packed into *bona fide* LDs (Fig. 3.6). Our data shows that TAG accumulation is abrogated if the Diacylglycerol-O-transferase Dga1 is deleted (Fig. 3.9). Therefore, stimulated TAG synthesis is mediated by Dga1. We tested if Dga1 levels, its localization or its activity were altered in cells overexpressing Osw5L (Fig. 3.10). According to our findings, none of these were the case. However, we cannot exclude that our methods, especially the enzymatic assay for Dga1 activity, were not sensitive enough to detect such differences.

In conclusion, our data suggests that elevated TAG levels are not due to a direct influence on Dga1 levels, activity or distribution. Therefore, Osw5L could possibly increase TAG precursor pools or deregulate the dynamic balance between TAG storage and breakdown.

TAG overstorage in these cells starts very early on in logarithmic phase, when TAG precursors are usually used to supply the cell with the necessary membrane precursors for growth (Henry, Kohlwein et al. 2012). The precise signals controlling TAG storage and breakdown are not well understood but they are tightly intertwined with the cell-cycle (Kohlwein, Veenhuis et al. 2013). The PA phosphatase Pah1, involved in TAG catabolism and the lipase Tgl4, involved in TAG anabolism, are both regulated through a cell cycle dependent phosphorylation by Cdk1/Cdc28 (Kurat, Wolinski et al. 2009, Kohlwein, Veenhuis et al. 2013). Osw5L overexpression could also interfere with the regulatory circuits which tell the cell to store or break down storage lipids.

We also observed that overexpressed Osw5L localized in the vicinity of LDs (Fig.3.8). This protein accumulation could inhibit the access of TAG lipases and therefore impair lipolysis. This could also lead to increased TAG levels. This possibility is supported by the observation that various proteins, including the lipase Tgl3, are excluded from Osw5L induced LD aggregates (Fig. 3.11). Future experiments should discriminate effects of increased TAG storage and diminished breakdown.

Summarizing, Osw5L overexpression mediated TAG overstorage could be achieved through stimulation of precursor formation, inhibition of breakdown, or manipulation of the storage signaling pathways.

4.5. Osw5L could modulate lipid droplet surface properties

As mentioned before, deletion of the Seipin complex leads to major defects in LD protein targeting (Grippa, Buxo et al. 2015). In contrast, in *osw5LΔ* cells only one protein was mislocalized: Pdr16 (Fig. 3.12A, 3.13A). Pdr16 is a soluble lipid transfer protein that normally localizes to LDs. Consistent with a putative function in lipid transfer, Pdr16 binds PI and sterols *in vitro* (Schnabl, Oskolkova et al. 2003, Holic, Simova et al. 2014). Since Osw5L cannot be found on the LD (Fig. 3.4, 1.1B) and targeting in Seipin core mutant to aberrant LDs is Osw5L independent (Fig. 3.13A), it is likely that Pdr16 is not recruited to the LD by a direct interaction with Osw5L but rather recognizes certain surface properties of the LD monolayer. Reciprocally, Osw5L overexpression leads to strong accumulation of Pdr16 at the induced LD aggregates (Fig. 3.14).

Another lipid transfer protein, Kes1, is also recruited to theses aggregates (Fig. 3.16A). Kes1 is an amphipathic helix containing protein that detects packaging defect in membranes (Drin, Casella et al. 2007). Usually, Kes1 does not localize to LD, but the Golgi and the ER. Ectopical recruitment of Kes1 indicates altered LD surface properties in Osw5L overexpression induced LDs.

In Seipin complex mutants, Kes1 is also recruited to small LD clusters which are formed upon phospholipid surplus (Grippa, Buxo et al. 2015). Here, the amphipathic helix of Kes1 is necessary and sufficient to mediate the recruitment (Fig. 3.16C). However, this is not the case for Osw5L overexpression induced LD aggregates (Fig. 3.16C). This indicates, that Kes1 might not recognize the same membrane packaging defect in Seipin complex mutants as in Osw5L overexpression mutants.

Presumably, Pdr16 and Kes1 are both proteins involved in non-vesicular lipid transport in cells (Mesmin, Antonny et al. 2013, Holic, Simova et al. 2014). Whereas Pdr16 is thought to transport PI and sterols, Kes1 is involved in sterol- PI(4)P exchange. A Pdr16 mutant that is defective in PI binding shows no localization abnormalities (Fig. 3.15A). Therefore, in this experiment PI seems not to be involved in targeting it to LDs.

Since Pdr16 and Kes1 are both recruited to Osw5L induced LD aggregates (Fig. 3.14, 3.16) they could be recognizing the same membrane feature. Kes1 and Pdr16 are both reported to bind sterols (Im, Raychaudhuri et al. 2005, Holic, Simova et al. 2014). When we deleted the sterol acyltransferases ARE1 and ARE2 in the presence of Osw5L overexpression, LD aggregates do not contain SE anymore, but only TAG. Under these conditions, Pdr16 super-recruitment to LDs aggregates was persistent (Fig. 3.15B). Therefore, we conclude that SE are not important for Pdr16 recruitment to LDs.

Apart from SE, there are several sterol intermediates which could mediate Pdr16 and Kes1 recruitment. A study by Moldavski, Amen et al. (2015) implicates a soluble sterol derivate in the LD mediated clearance of inclusion bodies in yeast. LDs had an active role in inclusion body clearance which was dependent on the presence of sterols. Interestingly, Pdr16 mediated the contact between inclusion bodies and LDs. Upon PDR16 deletion, the contact was lost and the cells displayed an inclusion body clearance defect. A strain deleted for the acyltransferases ARE1 and ARE2, and therefore without SE, displayed the same clearance defects.

Taken together, sterols or sterol derivate could be involved in Kes1 and Pdr16 LD targeting. This could be addressed by altering sterol synthesis in these cells either biochemically or genetically.

4.6. A model of Osw5 protein function in the cell

The current study suggests that the Seipin complex could be integrating various events regulating LD properties. Its privileged localization at the ER-LD contact site makes it a prime candidate to regulate protein and lipid composition of the LD. Low affinity interactions with different proteins regulated by the metabolic state of the cell could enable fine tuning of LD biogenesis and LD dynamics according to nutrient availability in the media. These events are largely dependent on the LD surface and LD size which, to our current knowledge, influence the LD proteome and therefore its formation and breakdown (Grippa, Buxo et al. 2015). Both, LD surface, size and content are altered if the expression levels of the Osw5 proteins are changed. Therefore, this gives hints on how the information about the metabolic state of the cell could be integrated with LD integrity and dynamics.

The current work contributes to the functional understanding of LD regulation by the Seipin complex and a more integrative view of lipid metabolism in the cell. It also raises the question if and how the cell uses the ER-LD organelle contact site to regulate metabolic processes. It is an intriguing idea that Seipin controls more global features of the LD apart from phospholipid coating, for example protein access. Here, it would be interesting to explore the functions of Osw5S on the LD and to understand if its role is connected to the one in the Seipin complex. Also, future experiments should aim to elucidate the mechanism by which the ER protein Osw5L regulates Pdr16 recruitment to the LD. The conceptual framework that Osw5L, in complex with Seipin, influences the membrane properties of the LD monolayer, suggests that Seipin could not only passively gate phospholipid access to the LD, but there could be selection processes for, for example, certain lipid species.

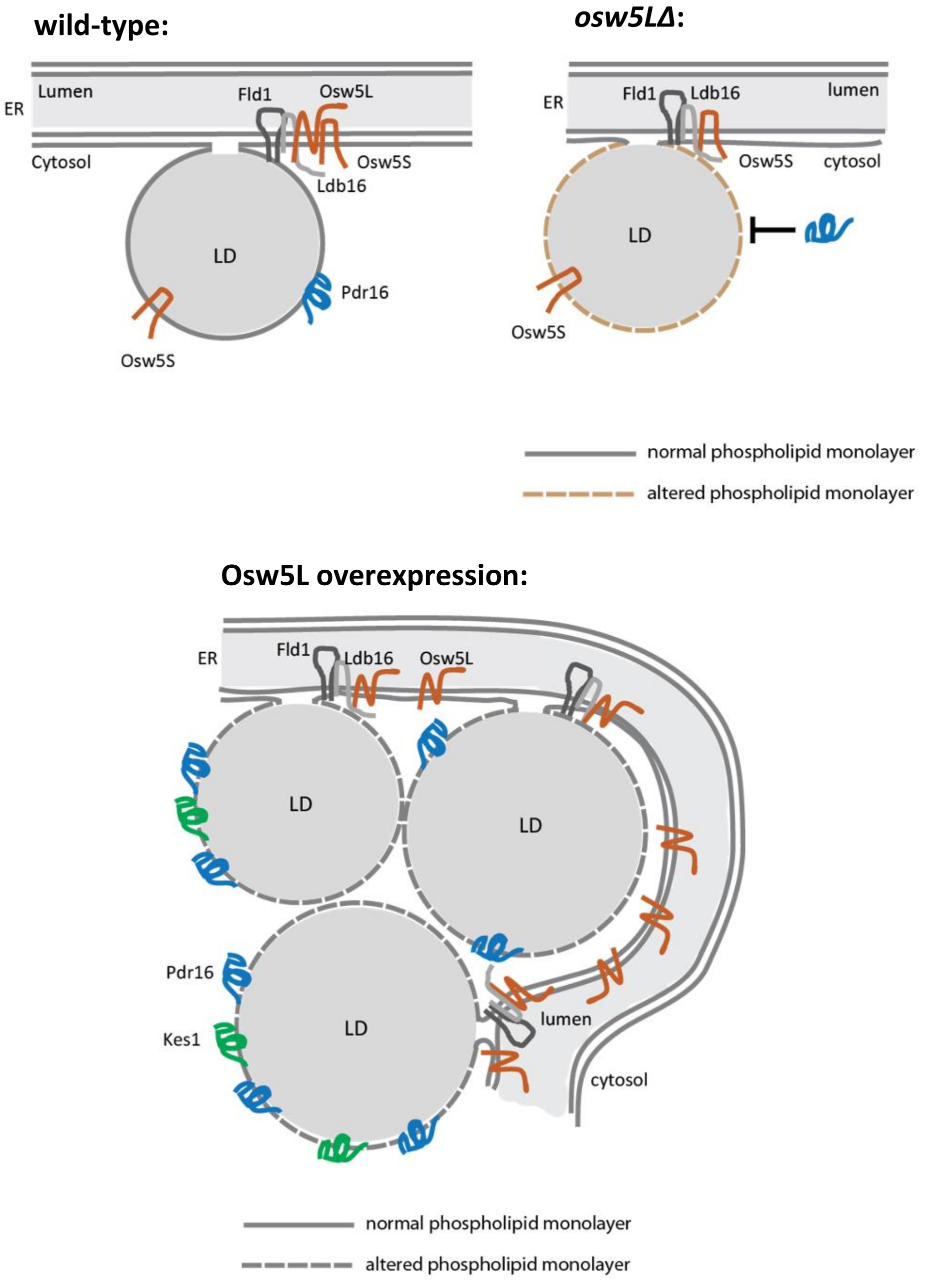

Figure 4.1. Model of Osw5L and Osw5S action at the ER-LD contact site.
The Seipin complex core components Fld1 and Ldb16 are localized to the ER-LD contact site. In wt cells, Osw5L and Osw5S are accessory protein of the Seipin complex. Osw5S also moves into the LD. Pdr16 recruitment to LDs in wt cells depends on the presence of Osw5L. When Osw5L is absent in cells, the LD monolayer seems to be altered. This inhibits Pdr16 recruitment to the LD surface. Upon Osw5L overexpression, Osw5S expression is shut down. Osw5L overexpression induces TAG overstorage and clustered LDs. Osw5L accumulates at the ER membrane in the vicinity of the LD aggregates. Osw5L overexpression leads to Pdr16 super-recruitment and ectopic recruitment of Kes1 to LD aggregates probably due to changes in the phospholipid monolayer.

5. References

(1991). "Guide to yeast genetics and molecular biology." Methods Enzymol 194: 1-863.

Abell, B. M., S. High and M. M. Moloney (2002). "Membrane protein topology of oleosin is constrained by its long hydrophobic domain." J Biol Chem 277(10): 8602-8610.

Abell, B. M., L. A. Holbrook, M. Abenes, D. J. Murphy, M. J. Hills and M. M. Moloney (1997). "Role of the proline knot motif in oleosin endoplasmic reticulum topology and oil body targeting." Plant Cell 9(8): 1481-1493.

Athenstaedt, K. and G. Daum (2003). "YMR313c/TGL3 encodes a novel triacylglycerol lipase located in lipid particles of Saccharomyces cerevisiae." J Biol Chem 278(26): 23317-23323.

Atkinson, K. D., B. Jensen, A. I. Kolat, E. M. Storm, S. A. Henry and S. Fogel (1980). "Yeast mutants auxotrophic for choline or ethanolamine." J Bacteriol 141(2): 558-564.

Bankaitis, V. A., C. J. Mousley and G. Schaaf (2010). "The Sec14 superfamily and mechanisms for crosstalk between lipid metabolism and lipid signaling." Trends Biochem Sci 35(3): 150-160.

Bankaitis, V. A., S. Phillips, L. Yanagisawa, X. Li, S. Routt and Z. Xie (2005). "Phosphatidylinositol transfer protein function in the yeast Saccharomyces cerevisiae." Adv Enzyme Regul 45: 155-170.

Bartz, R., W. H. Li, B. Venables, J. K. Zehmer, M. R. Roth, R. Welti, R. G. Anderson, P. Liu and K. D. Chapman (2007). "Lipidomics reveals that adiposomes store ether lipids and mediate phospholipid traffic." J Lipid Res 48(4): 837-847.

Beh, C. T., L. Cool, J. Phillips and J. Rine (2001). "Overlapping functions of the yeast oxysterol-binding protein homologues." Genetics 157(3): 1117-1140.

Beh, C. T. and J. Rine (2004). "A role for yeast oxysterol-binding protein homologs in endocytosis and in the maintenance of intracellular sterol-lipid distribution." J Cell Sci 117(Pt 14): 2983-2996.

Bell, R. M., L. M. Ballas and R. A. Coleman (1981). "Lipid topogenesis." J Lipid Res 22(3): 391-403.

Beller, M., C. Sztalryd, N. Southall, M. Bell, H. Jackle, D. S. Auld and B. Oliver (2008). "COPI complex is a regulator of lipid homeostasis." PLoS Biol 6(11): e292.

Bi, J., W. Wang, Z. Liu, X. Huang, Q. Jiang, G. Liu, Y. Wang and X. Huang (2014). "Seipin promotes adipose tissue fat storage through the ER Ca(2)(+)-ATPase SERCA." Cell Metab 19(5): 861-871.

Bickel, P. E., J. T. Tansey and M. A. Welte (2009). "PAT proteins, an ancient family of lipid droplet proteins that regulate cellular lipid stores." Biochim Biophys Acta 1791(6): 419-440.

Binns, D., S. Lee, C. L. Hilton, Q. X. Jiang and J. M. Goodman (2010). "Seipin is a discrete homooligomer." Biochemistry 49(50): 10747-10755.

Blaner, W. S., S. M. O'Byrne, N. Wongsiriroj, J. Kluwe, D. M. D'Ambrosio, H. Jiang, R. F. Schwabe, E. M. Hillman, R. Piantedosi and J. Libien (2009). "Hepatic stellate cell lipid droplets: a specialized lipid droplet for retinoid storage." Biochim Biophys Acta 1791(6): 467-473.

Botstein, D. and G. R. Fink (1988). "Yeast: an experimental organism for modern biology." Science 240(4858): 1439-1443.

Botstein, D. and G. R. Fink (2011). "Yeast: an experimental organism for 21st Century biology." Genetics 189(3): 695-704.

Broach, J. R. (2012). "Nutritional control of growth and development in yeast." Genetics 192(1): 73-105.

Casanovas, A., R. R. Sprenger, K. Tarasov, D. E. Ruckerbauer, H. K. Hannibal-Bach, J. Zanghellini, O. N. Jensen and C. S. Ejsing (2015). "Quantitative analysis of proteome and lipidome dynamics reveals functional regulation of global lipid metabolism." Chem Biol 22(3): 412-425.

Carman, G. M. and S. A. Henry (2007). "Phosphatidic acid plays a central role in the transcriptional regulation of glycerophospholipid synthesis in Saccharomyces cerevisiae." J Biol Chem 282(52): 37293-37297.

Cartwright, B. R., D. D. Binns, C. L. Hilton, S. Han, Q. Gao and J. M. Goodman (2015). "Seipin performs dissectible functions in promoting lipid droplet biogenesis and regulating droplet morphology." Mol Biol Cell 26(4): 726-739.

Cartwright, B. R. and J. M. Goodman (2012). "Seipin: from human disease to molecular mechanism." J Lipid Res 53(6): 1042-1055.

Carvalho, P., V. Goder and T. A. Rapoport (2006). "Distinct ubiquitin-ligase complexes define convergent pathways for the degradation of ER proteins." Cell 126(2): 361-373.

Cermelli, S., Y. Guo, S. P. Gross and M. A. Welte (2006). "The lipid-droplet proteome reveals that droplets are a protein-storage depot." Curr Biol 16(18): 1783-1795.

Chen, W., B. Chang, P. Saha, S. M. Hartig, L. Li, V. T. Reddy, Y. Yang, V. Yechoor, M. A. Mancini and L. Chan (2012). "Berardinelli-seip congenital lipodystrophy 2/seipin is a cell-autonomous regulator of lipolysis essential for adipocyte differentiation." Mol Cell Biol 32(6): 1099-1111.

Chiapparino, A., K. Maeda, D. Turei, J. Saez-Rodriguez and A. C. Gavin (2016). "The orchestra of lipid-transfer proteins at the crossroads between metabolism and signaling." Prog Lipid Res 61: 30-39.

Choi, H. S., W. M. Su, G. S. Han, D. Plote, Z. Xu and G. M. Carman (2012). "Pho85p-Pho80p phosphorylation of yeast Pah1p phosphatidate phosphatase regulates its activity, location, abundance, and function in lipid metabolism." J Biol Chem 287(14): 11290-11301.

Choudhary, V., N. Ojha, A. Golden and W. A. Prinz (2015). "A conserved family of proteins facilitates nascent lipid droplet budding from the ER." J Cell Biol 211(2): 261-271.

Connerth, M., K. Grillitsch, H. Kofeler and G. Daum (2009). "Analysis of lipid particles from yeast." Methods Mol Biol 579: 359-374.

Currie, E., X. Guo, R. Christiano, C. Chitraju, N. Kory, K. Harrison, J. Haas, T. C. Walther and R. V. Farese, Jr. (2014). "High confidence proteomic analysis of yeast LDs identifies additional droplet proteins and reveals connections to dolichol synthesis and sterol acetylation." J Lipid Res 55(7): 1465-1477.

do Valle Matta, M. A., J. L. Jonniaux, E. Balzi, A. Goffeau and B. van den Hazel (2001). "Novel target genes of the yeast regulator Pdr1p: a contribution of the TPO1 gene in resistance to quinidine and other drugs." Gene 272(1-2): 111-119.

Drin, G., J. F. Casella, R. Gautier, T. Boehmer, T. U. Schwartz and B. Antonny (2007). "A general amphipathic alpha-helical motif for sensing membrane curvature." Nat Struct Mol Biol 14(2): 138-146.

Ernster, L. and G. Schatz (1981). "Mitochondria: a historical review." J Cell Biol 91(3 Pt 2): 227s-255s.

Espenshade, P. J. and A. L. Hughes (2007). "Regulation of sterol synthesis in eukaryotes." Annu Rev Genet 41: 401-427.

Fagone, P. and S. Jackowski (2009). "Membrane phospholipid synthesis and endoplasmic reticulum function." J Lipid Res 50 Suppl: S311-316.

Fakas, S., C. Konstantinou and G. M. Carman (2011). "DGK1-encoded diacylglycerol kinase activity is required for phospholipid synthesis during growth resumption from stationary phase in Saccharomyces cerevisiae." J Biol Chem 286(2): 1464-1474.

Fang, M., B. G. Kearns, A. Gedvilaite, S. Kagiwada, M. Kearns, M. K. Fung and V. A. Bankaitis (1996). "Kes1p shares homology with human oxysterol binding protein and participates in a novel regulatory pathway for yeast Golgi-derived transport vesicle biogenesis." EMBO J 15(23): 6447-6459.

Farquhar, M. G. and G. E. Palade (1998). "The Golgi apparatus: 100 years of progress and controversy." Trends Cell Biol 8(1): 2-10.

Fei, W., G. Shui, B. Gaeta, X. Du, L. Kuerschner, P. Li, A. J. Brown, M. R. Wenk, R. G. Parton and H. Yang (2008). "Fld1p, a functional homologue of human seipin, regulates the size of lipid droplets in yeast." J Cell Biol 180(3): 473-482.

Fei, W., G. Shui, Y. Zhang, N. Krahmer, C. Ferguson, T. S. Kapterian, R. C. Lin, I. W. Dawes, A. J. Brown, P. Li, X. Huang, R. G. Parton, M. R. Wenk, T. C. Walther and H. Yang (2011). "A role for phosphatidic acid in the formation of "supersized" lipid droplets." PLoS Genet 7(7): e1002201.

Folch, J., M. Lees and G. H. Sloane Stanley (1957). "A simple method for the isolation and purification of total lipides from animal tissues." J Biol Chem 226(1): 497-509.

Foresti, O., A. Ruggiano, H. K. Hannibal-Bach, C. S. Ejsing and P. Carvalho (2013). "Sterol homeostasis requires regulated degradation of squalene monooxygenase by the ubiquitin ligase Doa10/Teb4." Elife 2: e00953.

Gaspar, M. L., S. A. Jesch, R. Viswanatha, A. L. Antosh, W. J. Brown, S. D. Kohlwein and S. A. Henry (2008). "A block in endoplasmic reticulum-to-Golgi trafficking inhibits phospholipid synthesis and induces neutral lipid accumulation." J Biol Chem 283(37): 25735-25751.

Georgiev, A. G., D. P. Sullivan, M. C. Kersting, J. S. Dittman, C. T. Beh and A. K. Menon (2011). "Osh proteins regulate membrane sterol organization but are not required for sterol movement between the ER and PM." Traffic 12(10): 1341-1355.

Gong, J., Z. Sun, L. Wu, W. Xu, N. Schieber, D. Xu, G. Shui, H. Yang, R. G. Parton and P. Li (2011). "Fsp27 promotes lipid droplet growth by lipid exchange and transfer at lipid droplet contact sites." J Cell Biol 195(6): 953-963.

Grillitsch, K., M. Connerth, H. Kofeler, T. N. Arrey, B. Rietschel, B. Wagner, M. Karas and G. Daum (2011). "Lipid particles/droplets of the yeast Saccharomyces cerevisiae revisited: lipidome meets proteome." Biochim Biophys Acta 1811(12): 1165-1176.

Guo, Y., T. C. Walther, M. Rao, N. Stuurman, G. Goshima, K. Terayama, J. S. Wong, R. D. Vale, P. Walter and R. V. Farese (2008). "Functional genomic screen reveals genes involved in lipid-droplet formation and utilization." Nature 453(7195): 657-661.

Grippa, A., L. Buxo, G. Mora, C. Funaya, F. Z. Idrissi, F. Mancuso, R. Gomez, J. Muntanya, E. Sabido and P. Carvalho (2015). "The seipin complex Fld1/Ldb16 stabilizes ER-lipid droplet contact sites." J Cell Biol 211(4): 829-844.

Han, G. S., W. I. Wu and G. M. Carman (2006). "The Saccharomyces cerevisiae Lipin homolog is a Mg2+-dependent phosphatidate phosphatase enzyme." J Biol Chem 281(14): 9210-9218.

Han, S., D. D. Binns, Y. F. Chang and J. M. Goodman (2015). "Dissecting seipin function: the localized accumulation of phosphatidic acid at ER/LD junctions in the absence of seipin is suppressed by Sei1p(DeltaNterm) only in combination with Ldb16p." BMC Cell Biol 16: 29.

Harris, H (2000). The Birth of the Cell. New Haven: Yale University Press. ISBN 0-300-07384-4.

Henry, S. A., S. D. Kohlwein and G. M. Carman (2012). "Metabolism and regulation of glycerolipids in the yeast Saccharomyces cerevisiae." Genetics 190(2): 317-349.

Herker, E. and M. Ott (2011). "Unique ties between hepatitis C virus replication and intracellular lipids." Trends Endocrinol Metab 22(6): 241-248.

Hofbauer, H. F., F. H. Schopf, H. Schleifer, O. L. Knittelfelder, B. Pieber, G. N. Rechberger, H. Wolinski, M. L. Gaspar, C. O. Kappe, J. Stadlmann, K. Mechtler, A. Zenz, K. Lohner, O. Tehlivets, S. A. Henry and S. D. Kohlwein (2014). "Regulation of gene expression through a transcriptional repressor that senses acyl-chain length in membrane phospholipids." Dev Cell 29(6): 729-739.

Holic, R., Z. Simova, T. Ashlin, V. Pevala, K. Poloncova, D. Tahotna, E. Kutejova, S. Cockcroft and P. Griac (2014). "Phosphatidylinositol binding of Saccharomyces cerevisiae Pdr16p represents an essential feature of this lipid transfer protein to provide protection against azole antifungals." Biochim Biophys Acta 1842(10): 1483-1490.

Holthuis, J. C. and A. K. Menon (2014). "Lipid landscapes and pipelines in membrane homeostasis." Nature 510(7503): 48-57.

Hristova, K., W. C. Wimley, V. K. Mishra, G. M. Anantharamiah, J. P. Segrest and S. H. White (1999). "An amphipathic alpha-helix at a membrane interface: a structural study using a novel X-ray diffraction method." J Mol Biol 290(1): 99-117.

Hsieh, K. and A. H. Huang (2004). "Endoplasmic reticulum, oleosins, and oils in seeds and tapetum cells." Plant Physiol 136(3): 3427-3434.

Hunyady, L., A. J. Baukal, Z. Gaborik, J. A. Olivares-Reyes, M. Bor, M. Szaszak, R. Lodge, K. J. Catt and T. Balla (2002). "Differential PI 3-kinase dependence of early and late phases of recycling of the internalized AT1 angiotensin receptor." J Cell Biol 157(7): 1211-1222.

Im, Y. J., S. Raychaudhuri, W. A. Prinz and J. H. Hurley (2005). "Structural mechanism for sterol sensing and transport by OSBP-related proteins." Nature 437(7055): 154-158.

Jacquier, N., V. Choudhary, M. Mari, A. Toulmay, F. Reggiori and R. Schneiter (2011). "Lipid droplets are functionally connected to the endoplasmic reticulum in Saccharomyces cerevisiae." J Cell Sci 124(Pt 14): 2424-2437.

Jacquier, N., S. Mishra, V. Choudhary and R. Schneiter (2013). "Expression of oleosin and perilipins in yeast promotes formation of lipid droplets from the endoplasmic reticulum." J Cell Sci 126(Pt 22): 5198-5209.

Jandrositz, A., J. Petschnigg, R. Zimmermann, K. Natter, H. Scholze, A. Hermetter, S. D. Kohlwein and R. Leber (2005). "The lipid droplet enzyme Tgl1p hydrolyzes both steryl esters and triglycerides in the yeast, Saccharomyces cerevisiae." Biochim Biophys Acta 1735(1): 50-58.

Janke, C., M. M. Magiera, N. Rathfelder, C. Taxis, S. Reber, H. Maekawa, A. Moreno-Borchart, G. Doenges, E. Schwob, E. Schiebel and M. Knop (2004). "A versatile toolbox for PCR-based tagging of yeast genes: new fluorescent proteins, more markers and promoter substitution cassettes." Yeast 21(11): 947-962.

Kadereit, B., P. Kumar, W. J. Wang, D. Miranda, E. L. Snapp, N. Severina, I. Torregroza, T. Evans and D. L. Silver (2008). "Evolutionarily conserved gene family important for fat storage." Proc Natl Acad Sci U S A 105(1): 94-99.

Klein, I., L. Klug, C. Schmidt, M. Zandl, M. Korber, G. Daum and K. Athenstaedt (2016). "Regulation of the yeast triacylglycerol lipases Tgl4p and Tgl5p by the presence/absence of nonpolar lipids." Mol Biol Cell 27(13): 2014-2024.

Klug, L. and G. Daum (2014). "Yeast lipid metabolism at a glance." FEMS Yeast Res 14(3): 369-388.

Koffel, R., R. Tiwari, L. Falquet and R. Schneiter (2005). "The Saccharomyces cerevisiae YLL012/YEH1, YLR020/YEH2, and TGL1 genes encode a novel family of membrane-anchored lipases that are required for steryl ester hydrolysis." Mol Cell Biol 25(5): 1655-1668.

Kohlwein, S. D., M. Veenhuis and I. J. van der Klei (2013). "Lipid droplets and peroxisomes: key players in cellular lipid homeostasis or a matter of fat--store 'em up or burn 'em down." Genetics 193(1): 1-50.

Kory, N., R. V. Farese, Jr. and T. C. Walther (2016). "Targeting Fat: Mechanisms of Protein Localization to Lipid Droplets." Trends Cell Biol 26(7): 535-546.

Krahmer, N., R. V. Farese, Jr. and T. C. Walther (2013). "Balancing the fat: lipid droplets and human disease." EMBO Mol Med 5(7): 905-915.

Krahmer, N., Y. Guo, F. Wilfling, M. Hilger, S. Lingrell, K. Heger, H. W. Newman, M. Schmidt-Supprian, D. E. Vance, M. Mann, R. V. Farese, Jr. and T. C. Walther (2011). "Phosphatidylcholine synthesis for lipid droplet expansion is mediated by localized activation of CTP:phosphocholine cytidylyltransferase." Cell Metab 14(4): 504-515.

Krahmer, N., M. Hilger, N. Kory, F. Wilfling, G. Stoehr, M. Mann, R. V. Farese, Jr. and T. C. Walther (2013). "Protein correlation profiles identify lipid droplet proteins with high confidence." Mol Cell Proteomics 12(5): 1115-1126.

Kurat, C. F., H. Wolinski, J. Petschnigg, S. Kaluarachchi, B. Andrews, K. Natter and S. D. Kohlwein (2009). "Cdk1/Cdc28-dependent activation of the major triacylglycerol lipase Tgl4 in yeast links lipolysis to cell-cycle progression." Mol Cell 33(1): 53-63.

Leber, R., E. Zinser, G. Zellnig, F. Paltauf and G. Daum (1994). "Characterization of lipid particles of the yeast, Saccharomyces cerevisiae." Yeast 10(11): 1421-1428.

Lev, S. (2010). "Non-vesicular lipid transport by lipid-transfer proteins and beyond." Nat Rev Mol Cell Biol 11(10): 739-750.

Lev, S. (2012). "Nonvesicular lipid transfer from the endoplasmic reticulum." Cold Spring Harb Perspect Biol 4(10).

Li, X., M. P. Rivas, M. Fang, J. Marchena, B. Mehrotra, A. Chaudhary, L. Feng, G. D. Prestwich and V. A. Bankaitis (2002). "Analysis of oxysterol binding protein homologue Kes1p function in regulation of Sec14p-dependent protein transport from the yeast Golgi complex." J Cell Biol 157(1): 63-77.

Li, X., S. M. Routt, Z. Xie, X. Cui, M. Fang, M. A. Kearns, M. Bard, D. R. Kirsch and V. A. Bankaitis (2000). "Identification of a novel family of nonclassic yeast phosphatidylinositol transfer proteins whose function modulates phospholipase D activity and Sec14p-independent cell growth." Mol Biol Cell 11(6): 1989-2005.

Li, Z., M. R. Johnson, Z. Ke, L. Chen and M. A. Welte (2014). "Drosophila lipid droplets buffer the H2Av supply to protect early embryonic development." Curr Biol 24(13): 1485-1491.

Longtine, M. S., A. McKenzie, 3rd, D. J. Demarini, N. G. Shah, A. Wach, A. Brachat, P. Philippsen and J. R. Pringle (1998). "Additional modules for versatile and economical PCR-based gene deletion and modification in Saccharomyces cerevisiae." Yeast 14(10): 953-961.

Maeda, K., K. Anand, A. Chiapparino, A. Kumar, M. Poletto, M. Kaksonen and A. C. Gavin (2013). "Interactome map uncovers phosphatidylserine transport by oxysterol-binding proteins." Nature 501(7466): 257-261.

Magre, J., M. Delepine, E. Khallouf, T. Gedde-Dahl, Jr., L. Van Maldergem, E. Sobel, J. Papp, M. Meier, A. Megarbane, A. Bachy, A. Verloes, F. H. d'Abronzo, E. Seemanova, R. Assan, N. Baudic, C. Bourut, P. Czernichow, F. Huet, F. Grigorescu, M. de Kerdanet, D. Lacombe, P. Labrune, M. Lanza, H. Loret, F. Matsuda, J. Navarro, A. Nivelon-Chevalier, M. Polak, J. J. Robert, P. Tric, N. Tubiana-Rufi, C. Vigouroux, J. Weissenbach, S. Savasta, J. A. Maassen, O. Trygstad, P. Bogalho, P. Freitas, J. L. Medina, F. Bonnicci, B. I. Joffe, G. Loyson, V. R. Panz, F. J. Raal, S. O'Rahilly, T. Stephenson, C. R. Kahn, M. Lathrop, J. Capeau and B. W. Group (2001). "Identification of the gene altered in Berardinelli-Seip congenital lipodystrophy on chromosome 11q13." Nat Genet 28(4): 365-370.

Mesmin, B., B. Antonny and G. Drin (2013). "Insights into the mechanisms of sterol transport between organelles." Cell Mol Life Sci 70(18): 3405-3421.

Mesmin, B., J. Bigay, J. Moser von Filseck, S. Lacas-Gervais, G. Drin and B. Antonny (2013). "A four-step cycle driven by PI(4)P hydrolysis directs sterol/PI(4)P exchange by the ER-Golgi tether OSBP." Cell 155(4): 830-843.

Mishra, S. and R. Schneiter (2015). "Expression of perilipin 5 promotes lipid droplet formation in yeast." Commun Integr Biol 8(6): e1071728.

Miura, F., N. Kawaguchi, J. Sese, A. Toyoda, M. Hattori, S. Morishita and T. Ito (2006). "A large-scale full-length cDNA analysis to explore the budding yeast transcriptome." Proc Natl Acad Sci U S A 103(47): 17846-17851.

Möbius, K. A. (1884). “Das Sterben der einzelligen und der vielzelligen Tiere. Vergleichend Betrachtet,” Biol. Zent. Bl. 4:389–392.

Moir, R. D., D. A. Gross, D. L. Silver and I. M. Willis (2012). "SCS3 and YFT2 link transcription of phospholipid biosynthetic genes to ER stress and the UPR." PLoS Genet 8(8): e1002890.

Moldavski, O., T. Amen, S. Levin-Zaidman, M. Eisenstein, I. Rogachev, A. Brandis, D. Kaganovich and M. Schuldiner (2015). "Lipid Droplets Are Essential for Efficient Clearance of Cytosolic Inclusion Bodies." Dev Cell 33(5): 603-610.

Moser von Filseck, J., A. Copic, V. Delfosse, S. Vanni, C. L. Jackson, W. Bourguet and G. Drin (2015). "INTRACELLULAR TRANSPORT. Phosphatidylserine transport by ORP/Osh proteins is driven by phosphatidylinositol 4-phosphate." Science 349(6246): 432-436.

Mousley, C. J., P. Yuan, N. A. Gaur, K. D. Trettin, A. H. Nile, S. J. Deminoff, B. J. Dewar, M. Wolpert, J. M. Macdonald, P. K. Herman, A. G. Hinnebusch and V. A. Bankaitis (2012). "A sterol-binding protein integrates endosomal lipid metabolism with TOR signaling and nitrogen sensing." Cell 148(4): 702-715.

Nakanishi, H., P. de los Santos and A. M. Neiman (2004). "Positive and negative regulation of a SNARE protein by control of intracellular localization." Mol Biol Cell 15(4): 1802-1815.

Natter, K., P. Leitner, A. Faschinger, H. Wolinski, S. McCraith, S. Fields and S. D. Kohlwein (2005). "The spatial organization of lipid synthesis in the yeast Saccharomyces cerevisiae derived from large scale green fluorescent protein tagging and high resolution microscopy." Mol Cell Proteomics 4(5): 662-672.

Oelkers, P., D. Cromley, M. Padamsee, J. T. Billheimer and S. L. Sturley (2002). "The DGA1 gene determines a second triglyceride synthetic pathway in yeast." J Biol Chem 277(11): 8877-8881.

Oelkers, P., A. Tinkelenberg, N. Erdeniz, D. Cromley, J. T. Billheimer and S. L. Sturley (2000). "A lecithin cholesterol acyltransferase-like gene mediates diacylglycerol esterification in yeast." J Biol Chem 275(21): 15609-15612.

Palade, G. E. and K. R. Porter (1954). "Studies on the endoplasmic reticulum. I. Its identification in cells in situ." J Exp Med 100(6): 641-656.

Pascual, F., L. S. Hsieh, A. Soto-Cardalda and G. M. Carman (2014). "Yeast Pah1p phosphatidate phosphatase is regulated by proteasome-mediated degradation." J Biol Chem 289(14): 9811-9822.

Patel, H., P. E. Hart, T. T. Warner, R. S. Houlston, M. A. Patton, S. Jeffery and A. H. Crosby (2001). "The Silver syndrome variant of hereditary spastic paraplegia maps to chromosome 11q12-q14, with evidence for genetic heterogeneity within this subtype." Am J Hum Genet 69(1): 209-215.

Phillips, M. J. and G. K. Voeltz (2016). "Structure and function of ER membrane contact sites with other organelles." Nat Rev Mol Cell Biol 17(2): 69-82.

Pol, A., S. P. Gross and R. G. Parton (2014). "Review: biogenesis of the multifunctional lipid droplet: lipids, proteins, and sites." J Cell Biol 204(5): 635-646.

Porter, K. R. (1953). "Observations on a submicroscopic basophilic component of cytoplasm." J Exp Med 97(5): 727-750.

Prieur, X., L. Dollet, M. Takahashi, M. Nemani, B. Pillot, C. Le May, C. Mounier, H. Takigawa-Imamura, D. Zelenika, F. Matsuda, B. Feve, J. Capeau, M. Lathrop, P. Costet, B. Cariou and J. Magre (2013). "Thiazolidinediones partially reverse the metabolic disturbances observed in Bscl2/seipin-deficient mice." Diabetologia 56(8): 1813-1825.

Prinz, W. A. (2014). "Bridging the gap: membrane contact sites in signaling, metabolism, and organelle dynamics." J Cell Biol 205(6): 759-769.

Raychaudhuri, S., Y. J. Im, J. H. Hurley and W. A. Prinz (2006). "Nonvesicular sterol movement from plasma membrane to ER requires oxysterol-binding protein-related proteins and phosphoinositides." J Cell Biol 173(1): 107-119.

Ren, J., C. Pei-Chen Lin, M. C. Pathak, B. R. Temple, A. H. Nile, C. J. Mousley, M. C. Duncan, D. M. Eckert, T. J. Leiker, P. T. Ivanova, D. S. Myers, R. C. Murphy, H. A. Brown, J. Verdaasdonk, K. S. Bloom, E. A. Ortlund, A. M. Neiman and V. A. Bankaitis (2014). "A phosphatidylinositol transfer protein integrates phosphoinositide signaling with lipid droplet metabolism to regulate a developmental program of nutrient stress-induced membrane biogenesis." Mol Biol Cell 25(5): 712-727.

Ren, J., G. Schaaf, V. A. Bankaitis, E. A. Ortlund and M. C. Pathak (2011). "Crystallization and preliminary X-ray diffraction analysis of Sfh3, a member of the Sec14 protein superfamily." Acta Crystallogr Sect F Struct Biol Cryst Commun 67(Pt 10): 1239-1243.

Roy, A. and T. P. Levine (2004). "Multiple pools of phosphatidylinositol 4-phosphate detected using the pleckstrin homology domain of Osh2p." J Biol Chem 279(43): 44683-44689.

Ruggiano, A., G. Mora, L. Buxo and P. Carvalho (2016). "Spatial control of lipid droplet proteins by the ERAD ubiquitin ligase Doa10." EMBO J 35(15): 1644-1655.

Saidane, S., S. Weber, X. De Deken, G. St-Germain and M. Raymond (2006). "PDR16-mediated azole resistance in Candida albicans." Mol Microbiol 60(6): 1546-1562.

Sandager, L., M. H. Gustavsson, U. Stahl, A. Dahlqvist, E. Wiberg, A. Banas, M. Lenman, H. Ronne and S. Stymne (2002). "Storage lipid synthesis is non-essential in yeast." J Biol Chem 277(8): 6478-6482.

Santos-Rosa, H., J. Leung, N. Grimsey, S. Peak-Chew and S. Siniossoglou (2005). "The yeast lipin Smp2 couples phospholipid biosynthesis to nuclear membrane growth." EMBO J 24(11): 1931-1941.

Schimper, A. F. W.(1883). “Über die Entwicklung der Chlorophyllkörner und Farbkörper.” Bot. Ztg. 41:105–162.

Schindelin, J., I. Arganda-Carreras, E. Frise, V. Kaynig, M. Longair, T. Pietzsch, S. Preibisch, C. Rueden, S. Saalfeld, B. Schmid, J. Y. Tinevez, D. J. White, V. Hartenstein, K. Eliceiri, P. Tomancak and A. Cardona (2012). "Fiji: an open-source platform for biological-image analysis." Nat Methods 9(7): 676-682.

Schnabl, M., O. V. Oskolkova, R. Holic, B. Brezna, H. Pichler, M. Zagorsek, S. D. Kohlwein, F. Paltauf, G. Daum and P. Griac (2003). "Subcellular localization of yeast Sec14 homologues and their involvement in regulation of phospholipid turnover." European Journal of Biochemistry 270(15): 3133-3145.

Schuller, H. J. (2003). "Transcriptional control of nonfermentative metabolism in the yeast Saccharomyces cerevisiae." Curr Genet 43(3): 139-160.

Selitrennik, M. and S. Lev (2016). "The role of phosphatidylinositol-transfer proteins at membrane contact sites." Biochem Soc Trans 44(2): 419-424.

Shibata, Y., G. K. Voeltz and T. A. Rapoport (2006). "Rough sheets and smooth tubules." Cell 126(3): 435-439.

Sim, M. F., R. J. Dennis, E. M. Aubry, N. Ramanathan, H. Sembongi, V. Saudek, D. Ito, S. O'Rahilly, S. Siniossoglou and J. J. Rochford (2012). "The human lipodystrophy protein seipin is an ER membrane adaptor for the adipogenic PA phosphatase lipin 1." Mol Metab 2(1): 38-46.

Simova, Z., K. Poloncova, D. Tahotna, R. Holic, I. Hapala, A. R. Smith, T. C. White and P. Griac (2013). "The yeast Saccharomyces cerevisiae Pdr16p restricts changes in ergosterol biosynthesis caused by the presence of azole antifungals." Yeast 30(6): 229-241.

Soni, K. G., G. A. Mardones, R. Sougrat, E. Smirnova, C. L. Jackson and J. S. Bonifacino (2009). "Coatomer-dependent protein delivery to lipid droplets." J Cell Sci 122(Pt 11): 1834-1841.

Sorger, D. and G. Daum (2002). "Synthesis of triacylglycerols by the acyl-coenzyme A:diacyl-glycerol acyltransferase Dga1p in lipid particles of the yeast Saccharomyces cerevisiae." J Bacteriol 184(2): 519-524.

Spanova, M., D. Zweytick, K. Lohner, L. Klug, E. Leitner, A. Hermetter and G. Daum (2012). "Influence of squalene on lipid particle/droplet and membrane organization in the yeast Saccharomyces cerevisiae." Biochim Biophys Acta 1821(4): 647-653.

Stefan, C. J., A. Audhya and S. D. Emr (2002). "The yeast synaptojanin-like proteins control the cellular distribution of phosphatidylinositol (4,5)-bisphosphate." Mol Biol Cell 13(2): 542-557.

Suda, Y., R. K. Rodriguez, A. E. Coluccio and A. M. Neiman (2009). "A screen for spore wall permeability mutants identifies a secreted protease required for proper spore wall assembly." PLoS One 4(9): e7184.

Sztalryd, C. and A. R. Kimmel (2014). "Perilipins: lipid droplet coat proteins adapted for tissue-specific energy storage and utilization, and lipid cytoprotection." Biochimie 96: 96-101.

Szymanski, K. M., D. Binns, R. Bartz, N. V. Grishin, W. P. Li, A. K. Agarwal, A. Garg, R. G. Anderson and J. M. Goodman (2007). "The lipodystrophy protein seipin is found at endoplasmic reticulum lipid droplet junctions and is important for droplet morphology." Proc Natl Acad Sci U S A 104(52): 20890-20895.

Talukder, M. M., M. F. Sim, S. O'Rahilly, J. M. Edwardson and J. J. Rochford (2015). "Seipin oligomers can interact directly with AGPAT2 and lipin 1, physically scaffolding critical regulators of adipogenesis." Mol Metab 4(3): 199-209.

Tauchi-Sato, K., S. Ozeki, T. Houjou, R. Taguchi and T. Fujimoto (2002). "The surface of lipid droplets is a phospholipid monolayer with a unique Fatty Acid composition." J Biol Chem 277(46): 44507-44512.

Terasaki, M., T. Shemesh, N. Kasthuri, R. W. Klemm, R. Schalek, K. J. Hayworth, A. R. Hand, M. Yankova, G. Huber, J. W. Lichtman, T. A. Rapoport and M. M. Kozlov (2013). "Stacked endoplasmic reticulum sheets are connected by helicoidal membrane motifs." Cell 154(2): 285-296.

Terzi, E., G. Holzemann and J. Seelig (1997). "Interaction of Alzheimer beta-amyloid peptide(1-40) with lipid membranes." Biochemistry 36(48): 14845-14852.

Thiam, A. R., R. V. Farese, Jr. and T. C. Walther (2013). "The biophysics and cell biology of lipid droplets." Nat Rev Mol Cell Biol 14(12): 775-786.

Thiam, A. R. and L. Foret (2016). "The physics of lipid droplet nucleation, growth and budding." Biochim Biophys Acta 1861(8 Pt A): 715-722.

Thoms, S., M. O. Debelyy, M. Connerth, G. Daum and R. Erdmann (2011). "The putative Saccharomyces cerevisiae hydrolase Ldh1p is localized to lipid droplets." Eukaryot Cell 10(6): 770-775.

Tsirigos, K. D., C. Peters, N. Shu, L. Kall and A. Elofsson (2015). "The TOPCONS web server for consensus prediction of membrane protein topology and signal peptides." Nucleic Acids Res 43(W1): W401-407.

Turner, W. (1890). "The Cell Theory, Past and Present." J Anat Physiol 24(Pt 2): 253-287.

van den Hazel, H. B., H. Pichler, M. A. do Valle Matta, E. Leitner, A. Goffeau and G. Daum (1999). "PDR16 and PDR17, two homologous genes of Saccharomyces cerevisiae, affect lipid biosynthesis and resistance to multiple drugs." J Biol Chem 274(4): 1934-1941.

van Meer, G., D. R. Voelker and G. W. Feigenson (2008). "Membrane lipids: where they are and how they behave." Nat Rev Mol Cell Biol 9(2): 112-124.

Veratti, E. (1961). "Investigations on the fine structure of striated muscle fiber read before the Reale Istituto Lombardo, 13 March 1902." J Biophys Biochem Cytol 10(4)Suppl: 1-59.

Villasmil, M. L., V. A. Bankaitis and C. J. Mousley (2012). "The oxysterol-binding protein superfamily: new concepts and old proteins." Biochem Soc Trans 40(2): 469-473.

Walther, T. C. and R. V. Farese, Jr. (2012). "Lipid droplets and cellular lipid metabolism." Annu Rev Biochem 81: 687-714.

Wang, C. W., Y. H. Miao and Y. S. Chang (2014). "Control of lipid droplet size in budding yeast requires the collaboration between Fld1 and Ldb16." J Cell Sci 127(Pt 6): 1214-1228.

Wee, K., W. Yang, S. Sugii and W. Han (2014). "Towards a mechanistic understanding of lipodystrophy and seipin functions." Biosci Rep 34(5).

Westrate, L. M., J. E. Lee, W. A. Prinz and G. K. Voeltz (2015). "Form follows function: the importance of endoplasmic reticulum shape." Annu Rev Biochem 84: 791-811.

Wilfling, F., J. T. Haas, T. C. Walther and R. V. Farese, Jr. (2014). "Lipid droplet biogenesis." Curr Opin Cell Biol 29: 39-45.

Wilfling, F., A. R. Thiam, M. J. Olarte, J. Wang, R. Beck, T. J. Gould, E. S. Allgeyer, F. Pincet, J. Bewersdorf, R. V. Farese, Jr. and T. C. Walther (2014). "Arf1/COPI machinery acts directly on lipid droplets and enables their connection to the ER for protein targeting." Elife 3: e01607.

Windpassinger, C., M. Auer-Grumbach, J. Irobi, H. Patel, E. Petek, G. Horl, R. Malli, J. A. Reed, I. Dierick, N. Verpoorten, T. T. Warner, C. Proukakis, P. Van den Bergh, C. Verellen, L. Van Maldergem, L. Merlini, P. De Jonghe, V. Timmerman, A. H. Crosby and

K. Wagner (2004). "Heterozygous missense mutations in BSCL2 are associated with distal hereditary motor neuropathy and Silver syndrome." Nat Genet 36(3): 271-276.

Windpassinger, C., K. Wagner, E. Petek, R. Fischer and M. Auer-Grumbach (2003). "Refinement of the Silver syndrome locus on chromosome 11q12-q14 in four families and exclusion of eight candidate genes." Hum Genet 114(1): 99-109.

Wolinski, H., H. F. Hofbauer, K. Hellauer, A. Cristobal-Sarramian, D. Kolb, M. Radulovic, O. L. Knittelfelder, G. N. Rechberger and S. D. Kohlwein (2015). "Seipin is involved in the regulation of phosphatidic acid metabolism at a subdomain of the nuclear envelope in yeast." Biochim Biophys Acta 1851(11): 1450-1464.

Wolinski, H., D. Kolb, S. Hermann, R. I. Koning and S. D. Kohlwein (2011). "A role for seipin in lipid droplet dynamics and inheritance in yeast." J Cell Sci 124(Pt 22): 3894-3904.

Woods, A., M. R. Munday, J. Scott, X. Yang, M. Carlson and D. Carling (1994). "Yeast SNF1 is functionally related to mammalian AMP-activated protein kinase and regulates acetyl-CoA carboxylase in vivo." J Biol Chem 269(30): 19509-19515.

Yang, H., M. Bard, D. A. Bruner, A. Gleeson, R. J. Deckelbaum, G. Aljinovic, T. M. Pohl, R. Rothstein and S. L. Sturley (1996). "Sterol esterification in yeast: a two-gene process." Science 272(5266): 1353-1356.

Yang, H., A. Galea, V. Sytnyk and M. Crossley (2012). "Controlling the size of lipid droplets: lipid and protein factors." Curr Opin Cell Biol 24(4): 509-516.

Yang, H., J. Tong, T. A. Leonard and Y. J. Im (2013). "Structural determinants for phosphatidylinositol recognition by Sfh3 and substrate-induced dimer-monomer transition during lipid transfer cycles." FEBS Lett 587(11): 1610-1616.

Yang, W., S. Thein, X. Guo, F. Xu, B. Venkatesh, S. Sugii, G. K. Radda and W. Han (2013). "Seipin differentially regulates lipogenesis and adipogenesis through a conserved core sequence and an evolutionarily acquired C-terminus." Biochem J 452(1): 37-44.

Yang, W., S. Thein, X. Wang, X. Bi, R. E. Ericksen, F. Xu and W. Han (2014). "BSCL2/seipin regulates adipogenesis through actin cytoskeleton remodelling." Hum Mol Genet 23(2): 502-513.

Yeung, T., G. E. Gilbert, J. Shi, J. Silvius, A. Kapus and S. Grinstein (2008). "Membrane phosphatidylserine regulates surface charge and protein localization." Science 319(5860): 210-213.

Yu, C., N. J. Kennedy, C. C. Chang and J. A. Rothblatt (1996). "Molecular cloning and characterization of two isoforms of Saccharomyces cerevisiae acyl-CoA:sterol acyltransferase." J Biol Chem 271(39): 24157-24163.

Yu, J. W., J. M. Mendrola, A. Audhya, S. Singh, D. Keleti, D. B. DeWald, D. Murray, S. D. Emr and M. A. Lemmon (2004). "Genome-wide analysis of membrane targeting by S. cerevisiae pleckstrin homology domains." Mol Cell 13(5): 677-688.

Zinser, E., F. Paltauf and G. Daum (1993). "Sterol composition of yeast organelle membranes and subcellular distribution of enzymes involved in sterol metabolism." J Bacteriol 175(10): 2853-2858.

Zinser, E., C. D. Sperka-Gottlieb, E. V. Fasch, S. D. Kohlwein, F. Paltauf and G. Daum (1991). "Phospholipid synthesis and lipid composition of subcellular membranes in the unicellular eukaryote Saccharomyces cerevisiae." J Bacteriol 173(6): 2026-2034.

Zheng, L., U. Baumann and J. L. Reymond (2004). "An efficient one-step site-directed and site-saturation mutagenesis protocol." Nucleic Acids Res 32(14): e115.